



UNIVERSITEIT•STELLENBOSCH•UNIVERSITY  
jou kennisvennoot • your knowledge partner

# Evaluation of next-generation low-power communication technologies to replace GSM in IoT-applications

by

Thomas Gerhardus Durand



UNIVERSITEIT  
iYUNIVESITHI  
STELLENBOSCH  
UNIVERSITY

Thesis presented in partial fulfilment of the requirements for the degree of  
Masters of Engineering (Research) in the Department of Electrical and  
Electronic Engineering at Stellenbosch University

Study leader: Prof. M.J. Booysen

Co-study leader: Dr. L. Visagie

December 2018

# Declaration

By submitting this report electronically, I declare that the entirety of the work contained therein is my own, original work, that I am the sole author thereof (save to the extent explicitly otherwise stated), that reproduction and publication thereof by Stellenbosch University will not infringe any third party rights and that I have not previously in its entirety or in part submitted it for obtaining any qualification.

Date: ..... December 2018 .....

Copyright © 2018 Stellenbosch University  
All rights reserved.

# Abstract

In today's world smart metering and control has become a critical component of our modern lifestyle. Smart Internet of Things (IoT) devices are used in a variety of applications in all sectors. Due to the rapid expansion of IoT applications, various IoT-focused communication networks are being developed and deployed. Although many technologies are available and being pursued, they do not all perform equally for all key metrics of the various applications. Choosing the right technology for the right application is difficult with the plethora of technologies and their claims.

This thesis provides an impartial and fair overview of the performance of alternative communication technologies available to the current cellular standard. Specifically, Sigfox, LoRaWAN and NB-IoT are compared to determine the best application for each technology.

Through investigating current literature, a suitable set of test metrics are identified, motivated, and used to compare the different communication technologies. The comparative metrics consists of two categories. Firstly, performance is compared through practically testing the power-consumption, maximum coupling loss (MCL), throughput and simulating the scalability. Secondly, different application metrics that affect performance, specifically the antenna, polarization, near-field interference, transmission power, path loss and coverage are evaluated.

To compare the technologies, four identical test devices were built and the firmware for each developed, each with their own communication module and test points in order to test power consumption. A LoRaWAN TTN base station was built to provide coverage in the testing area. To measure the power consumption of the communications modules accurately, a current measurement solution is designed, developed, built and tested. A complete back-end system is developed to store data transmitted by devices, used in the different testing procedures.

The research objective to develop, test and compare the hardware and firmware of the different communication technologies is achieved. The results indicate that there is no one solution to all IoT applications, however certain technologies are better suited, based on their performance metrics.

The test verified the ultra-low power consumption of LoRaWAN and Sigfox, while it indicated that NB-IoT's network process currently limits the power consumption savings of NB-IoT. NB-IoT and Sigfox performed the best in MCL tests, while GPRS performed the worst. Due to LoRaWAN and Sigfox's radio band duty cycle limitations, throughput is relatively limited compared to NB-IoT and GPRS.

# Uittreksel

In die wêreld van vandag, het slim meting en beheer 'n kritiese aspek van ons moderne leefstyl geword. Slim Internet van Dinge (IoD) toestelle word gebruik in 'n verskeidenheid toepassings in alle sektore van ons lewens. As gevolg van die vinnige ontwikkeling van slim toestel toepassings het verskeie IoD kommunikasie netwerke ontwikkel en word tans wêreldwyd ontplooi. Alhoewel verskeie kommunikasie tegnologieë beskikbaar is en nagevors word, het die verskeie tegnologieë meer toepaslike werkverrigtinge eienskappe wat beter vaar in verskillende toepassings. Die keuse van die regte tegnologie vir die regte toepassing is moeilik as gevolg van die oorfloed tipes tegnologieë en hul beweerde eienskappe.

Hierdie tesis bied 'n onpartydige en regverdige oorsig van die werkverrigting van alternatiewe kommunikasie netwerke wat saamding om die huidige GSM selulêre netwerk in IoD toepassings te vervang. Die tesis fokus spesifiek op Sigfox, LoRaWAN en NB-IoT, en beoog om die beste toepassing vir elke tipe tegnologie te vind.

Deur navorsing van die huidige literatuur word 'n stel toetsmetings geïdentifiseer en gemotiveer wat gebruik word om die verskillende IoD netwerke te vergelyk. Die vergelykende toets bestaan uit twee kategorieë. Eerstens, word die werkverrigting van netwerke getoets deur prakties kragverbruik, maksimum skakel verlies en deurset te meet. Die skalering van die verskillende netwerke word deur simulاسie bepaal. Tweedens, word toepassings metings getoets wat werkswirigting kan beïnvloed. Spesifiek word die invloed van antenna keuse, polarisasie, naby-veld versteurings, transmissie drywing, padverlies en dekking geëvalueer.

Om die tegnologie te vergelyk, is vier identiese toets appaarte gebou en die fermware vir elk ontwikkel, elk met hul eie kommunikasiemodule en toetspunte om die kragverbruik te meet. 'n LoRaWAN TTN-basisstasie is gebou om dekking in die toetsarea te bied. Om die kragverbruik van die kommunikasiemodules akkuraat te meet, word 'n meetoplossing ontwerp, ontwikkel, gebou en getoets. 'n Volledige agtergrondprogram stelsel is ontwikkel om data wat deur toestelle oorgedra word, te stoor, wat gebruik word in die verskillende toetsprosedures.

Die navorsingsdoelwit om die hardeware en fermware van die verskillende kommunikasietegnologieë te ontwikkel, te toets en te vergelyk, word behaal. Die resultate dui daarop dat daar geen oplossing vir alle IoD toepassings is nie, maar sekere tegnologieë is beter geskik, gebaseer op hul werkverrigting statistieke.

Die toetse het die ultra lae kragverbruik van LoRaWAN en Sigfox geverifieer, terwyl dit aangedui het dat NB-IoT se netwerkproses tans die lae kragverbruik van NB-IoT beperk. NB-IoT en Sigfox het die beste presteer in maksimum skakel verlies toetse, terwyl GPRS die swakste presteer het. As gevolg van LoRaWAN en Sigfox se radio-band-siklusbeperkings, is deurvoer relatief beperk in vergelyking met NB-IoT en GPRS.

# Acknowledgements

I would like to express my sincere gratitude to the following people and organizations ...

- Prof. Thinus Booysen, for assistance and financial support throughout the project.
- Dr. Lourens Visagie, for impartial independent and exceptional advice keeping my project on track.
- My family for their support and assistance throughout the project.
- Retha de Wet, for cheering me on through the tough times and believing in me.
- My friends and housemates for livening up the days when there was just too much work.
- Bridgiot for allowing me to test the Sigfox network in practice and allowing me access to Sigfox signal quality data.
- MTN for the Mobile Intelligence Lab

# Contents

<b>Declaration</b>	<b>i</b>
<b>Abstract</b>	<b>ii</b>
<b>Uittreksel</b>	<b>iii</b>
<b>Acknowledgements</b>	<b>iv</b>
<b>Contents</b>	<b>v</b>
<b>List of Figures</b>	<b>ix</b>
<b>List of Tables</b>	<b>xii</b>
<b>Abbreviations</b>	<b>xiii</b>
<b>1 Introduction</b>	<b>1</b>
1.1 Problem Statement . . . . .	1
1.2 Research Objectives . . . . .	2
1.3 Scope of Work . . . . .	3
1.4 Research contributions . . . . .	3
1.5 Noteworthy non-research contributions . . . . .	3
1.6 Thesis Structure . . . . .	4
<b>2 Literature Review</b>	<b>6</b>
2.1 Wide-area massive IoT networks overview . . . . .	6
2.1.1 Long-range . . . . .	7
2.1.2 Low-power consumption . . . . .	7
2.1.3 Low cost . . . . .	8
2.1.4 Scalability . . . . .	8
2.1.5 Existing wide-area massive IoT networks research . . . . .	9
2.2 GSM/GPRS . . . . .	10
2.2.1 Overview . . . . .	10
2.2.2 Architecture . . . . .	11
2.2.3 Data rate, link-budget and coding scheme . . . . .	11
2.2.4 Quality of Service . . . . .	12
2.2.5 Network processes . . . . .	12
2.2.6 GPRS applications . . . . .	13
2.3 Sigfox . . . . .	13
2.4 LoRaWAN . . . . .	15

2.4.1	LoRaWAN overview . . . . .	15
2.4.2	LoRaWAN device classes . . . . .	16
2.4.3	LoRaWAN registration . . . . .	16
2.4.4	LoRa Physical Layer overview and advantages . . . . .	17
2.4.5	LoRa parameters of the Physical layer . . . . .	17
2.4.6	LoRaWAN security . . . . .	19
2.4.7	The Things Network . . . . .	19
2.5	NB-IoT . . . . .	20
2.6	Other LPWAN solutions . . . . .	22
2.6.1	Weightless-P . . . . .	22
2.6.2	WAVIoT . . . . .	23
2.6.3	N-Wave . . . . .	23
2.6.4	INGENU RPMA . . . . .	23
2.6.5	Dash7 . . . . .	24
2.7	Comparison of the different solutions . . . . .	24
2.7.1	Power-consumption . . . . .	24
2.7.2	Range . . . . .	25
2.7.3	Throughput . . . . .	25
2.7.4	Down link latency . . . . .	26
2.7.5	Interference immunity . . . . .	26
2.8	Application metrics . . . . .	26
2.8.1	Antenna Performance . . . . .	27
2.8.2	Link budget and path loss . . . . .	29
2.8.3	Near field interference . . . . .	31
2.8.4	Transmission power . . . . .	32
2.9	Conclusion . . . . .	32
<b>3</b>	<b>Methodology and Research Design</b>	<b>33</b>
3.1	Performance testing methodology . . . . .	33
3.1.1	Link budget . . . . .	33
3.1.2	Power-consumption . . . . .	34
3.1.3	Throughput . . . . .	34
3.1.4	Scalability . . . . .	34
3.2	Application testing methodology . . . . .	37
3.2.1	Antenna . . . . .	37
3.2.2	Polarisation . . . . .	38
3.2.3	Near-field interference . . . . .	38
3.2.4	Transmission power . . . . .	38
3.2.5	Path-loss . . . . .	39
3.2.6	Coverage . . . . .	39
3.3	Conceptual test system overview . . . . .	40
3.4	Test device firmware requirements . . . . .	41
3.5	Generic testing devices available . . . . .	42
3.5.1	FiPy and LoPy . . . . .	43
3.5.2	Telit 868s Sigfox development board . . . . .	43
3.5.3	The Things Uno . . . . .	43
3.6	Test device hardware design . . . . .	43
3.6.1	General test device hardware design . . . . .	43

3.6.2	Test device hardware summary . . . . .	46
3.7	Power-consumption measurement . . . . .	47
3.8	Network base stations . . . . .	49
3.8.1	GSM and NB-IoT base stations . . . . .	49
3.8.2	Sigfox base stations . . . . .	50
3.8.3	LoRaWAN TTN base stations . . . . .	50
3.9	Firmware and back-end architecture . . . . .	51
3.9.1	Firmware architecture . . . . .	52
3.9.2	Back-end architecture . . . . .	58
3.9.3	Closing remarks on the firmware and back-end architecture . . . . .	60
<b>4</b>	<b>Results</b>	<b>61</b>
4.1	Performance results analysis . . . . .	61
4.1.1	Link budget . . . . .	61
4.1.2	Power-Consumption . . . . .	62
4.1.3	Throughput . . . . .	71
4.1.4	Scalability . . . . .	73
4.2	Application results analysis . . . . .	75
4.2.1	Antenna . . . . .	75
4.2.2	Polarization . . . . .	76
4.2.3	Near-field interference . . . . .	77
4.2.4	Path Loss . . . . .	78
4.2.5	Coverage . . . . .	79
4.3	Practical results analysis . . . . .	79
4.3.1	Sigfox results . . . . .	79
4.3.2	LoRaWAN results . . . . .	81
4.3.3	Summary . . . . .	83
<b>5</b>	<b>Conclusion and recommendations</b>	<b>84</b>
5.1	Comparative conclusion . . . . .	84
5.2	Use cases . . . . .	85
5.2.1	Smart farming . . . . .	85
5.2.2	Smart cities . . . . .	85
5.2.3	Vehicle tracking . . . . .	85
5.2.4	Smart homes . . . . .	85
5.2.5	Predictive maintenance . . . . .	86
5.3	Conclusion . . . . .	86
5.4	Open research challenges . . . . .	87
5.5	Recommendations . . . . .	87
5.5.1	Test devices . . . . .	87
5.5.2	Test system . . . . .	88
	<b>List of References</b>	<b>89</b>
	<b>A Antenna Tests</b>	<b>95</b>
	<b>B Hardware Development</b>	<b>100</b>
	<b>C Backend systems</b>	<b>107</b>



*CONTENTS*

viii

<b>D Power consumption calculations</b>	<b>110</b>
<b>E Scalability simulations</b>	<b>112</b>

# List of Figures

2.1	A comparison of LPWAN vs. different solutions available [1]	7
2.2	Wide-area massive IoT networks' coverage in smart cities [2]	8
2.3	GPRS architecture [3]	11
2.4	Resilience to interferes provided by UNB [1]	14
2.5	Sigfox transmission time- and frequency diversity	14
2.6	LoRaWAN complete architecture overview [4]	15
2.7	LoRa linear frequency modulated upchirp . [5]	17
2.8	LoRa transmission frame modulation [6]	18
2.9	Comparison of LoRa spreading factors [5]	18
2.10	NB-IoT deployment options	20
2.11	Extended Discontinuous Reception for NB-IoT [7]	22
2.12	Power Saving Mode for NB-IoT [7]	22
2.13	Different types of antennas tested	28
2.14	The Fresnel zone in communication systems	30
2.15	900MHz GSM signal attenuation [8]	31
2.16	433MHz antenna detuning [9]	32
3.1	LoRaWAN packet error rate at 1% duty cycle transmitting on 8 channels, theoretically calculated from Equation 3.4	36
3.2	LoRaWAN packet error rate at 1% duty cycle transmitting on 8 channels, practically simulated	36
3.3	Sigfox devices transmitting three frames with frequency and time diversity	37
3.4	Complete system architecture overview	40
3.5	Generic testing device	41
3.6	Coplanar Waveguide transmission line (Left) vs design Micro-strip (Right) [10]	46
3.7	Designed test devices	47
3.8	Spice model of current measurement solution mk I	48
3.9	Spice model of current measurement solution mk II	48
3.10	Current measurement solution mk II validation	49
3.11	LoRaWAN The Things Network base station overview	51
3.12	LoRaWAN TTN base station coverage [11]	51
3.13	Up-link centric device firmware overview	52
3.14	Basic overview of the communication modem firmware sections	53
3.15	GSM MCU-communication sequence diagram	55
3.16	Sigfox MCU-communication sequence diagram	56
3.17	LoRaWAN MCU-communication sequence diagram	57
3.18	NB-IoT MCU-communication sequence diagram	58

4.1	Packet delivery ratio of different communication technologies in different field test conditions . . . . .	62
4.2	LoRaWAN SF 7 (RN2483) 12 byte transmission current-consumption at 3.3V . . . . .	63
4.3	LoRaWAN SF 12 (RN2483) 12 byte transmission current-consumption at 3.3V . . . . .	63
4.4	Sigfox (Sfm10r1) 12 byte transmission current-consumption at 3.3V . . . . .	63
4.5	NB-IoT 12-byte transmission current-consumption profile at 3.4V . . . . .	64
4.6	NB-IoT 12 byte transmission and RCC connection release current-consumption profile at 3.4V . . . . .	64
4.7	NB-IoT RCC connected current-consumption profile at 3.4V . . . . .	65
4.8	NB-IoT RCC window close-up current-consumption profile at 3.4V . . . . .	65
4.9	Theoretically calculated vs. empirically measured battery life expectation of the different communication technologies transmitting 6, 12-byte messages per hour, no MCU included . . . . .	66
4.10	LPWAN battery life vs transmission packet size @ 6 messages per hour . . . . .	68
4.11	LPWAN battery life vs transmission rate @ 12 byte messages . . . . .	68
4.12	Sigfox transmitted power vs received power for 10 tests . . . . .	69
4.13	LoRaWAN SF7 transmitted power vs received power for 10 tests . . . . .	69
4.14	LoRaWAN SF12 transmitted power vs received power for 10 tests . . . . .	69
4.15	GPRS current consumption profile during network connection at 3.4 V . . . . .	69
4.16	GPRS current consumption profile during network idle at 3.4 V . . . . .	70
4.17	GPRS current consumption profile connecting to network from sleep at 3.4 V . . . . .	70
4.18	LoRa time on air vs spreading factor with CR 4/5 and 125 kHz bandwidth . . . . .	71
4.19	LoRaWAN SF7 packet delivery ratio vs. number of devices @ a single 12-byte message every 1000s . . . . .	74
4.20	LoRaWAN SF12 packet delivery ratio vs. number of devices @ a single 12-byte message every 1000s . . . . .	74
4.21	LoRaWAN SF7 packet delivery ratio vs. number of devices @ a single 12-byte message every 6.16s (1% duty cycle) . . . . .	74
4.22	LoRaWAN SF12 packet delivery ratio vs. number of devices @ a single 12-byte message every 148s (1% duty cycle) . . . . .	74
4.23	Sigfox number of simultaneous transmissions vs. number of devices transmitting . . . . .	75
4.24	Sigfox packet error rate vs. number of devices transmitting . . . . .	75
4.25	Comparison of different antennas in terms of signal strength (LoRaWAN) . . . . .	75
4.26	Comparison of different antennas in terms of signal strength (GSM) . . . . .	75
4.27	Comparison of different antennas in terms of signal strength (Sigfox) . . . . .	76
4.28	Comparison of different antennas in terms of signal strength (NB-IoT) . . . . .	76
4.29	% RSSI reduction due to 90° angle polarization shift . . . . .	76
4.30	Average % RSSI drop from baseline caused by near-field interference . . . . .	77
4.31	Sigfox theoretical free-space path-loss vs measured path-loss . . . . .	78
4.32	LoRaWAN theoretical SF7 free-space path-loss vs measured path-loss . . . . .	78
4.33	Measured RSSI (dB) network coverage of the different networks in the testing area . . . . .	79
4.34	Sigfox field-test RSSI . . . . .	81
4.35	Sigfox field-test SNR . . . . .	81
4.36	TTN LoRaWAN packets RSSI distribution at CR=4/5, BW=125 . . . . .	82
4.37	TTN LoRaWAN packets SNR distribution at CR=4/5, BW=125 . . . . .	82
4.38	TTN LoRaWAN packet frequency distribution at CR=4/5, BW=125 . . . . .	82
4.39	LoRaWAN performance summary . . . . .	83

4.40	Sigfox performance summary . . . . .	83
4.41	NB-IoT performance summary . . . . .	83
4.42	GPRS performance summary . . . . .	83
A.1	868MHz Dipole Antenna Far-Field vertical radiation pattern tested at 868MHz	95
A.2	868MHz Stub Antenna Far-Field vertical radiation pattern tested at 868MHz .	96
A.3	90 Deg 868MHz Stub Antenna Far-Field vertical radiation pattern tested at 868MHz . . . . .	96
A.4	GSM Dipole Antenna Far-Field vertical radiation pattern tested at 868MHz .	97
A.5	90 Deg GSM Stub Antenna Far-Field vertical radiation pattern tested at 868MHz	97
A.6	3dBi GSM helical stubby antenna, with 90deg connector VSWR . . . . .	98
A.7	3dBi 868MHz helical stubby antenna, with 90deg connector VSWR . . . . .	98
A.8	3dBi 868MHz dipole antenna, straight VSWR . . . . .	98
A.9	0.5dBi GSM dipole antenna, straight VSWR . . . . .	98
A.10	2.2dBi 868MHz helical stubby antenna, straight VSWR . . . . .	99
B.1	Different base stations deployed . . . . .	100
B.2	LoRaWAN device PCB design . . . . .	101
B.3	GPRS device PCB design . . . . .	102
B.4	NB-IoT device PCB design Part I . . . . .	103
B.5	NB-IoT device PCB design Part II . . . . .	104
B.6	Sigfox device PCB design . . . . .	105
C.1	The Things network LoRaWAN device back-end . . . . .	107
C.2	Sigfox device back-end . . . . .	108
C.3	MEAN-stack front-end web development . . . . .	108
C.4	Data translation layer overview . . . . .	109
E.1	LoRaWAN SF12 Scalability simulation, for device transmitting a single packet in 1000s intervals . . . . .	112
E.2	LoRaWAN SF7 Scalability simulation, for device transmitting a single packet in 1000s intervals . . . . .	113
E.3	Sigfox Scalability simulation, for device transmitting a single packet in 1000s intervals . . . . .	113

# List of Tables

2.1	Summary of technologies covered, metrics evaluated, and methodology used by current wide-area network research. . . . .	9
2.2	GPRS performance at different coding rates [12] . . . . .	12
2.3	Sigfox tiered device message limits per day . . . . .	14
2.4	LoRa receive sensitivity vs SF and Bandwidth . . . . .	19
2.5	Comparison of the different wide-area massive IoT networks . . . . .	25
2.6	Shanon maximum theoretical bit rate . . . . .	26
2.7	Overview of main antenna types categories used in wide-area massive IoT solutions . . . . .	27
2.8	Summary of different antenna's data sheets . . . . .	29
3.1	Test device firmware design specifications . . . . .	42
3.2	Current measurement solution mk II measurement range . . . . .	49
4.1	Measured link-budget of different communication technologies . . . . .	62
4.2	Measured Sigfox, LoRaWAN, NB-IoT modem and MCU sleep and idle currents	66
4.3	Power consumption calculations for the different technologies transmitting a single 12-byte message once per hour . . . . .	67
4.4	LoRaWAN and Sigfox transmission current draw at different transmission powers	68
4.5	LoRaWAN max messages per 24h vs spreading factor at CR=4/5 and BW=125 kHz . . . . .	72
4.6	LoRaWAN measured transmission speed vs spreading factor at CR=4/5 and BW=125 kHz . . . . .	72
4.7	Sigfox measured transmission speed . . . . .	72
4.8	NB-IoT measured up link and down link rate . . . . .	73
4.9	Throughput comparison of the different technologies . . . . .	73
4.10	Sigfox water meters signal quality analysis . . . . .	80
5.1	IoT use case requirements . . . . .	86
5.2	IoT use case applicability . . . . .	86
D.1	Battery life estimation of each type of technology . . . . .	110
D.2	LoRaWAN SF7 power consumption calculations . . . . .	110
D.3	LoRaWAN SF12 power consumption calculations . . . . .	110
D.4	Sigfox power consumption calculations . . . . .	111
D.5	NB-IoT power consumption calculations . . . . .	111

# Abbreviations

<b>3GPP</b>	3rd Generation Partnership Project
<b>ABP</b>	Activation by Personalization
<b>AES</b>	Advanced Encryption Standard
<b>API</b>	Application Programming Interface
<b>Bd</b>	Baud
<b>BPSK</b>	Binary Phase Shift keying
<b>BSC</b>	Base Station Controller
<b>BTS</b>	Base Transceiver Station
<b>BW</b>	Band Width
<b>CDMA</b>	Code-division multiple access
<b>CoAP</b>	Constrained Application Protocol
<b>CR</b>	Coding rate
<b>CS</b>	Coding Scheme
<b>CSS</b>	Chirp Spread Spectrum
<b>DNS</b>	Domain Name Server
<b>FEC</b>	Forward error correction
<b>FDMA</b>	Frequency-division multiple access
<b>FHSS</b>	Frequency-hopping spread spectrum
<b>FOTA</b>	Firmware Over-The-Air
<b>FSK</b>	Frequency Shift keying
<b>GGSN</b>	Gateway GPRS Service Node
<b>GMSK</b>	Gaussian Minimum Shift Keying
<b>GPRS</b>	General Packet Radio Service
<b>GPS</b>	Global Positioning System
<b>GSM</b>	Global System for Mobile communications
<b>GSMA</b>	Global System for Mobile communications Association
<b>HAL</b>	Hardware Abstraction Layer
<b>HTTP</b>	The Hypertext Transfer Protocol
<b>IDE</b>	Integrated Development Environment
<b>IMEI</b>	International Mobile Equipment Identity
<b>IoT</b>	Internet of Things
<b>IP</b>	Internet Protocol
<b>IMSI</b>	International Mobile Subscriber Identity
<b>ISM</b>	Industrial, Scientific and Medical

<b>LED</b>	Light emitting diode
<b>LoRaWAN</b>	Long Range Wide Area Network
<b>LPWAN</b>	Low Powered Wide Area Network
<b>LTE-M</b>	Long Term Evolution , Category M1
<b>MAC</b>	Medium Access Control
<b>MCL</b>	Maximum Coupling Loss
<b>MCU</b>	Micro Controller Unit
<b>MQTT</b>	Message Queuing Telemetry Transport
<b>NB-IoT</b>	Narrowband Internet of Things
<b>NB-Fi</b>	Narrow band Fidelity
<b>OFDM</b>	Orthogonal Frequency Division Multiplexing
<b>OTAA</b>	Over the Air Activation
<b>PDP</b>	Packet data protocol
<b>PDR</b>	Packet Delivery Ratio
<b>PER</b>	Packet Error Rate
<b>PSM</b>	Power saving mode
<b>QoS</b>	Quality of Service
<b>QPSK</b>	Quadrature Phase Shift keying
<b>RPMA</b>	Random Phase Multiple Access
<b>RSSI</b>	Received Signal Strength Indicator
<b>SC-FDMA</b>	Single-carrier Frequency-division multiple access
<b>SF</b>	Spreading Factor
<b>SGSN</b>	Serving GPRS Service Node
<b>SIM</b>	Subscriber Identity Module
<b>SMPS</b>	Switch Mode Power Supply
<b>SNR</b>	Signal-to-noise ratio
<b>SPI</b>	Serial Peripheral Interface
<b>TDMA</b>	Time-division multiple access
<b>UART</b>	Universal Asynchronous Receiver/Transmitter
<b>UNB</b>	Ultra Narrow Band
<b>Wi-Fi</b>	Wireless Fidelity

# Chapter 1

## Introduction

According to a mobility report by Ericsson in 2016, the Internet of Things consists of 5.2 billion short-range network IoT devices and 0.4 billion IoT devices utilizing long-range IoT networks [13]. These IoT devices (excluding PCs, laptops, smart phones or fixed phones) are all used to enable communication between various applications to enable a more connected society. The number is expected to grow to an estimated 2.1 billion long-range network IoT devices and 16 billion short-range network IoT devices by 2022. The short-range network segment mostly makes use of the unlicensed radio spectrum with a typical range of up to 100 meters and technologies include Wi-Fi, Bluetooth and ZigBee. The wide-area network segment consists mostly of devices using cellular connections (3GPP-based with some CDMA), as well as unlicensed low-power technologies, such as Sigfox and LoRaWAN.

The IoT network market segment consists of two major categories: critical IoT, and massive IoT. Characteristics of critical IoT infrastructure are ultra-reliability, availability, low latency and high data throughput, while massive IoT connections are characterised by high device volumes, small data traffic volumes, low cost devices and low power consumption.

The research presented in this paper investigates the three major long-range massive IoT networks that are currently being adopted in South-Africa. These three major long-range massive IoT networks are compared to the dated 2G GSM network standard. As the current 2G GSM network standard is being phased out by mobile networks in countries such as Korea and USA [14][15], the focus shifts on finding long term alternatives. The comparison is done through investigating the important characteristics of the different networks and comparing the technologies in an impartial and fair overview. The research concludes the investigation by comparing the different technologies in different use cases, by evaluating them against commonly adopted performance metrics.

### 1.1 Problem Statement

Currently, the market is flooded with multiple long-range massive IoT networks which aims to compete with the current GSM standard to enable communication for the massive IoT market segment. Competing technologies include LTE-M, LoRaWAN, DASH7, Sigfox, NB-IoT, WAVIoT and Weightless SIG. Each of these technologies hold different advantages, as well as disadvantages, in terms of throughput, speed, latency, power consumption, cost and other factors. There is no clear leader in this market segment, therefore all the above-mentioned technologies aim to claim a part of the market seg-



ment. Small start-ups and local companies in South-Africa are faced with a vast amount of communication technologies available to be utilized in their IoT applications. The primary requirements of these long-range massive IoT network devices are:

- One directional (device-to-gateway) communication
- Low data throughput, typically in the order of 10 bytes per hour.
- Low power use. These IoT devices are typically powered from batteries, and a battery lifetime of 10 years is expected.
- Low cost, to enable large scale deployment

The different technologies that will be compared in this thesis are Sigfox, LoRaWAN, NB-IoT and GSM. Sigfox and LoRaWAN will be evaluated as they are the main long-range massive IoT networks currently available to developers in South Africa. Further, NB-IoT needs to be investigated, as it is currently under deployment in South-Africa as it offers an easy solution for mobile network providers to enter the long-range massive IoT networks market. This is mostly due to the fact that current GSM base stations can be adapted to support NB-IoT, reducing the need for additional infrastructure. These technologies need to be compared based on the digital communication specifications such as throughput, range, latency, interference immunity, etc. and power and energy specifications through an power-consumption analysis. Moreover, the principles of electromagnetic theory and antenna design needs to be investigated, as this will allow recommendations to be made to IoT end-device manufactures.

## 1.2 Research Objectives

The following research objectives were defined to evaluate the different long-range massive IoT networks:

1. Research and evaluate important, fair and commonly used test metrics to compare the different long-range IoT networks.
2. Investigate, design and build functional test equipment and setups that can be used to evaluate the different long-range IoT networks. The test system needs to fulfill the following requirements:
  - a) The different test configurations of setups need to stay fundamentally the same, with only the IoT network communication module the differentiating factor.
  - b) The complete test setup needs to be low-power as to enable battery driven applications.
  - c) Test setup needs to be practically usable in IoT applications such as smart metering, asset tracking and environmental monitoring.
3. Research and develop a back-end system to store data from the various communication technologies.
4. Research and develop a current measurement testbed to evaluate the different solutions.

5. Discuss and evaluate different use cases using the results of the performance metric comparison.

## 1.3 Scope of Work

Scope restrictions within the following areas are applied to this research:

- **Hardware development:** Only four different testbed devices were designed and implemented as they represent the four most common long-range massive IoT networks currently available in South-Africa. These devices were designed to be limited in complexity as only the core feature (communication module) needs to be tested.
- **Embedded Programming:** The firmware developed for the IoT devices is limited to only functions that are required by the metric testing. The ability to update firmware OTA was not included in firmware development, due to both the limitations of the communication technology, as well as to reduce development complexity.
- **Back-End development:** A practically usable and deployable back-end system needs to be developed. The scope is restricted to data-storage only, however a brief overview of the front-end is provided.
- **RF analysis:** Different tests need to be performed to evaluate the RF performance of the communication technologies. Parameters need to be clearly defined, and the different environmental variables have to stay constant during each of the tests.
- **LoRaWAN:** Although different deployment models of LoRa and LoRaWAN exist, this thesis specifically investigates the use on LoRaWAN in The Things Network (TTN), as it is the deployment option available in the research area.

## 1.4 Research contributions

The following contributions are made to the research field:

- The research provides a comprehensive overview and evaluation of the different IoT networks. Networks are compared based on commonly used performance metrics, either through practical testing or simulation of theoretical research.
- Design, develop and build of four IoT-network test devices, along with their complementing firmware which can be used to comprehensibly test the different networks.

## 1.5 Noteworthy non-research contributions

Throughout the process of this thesis, several practical contributions were made in order to conduct the tests. These contributions are listed below:

- Through close cooperation with teams from MTN-SA and ZTE, the first MTN NB-IoT base station was deployed in the Western-Cape, South-Africa. The NB-IoT base station required several hardware and software upgrades over the current 4G-LTE equipment already in place. The base station is currently live and provides

the first NB-IoT network coverage in Stellenbosch. The base station was launched on 20 August 2017 as a collaborative effort between ZTE, MTN and Stellenbosch University to drive innovation [16].

- Due to the limited The Things Network (TTN) LoRaWAN coverage in Stellenbosch, a TTN base station was built to support this thesis. This additional gateway increased the number of local gateways to three, thereby meeting the requirement of becoming a worldwide recognized TTN community [17].
- SqwidNET launched in November 2016 as the licensed Sigfox operator in South Africa. The mapping of the Sigfox network was still underdeveloped in the Western-Cape as of February 2017. Through cooperation with the SqwidNET development team, coverage issues were identified in Stellenbosch, which led to the deployment of a new Sigfox base station on the Engineering-building at Stellenbosch University campus.
- The Sigfox testing device that was implemented for this research, was used as part of a water-saving initiative run by a Stellenbosch based company, BrigIoT. The implementation of the Sigfox devices enabled a large data set, which can be used to analyse the Sigfox communication standard. Details on the success of the project can be found at [18] or on Bridgiot's home page at [www.bridgiot.co.za](http://www.bridgiot.co.za).

## 1.6 Thesis Structure

The thesis consists of the following basic structure:

**Chapter 2** presents an overview of the literature study that was conducted to gain insight into the vast number of IoT-networks available. Current literature is investigated and shortcomings are identified. A major focus is cast on the four long-range massive IoT-networks that are being tested. Various other communication technologies are also identified along with their shortcomings to the South-African market. This chapter also investigates important metrics which needs to be considered during the testing of the various communication technologies.

**Chapter 3** investigates the methodology followed to test the different metrics. Requirements for test devices are listed and off the shelf test solutions are investigated. A set of test devices are proposed. The chapter details the hardware design of the IoT test devices. A overview is provided of the different gateways used and built during the development, as well as the current measurement device testbed. Lastly, a detailed firmware design is outlined, which was implemented to enable the different communication modules, along with the back-end system architecture that was used to store data.

**Chapter 4** analyses the results obtained from the test devices. The chapter specifically looks at the tests performed in lab conditions to analyse the performance and application metrics of the different networks. The real world performance of the networks on a larger scale is also analysed to support the performance and application results.

**Chapter 5** discusses the results of the lab and real world tests, as well as evaluating use cases of the various networks. Finally the chapter draws a conclusion on the comparison of the different networks and suggests recommendations and future work to be done.

# Chapter 2

## Literature Review

This chapter presents a broad overview of the different IoT communication technologies. The field of IoT communication technology is rapidly expanding, thus boundaries are needed to limit the scope of the literature review. The focus of the literature review is exclusively to compare the performance of GSM with Low-power wide area network (LPWAN) technologies, that are regularly available to IoT device manufacturers in South Africa and that are also utilized globally. The first section of this literature review focuses on the complete wide-area massive IoT market and the performance advantages it holds. The following section critically investigates current literature available regarding wide-area massive IoT networks. This investigation identifies the lack of practical comparative testing in the current literature.

GSM and three major LPWAN technologies are evaluated theoretically regarding their power-consumption, link-budget, scalability and various other metrics. This is followed by a discussion on other alternative IoT communication technologies with a broad overview provided along with the shortcomings of these technologies. A comparison is drawn between three LPWAN technologies and GSM, as this provides the basis for the testing methodology in Chapter 3. Finally, the four main technologies are compared in Section 2.7. Different application metrics commonly affecting wide-area massive IoT networks are investigated. These metrics will be used in the tests, as discussed in Chapter 3, and needs to be taken into account when conducting the experiments to ensure consistency.

### 2.1 Wide-area massive IoT networks overview

The IoT spectrum consists of a vast number of various devices that are used to gather and transmit data in different applications. Due to the wide array of applications, GSM has become a standard, with an expected 70% of all IoT device being GSM based by 2022 [13]. These communication technologies will be used to connect all types of IoT devices in the smart metering, building automation, household appliances, wearable, agricultural and various other IoT sectors. The popularity of GSM-based solutions can be attributed to the excellent coverage provided by mobile network operators as well the flexibility due to IPv6 integration in the network layer. Traditionally, the problem with GSM is high modem cost, high power consumption and high data costs. However, newer 5G and LTE-M standard that are currently still under development, aim to address these problems to evolve GSM into a fully fledged IoT solution.

The legacy non-cellular wireless technologies e.g., ZigBee, Bluetooth-LE, Z-Wave and Wi-Fi are flawed in the sense that they either do not offer comparable range to GSM,

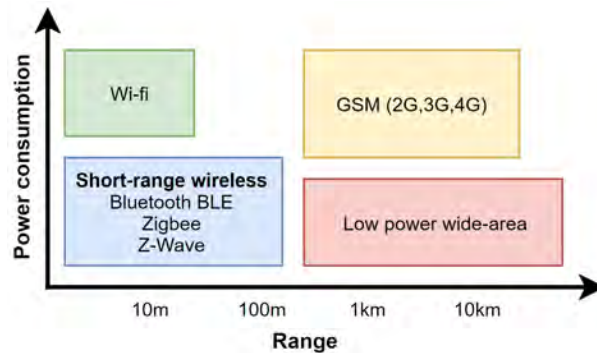


Figure 2.1: A comparison of LPWAN vs. different solutions available [1]

nor do they solve the power consumption limitation, as can be seen in Figure 2.1. Mesh networking can be implemented with a low-power solution such as ZigBee. However, this will increase the power consumption drastically as the nodes need to constantly be active and in receive mode to relay messages.

LPWAN networks are unique, as they compromise on data-rate, throughput and latency to compete with the rest of the communication technologies to achieve low-power consumption, long range, low module costs and massive amounts of devices per base station. To achieve these goals, various modulation and medium access (MAC) techniques are used, varying depending on the communication technology.

### 2.1.1 Long-range

LPWAN technologies typically operate in the sub-1GHz Industrial, Scientific and Medical (ISM) unlicensed radio bands. Globally the ISM bands are typically limited to a maximum transmission power of 15 dBm. This reduces the link budget compared to licensed bands, and lowers the range accordingly. However, due to the modulation scheme (discussed later in the text) used by LPWAN technologies, they typically offer a high receive sensitivity. This high receive sensitivity allows messages to be demodulated at extremely low received power. This increases the amount of attenuation of the radio signal can experience between the transmitter and receiver, maximum coupling loss (MCL), therefore increasing the range. MCL is the largest attenuation that a system can experience while still being able to demodulate the received signal. Figure 2.2 illustrates the attenuation experienced by various IoT applications. A higher MCL would increase coverage in deep indoor coverage locations, highlighted in Figure 2.2. The effects of low receive sensitivity and higher transmission powers will be discussed in greater detail in Section 2.8.2.

### 2.1.2 Low-power consumption

Star-network topology is used in LPWAN as opposed to mesh-networks, as this eliminates the need for energy inefficient repeaters, and allows the devices to be in sleep mode for as long as required. Also, connecting devices in a star network configuration increases scalability when compared to mesh networks, as certain nodes in a mesh network might become overloaded with traffic in a large scale network deployments. In a star-network topology, the base station or gateway is responsible to collect data from the end devices. Typically, the term gateway is used for a device that translate message protocols, for example LPWAN packets to IP based packets, while the term base station is used in a



Figure 2.2: Wide-area massive IoT networks' coverage in smart cities [2]

mobile and cellular communication connecting the end device to the back end network. Since the functionality is nearly identical in the network context the terms base station and gateway are used interchangeably in this thesis. To ensure further strict power consumption, LPWAN technologies typically require radio duty cycling specification. This allows LPWAN end devices to switch off their transceivers, when not in use as no synchronization with the network is required. The duty cycle is usage dependent and transceivers only need to be switched on when data has to be transmitted or received. A further advantage of LPWAN is a lightweight Medium Access Control (MAC) protocol, which reduces overhead drastically compared to short range and GSM MAC protocols. Lastly offloading processing complexity from end devices helps to improve power-consumption. This is done through shifting complex tasks from the end IoT devices to the back-end system. To allow IoT devices to transmit on any channel at will without the need of complex power-consuming communication initiation, base stations need to be able to receive multiple messages simultaneously on multiple channels. Complexity in the IoT device is thus traded for a more complex base station and back end design.

### 2.1.3 Low cost

To ensure the commercial success of LPWAN technologies, the module cost needs to be kept at a minimum to ensure large scale deployment, which further promotes an economy of scale for device manufacturers. Most LPWAN technologies aim to keep costs below ZAR 70 per communication module [19], as more active devices will also ensure a greater return on investment for network operators. Star type topologies, simple MAC protocol and reduced on-device processing, reduces the cost of the IoT device. Efficient modulation techniques and reduced transceiver complexity, peak data rates and memory sizes, also reduces hardware complexity and cost. The increased range of LPWAN technology reduces the amount of infrastructure needed to cover large areas, thus decreasing the set-up and maintenance costs for network operators, which in turn reduces the subscription cost for end users. Lastly, as most LPWAN technologies use the unlicensed ISM spectrum, there is no overhead cost associated with spectrum licensing.

### 2.1.4 Scalability

LPWAN technologies typically operate in the same frequency band, has no listen before talk (LBT) implemented and most LPWAN networks don't offer any acknowledgement of

Table 2.1: Summary of technologies covered, metrics evaluated, and methodology used by current wide-area network research.

Technologies covered	Metrics covered	Methodology	Ref
LoRaWAN, Sigfox, NB-IoT	Coverage, range, cost, latency, scalability, QoS, power-consumption	Purely research based	[20]
LoRaWAN, NB-IoT	Coverage, range, QoS, cost, latency, scalability, power-consumption	Purely research based	[21]
NB-IoT, LTE-M	Latency, coverage, power-consumption	Simulation based	[22]
LoRaWAN	Throughput, frequency usage, power-consumption, QoS	Large data set analysis and simulation based	[23]
LoRaWAN	Scalability, QoS	Simulation based and practical testing	[24]
LoRaWAN, Sigfox, NB-IoT, EC-GSM-IoT	Physical and MAC layer, business model	Purely research based	[25]
GPRS, NB-IoT, LoRaWAN, Sigfox	Coverage, path-loss, QoS	Simulation based	[26]
ZigBee, Bluetooth-LE, Wi-Fi, LoRaWAN	Scalability, transmission power, throughput	Purely research based	[27]

received packages. Therefore, best-effort LPWAN networks need to rely heavily on several modulation or software techniques to ensure reliable packet delivery in a scalable network. Two major categories of signal modulation can be identified in LPWAN: spread spectrum and ultra-narrow-band technologies, which helps to ensure packet delivery in a crowded frequency band. Specialized software techniques used in the end IoT devices include transmitting randomly on multiple channels and redundant time diverse transmissions, which decreases the chance of collision with a packet at same time and on the same channel or frequency. LPWAN also utilises a dense deployment of base stations, as this will ensure multiple reception to improve the chance of packet delivery in a scalable network.

### 2.1.5 Existing wide-area massive IoT networks research

The LPWAN market is growing rapidly due to an increasing number of IoT and M2M applications. Due to this drastic need for LPWAN technology, several standards have been set, which includes Sigfox, LoRaWAN, NB-IoT, EC-GSM-IoT, NWave, Weightless, LTE-M and the developing 5G-IoT.

The challenge regarding the vast number of LPWAN solutions is to determine a suitable set of technologies that can be practically implemented, tested and compared. Moreover, it is important to understand the differences and complexities of the LPWAN solution in order to compile a comprehensive list of testing metrics. Table 2.1 summarizes current research in the LPWAN field to provide an overview of the technologies investigated, whether the research was purely theoretical or practical, the metrics used to investigate/compare the technologies, and the methodology used to conduct the research in the literature.

Based on this overview, Sigfox, LoRaWAN, and NB-IoT were identified as being viable LPWAN technologies to investigate. This decision was based on the availability of network coverage, cost, performance and usability of the networks. Further, the need for



a baseline mobile-based IoT network was identified, to provide an overview comparison with the current GSM standard. GPRS is identified, due to its wide use as an IoT network technology, familiarity, and ease of use. Based on the overview of current research, a combination of a practical and theoretical research approach was identified as best suited, as there is a lack of comprehensive practical testing and comparison in the current literature. This lack of practical testing and comparison is due to the difficulty testing and comparing metric such as path-loss, packet-delivery ratio, polarisation and power consumption. Therefore, practical tests needs to be clearly defined to support theoretical work. Certain metrics, such as scalability can only be compared on a theoretical level as practical testing is not feasible.

## 2.2 GSM/GPRS

WAN 3rd Generation Partnership Project (3GPP) technologies like GSM, 3G, LTE and future 5G operate on licensed spectrum bands and historically have been intended for high-quality mobile voice, SMS and data services. GSM is the second-generation mobile telephone system, which was originally aimed at circuit-switched services namely voice and SMS, but also supports data transmission in the form of General Packet Radio Service (GPRS). GPRS uses packet-switched connections to carry data in small units, called IP packets, which are routed to a specific IP address. Due to the legacy of this system it is widely adopted, and hardware is available at low cost. The wide availability of cellular coverage encouraged IoT device manufactures to utilise it in a wide variety of IoT applications such as smart metering, industrial asset tracking, critical infrastructure monitoring etc. The scope of cellular networks is vast and cannot be covered in detail in this work.

Firstly, an overview of GPRS is provided which aims to explain the basic features and functionality. This is followed by a broad overview of the network architecture, which will be useful to understand how the current GPRS network can be used to support NB-IoT. Lastly, the QoS in a GPRS network is provided to understand how GPRS caters for various use-cases.

### 2.2.1 Overview

GPRS allows devices to connect in an "Always-On" state and transmit and receive IPv4 and IPv6 packets directly via the network layer. This always-on state allows down-link messages to be sent directly to the device nearly instantaneously, as opposed to waiting for a scheduled down-link frame, which most LPWAN technologies typically use. This allows GPRS to be used in mission critical IoT applications, such as remote shut off valves. Further, GSM allows packets to be acknowledged by both the base stations as well as the network server as there is no duty-cycle limitation. GPRS operates in the mobile network licensed spectrum in either the 850,900,1800 or 1900 MHz frequency spectrum dependent on region and network operator.

GPRS is based on the GSM standard where the international mobile station equipment identity (IMEI) uniquely identifies each GSM module, with each registered user being uniquely identified by its international mobile subscriber identity (IMSI). The IMSI is stored in the subscriber identity module (SIM), which is required to be valid and inserted into equipment with a valid IMEI to enable device to register to a network.

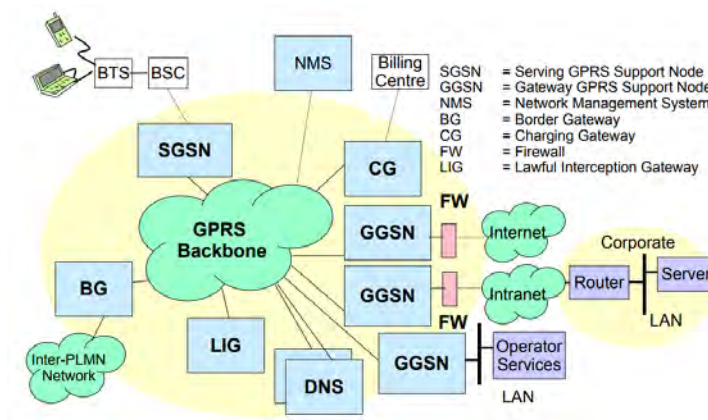


Figure 2.3: GPRS architecture [3]

## 2.2.2 Architecture

Enabling GPRS on a circuit-switched GSM network requires two core modules: the Gateway GPRS Service Node (GGSN), and the Serving GPRS Service Node (SGSN). The SGSN acts as a gateway between the GPRS network and the public data networks and is responsible for packet routing and transfers, mobility management (attach, detach and location management), logical link management (control upper sublayer of the data link layer multiplexing between several network protocols e.g. IP and X.25), authentication and charging users. Whereas the GGSN converts the GPRS packets coming from the SGSN into the appropriate packet data protocol (PDP) [28]. The addition of these two core modules, along with other upgrades, contributes to the high cost of GSM base station deployment to mobile network operators. Figure 2.3 presents an overview of the complete GPRS architecture. Devices connect to a base transceiver station (BTS), controlled by the base station controller (BSC), which further connects to the core network that enables connection to the internet (GGSN) through a firewall. Moreover, core network manages billing, authentication, management and connects to a Domain Name System (DNS) [29].

## 2.2.3 Data rate, link-budget and coding scheme

GPRS provides several benefits over the conventional circuit switched data GSM network, where connection setup takes several seconds and rates for data transmission are restricted to 9.6 Kbit/s. As GPRS is based on frequency division duplexing (FDD), each end-device is assigned to specific up-link and down-link 200 kHz frequency channels. Time-division multiple access (TDMA), is implemented along with FDD, which enables multiple end-devices to share the same frequency channel. TDMA divides the channels into 8 time-slots, allocating a single time slot to each end-device. In a single slot, the end-device transmits or receives a single packet containing both the user data and the error correction bits.

As end-devices operate in various signal strength environments, the amount of error correction bits can be varied, through the selection of the coding scheme [12]. Increasing the amount of error correction bits increases the error correction capability, however this results in a higher percentage of the transmitted data being error correction bits. Due to this increase, the effective user data rate decreases as the total data rate remains constant, as can be seen in Table 2.2.

Table 2.2: GPRS performance at different coding rates [12]

GPRS Coding scheme	User data rate (Kbps)	Error Correction capability	Worst link budget (dB)	Maximum cell range (m)
CS:1	9.05	Higest	135	450
CS:2	13.4		133	390
CS:3	15.6		131	350
CS:4	21.4	None	128.5	290

Theoretically, the data rate can be increased by allocating more time slots to each device. The actual data rate depends on the the following:

- Number of end-devices per cell
- Propagation delay between the end-device and the BTS
- Distance from the BTS

## 2.2.4 Quality of Service

GPRS allows defining different Quality of Service (QoS) profiles using four parameters to meet the requirements of different applications, such as real-time multimedia, web browsing, and basic message transfer. An in depth understanding of QoS is not required for the purpose of this research, however it enables a better understanding of the wide variety of GPRS applications [30].

- The service precedence (low, medium, high) defines the level of priority in a congested network.
- The reliability QoS defines the maximum transmission characteristics values in terms of probability of loss, duplication, mis-sequencing and corruption of packets.
- The delay QoS can also be specified, this includes all delays within the GPRS network e.g., the delay for request and assignment of radio resources and the transit delay in the GPRS backbone network. Transfer delays outside the GPRS network cannot be specified.
- The throughput QoS level can be negotiated between the network and end user to specify the maximum and mean throughput.

## 2.2.5 Network processes

A GPRS end-device undergoes several important network processes to establish and maintain a GPRS connection. The following network processes will be utilised to implement a GPRS connection [31].

- **Attach process**, through which the end device connects to the mobile network operator through connection to the SGSN in a GPRS network.
- **Authentication process**, were the SGSN authenticates the GPRS end-device by using the IMSI and IMEI.
- **PDP activation process**, which enables the end-device to connect to the GGSN allowing it access to the external network.

- **Detach procedure**, occurs when a GPRS end-device enters power-down mode or detaches from the SGSN in the GPRS network.

## 2.2.6 GPRS applications

GPRS end-devices are typically used in applications requiring vast amounts of data to be transmitted, such as mobile-phones, real-time asset tracking, industrial monitoring applications etc., due to its high speed, low latency and "always-on" state. GPRS end-devices popularity can be attributed to its wide-reaching coverage due to the legacy infrastructure in place. The high-power-consumption of GPRS, makes it less suitable for the IoT communication requirements that were defined in the problem statement in Chapter 1. When considering these requirements LPWAN alternatives provide an optimal replacement for GPRS.

## 2.3 Sigfox

Sigfox is a French company founded in 2009 that develops LPWAN technology aimed at connecting IoT devices with ultra-low bandwidth and power-consumption requirements. Sigfox employs a proprietary technology that enables communication using the ISM radio band, which uses 868MHz in Europe and Africa, 902MHz in North- and South-America, 923MHz in Japan and 920MHz in Asia [32]. Due to sub-1GHz modulation and a low receiver sensitivity, the network can cover large areas and penetrate objects easily, thus even subterranean IoT devices can be covered (depth depending on the distance between base-station and end-device). Sigfox utilises a wide-reaching Binary Phase Shift Keying (BPSK) signal modulation technique, which allows for a decreased PER/BER, in an ultra-narrow band (UNB). The network is based on one-hop star topology and requires local network operators to deploy a network of gateways.

Sqwidnet is the licensed Sigfox service provider in South-Africa and aim to provide countrywide coverage, with 83% of the South African population covered, March 2018 [33]. Sigfox covered 26 countries, February 2017, currently covers 51 countries (Jun 2018) and is on track to cover 60 countries by the end of 2018 [34]. This rapid expansion of the Sigfox network globally, indicates the volume of IoT-device manufactures utilizing the network and the amount of capital invested in reaching this global market. The aim of the Sigfox network is to enable devices to roam freely between countries that support the device's frequency band, without any re-registration or roaming costs. Sigfox network operators deploy multiple base stations to cover a single area to ensure cooperative reception of the Sigfox end-device's messages. This ensures that a message is still received by other base stations when the noise-level might be too high at one base station, or the base station is unavailable.

Sigfox utilizes 192 kHz of the ISM band to transmit a 100 Hz ultra-narrow band signal. This modulation technique concentrates all of the transmitted power in a small bandwidth, thus increasing the power spectral density significantly. This prevents signal jamming, as it is difficult to block such a high power signal at a random frequency, as can be seen in Figure 2.4. The small bandwidth also increases the number of channels, which reduces the probability of a collision with packets from other Sigfox devices. For a message to be received, the signal should be at least 8 dB above the noise floor [1].

The network is half-duplex with a two way communication limit of 140, 12 byte messages per day sent from the device to the gateway and two 8 byte messages per day sent

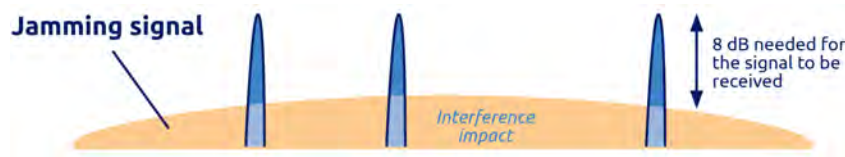


Figure 2.4: Resilience to interferes provided by UNB [1]

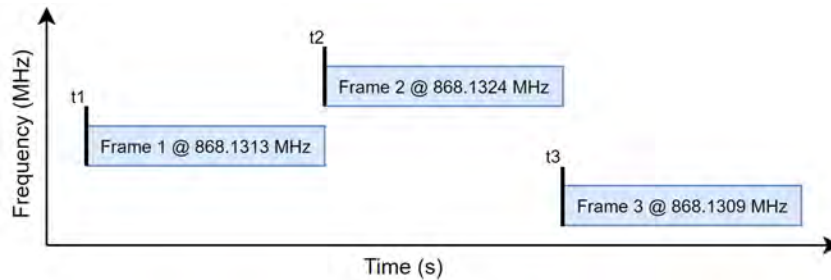


Figure 2.5: Sigfox transmission time- and frequency diversity

Table 2.3: Sigfox tiered device message limits per day

Tier	Uplink Messages	Downlink Messages
Platinum	101-140	4
Gold	51-100	2
Silver	3-50	1
One	1-2	0

from the gateway to the device. A single packet is transmitted three times, in three sequential frequency varying frames (transmissions). An example of this can be seen in Figure 2.5. Sigfox does not implement a listen-before-talk (LBT) protocol. This time- and frequency diversity increases the chance of reception, as simultaneous transmissions may occur **from** end-devices.

Sigfox is designed to be ultra-energy efficient with a maximum transmission power of 14 dBm (25 mW) allowed. Sigfox base stations have a receiver sensitivity of -140 dBm, which translates into a large link budget. There is no requirement for an end-device to sync with the network at any time and end-devices can transmit at will. Sigfox is aimed at being a "plug and play" technology. After powering the Sigfox device and registering the device to a Sigfox back-end account, see Appendix C, there are no extra steps necessary. Data is sent to a global back-end which the network operator manages. Device and contract management is also done through the Sigfox service provider. This back-end will grant access to the data in near real time (2-3 s back-end delay) and will execute a callback (HTTP post) to a customer's own proprietary back-end. Sigfox has partnered with several firms in the LPWAN industry such as Texas Instruments, Silicon Labs and Axom to provide Sigfox chip-sets [35].

Sigfox currently has a tiered option plan for how many up link transmissions a device is allocated per day, as well as how many down link transmissions are allowed (which is a different signal, using GFSK at 600 bd). The different message limit tiers can be seen in Table 2.3. The pricing of each message limit tiers depends on network service provider, and the amount of devices owned.

As Sigfox is responsible for transmitting large sets of collective data, security is of the utmost importance. The scope of Sigfox's security systems is vast and cannot be covered in detail in this work, for a comprehensive overview see [36]. The basis of Sigfox's security

is ensured through processing the received messages and validating the message sequence counter and the device's unique symmetrical authentication key. Communication between the Sigfox base stations and the Sigfox-core network is encrypted end-to-end where data is then stored on the secure Sigfox back-end. IoT device manufacturers can ensure an extra level of security by implementing application layer encryption.

## 2.4 LoRaWAN

Long-range wide area network (LoRaWAN) is an LPWAN with features that support low-cost, wide reaching, and secure bi-directional communication for low throughput IoT end-devices. Innovative features of LoRaWAN include support for redundant operation, geo-location, low-cost, and low complexity installation, which enables large scale deployment worldwide.

### 2.4.1 LoRaWAN overview

LoRaWAN is a network stack rooted in the LoRa physical layer to enable a network of IoT devices in a star-network topology. LoRa features data rates of up to 27 kbps with spreading factor 7 and 500 kHz channel or 50 kbps with Frequency-shift keying (FSK) modulation and long communication range of between 2-5 km in urban areas and more than 15 km in rural areas. World-Wide there are currently 83 network operators with 95 countries supporting some sort of LoRaWAN deployment [37]. A basic overview of a typical LoRaWAN setup can be seen in Figure 2.6. The flow of a transmitted packet starts with the MCU that interfaces with the LoRaWAN stack (LoRaWAN Master). The latter controls the hardware abstraction layer (HAL) which interfaces with the physical modulation. The message is transmitted using either LoRa or FSK modulation, which is received by a gateway's physical layer. The HAL in the base station or gateway then translates the message, which enable the gateway's packet forwarder to transmit the message via Ethernet, 3G, Wi-Fi or other networks. through the use of its IP stack. The network server receives the message that can then be further used in a customer application through an API.

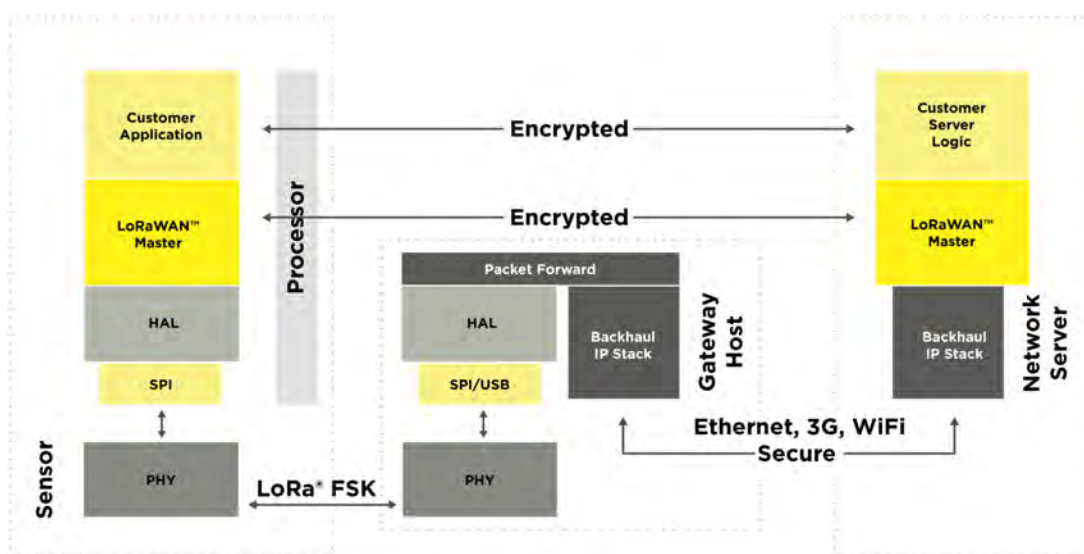


Figure 2.6: LoRaWAN complete architecture overview [4]

## 2.4.2 LoRaWAN device classes

Three different LoRaWAN device classes can be defined (Class A, B and C), each with their own capabilities [38]:

- Class A devices listen for a response during two down-link receive windows after transmitting an up-link frame. Each of the two receive windows are defined by a duration, time offset (with a default of one and two seconds respectively) and data rate. A down-link transmission is only allowed after a successful up-link message. The data rate and channel used in the first down-link window is based on the up-link data-rate and channel. The second receive window's offset and the data rate is fixed to a predetermined duration and 0.3 kbps respectively. The second down-link message window is disabled once data is successfully received in the first down-link window. This class of LoRaWAN device is the most power-efficient, however down-link latency is completely dependent on the transmission duty cycle. This prohibits this class of device being used in down-link centric mission critical applications such as IoT actuators.
- Class B devices are similar to class A devices, with two down-link frames, however they provide the option to add extra down-link frames at specified durations. The duration is specified by the gateway using a beacon frame, with the trade-off between down-link traffic and power consumption. The end user-application will be notified when a device is able to receive a down-link message. This class is ideal for non-critical low power actuators, as it provides relatively low latency (dependent on the amount of scheduled down-link frames), while still providing low-power consumption.
- Class C devices are completely down-link central, with virtually no down-link latency. After the transmission of a single up-link frame, one down-link frame is scheduled as described in Class A. However, the second receive frame is continuously active until a new up-link frame is sent. The down-link receive channel is dependent on the up-link channel. This is ideal for mission-critical actuators without strict power use limitations.

The three classes can co-exist in the same network, with devices switching between the different classes, however there is currently no class transition support for gateways, thus class transition needs to be implemented in the application layer.

## 2.4.3 LoRaWAN registration

Two types of LoRaWAN device network registration exist, namely Over-the-Air-Activation (OTAA) and Activation-by-Personalization (ABP), both of which are supported by the LoRaWAN stack and each having their own advantages and typical applications.

- Over-the-Air Activation (OTAA) requires devices perform a join-procedure with the network upon the first connection to a network, during which a dynamic device address (DevAddr) is assigned to the device and security keys are negotiated with the device. OTAA is the preferred way for large scale device manufacturers to manage devices and most secure way to connect. OTAA also allows a device to change networks without reprogramming the device.

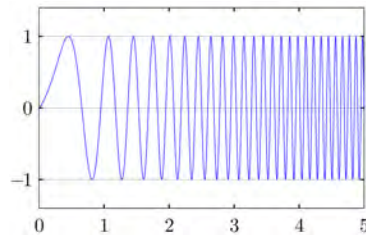


Figure 2.7: LoRa linear frequency modulated upchirp . [5]

- Activation-by-Personalization (ABP) is useful for development purposes where the DevAddr and security keys are hard coded into the firmware. This type of activation is not encouraged in large scale developments as the device can not easily change network, and any changes to the security keys requires device reprogramming resulting in compromised security.

#### 2.4.4 LoRa Physical Layer overview and advantages

LoRa utilizes chirp spread spectrum (CSS) modulation, to transfer data from the transmitter to receiver. CSS uses a sinusoidal signal (chirps), which has a linear variation in frequency over time, to encode data. An example of the modulation can be seen in Figure 2.8 and a linear frequency modulated upchirp in the time domain can be seen in Figure 2.7

Due to the linear nature of the chirps, the frequency offset between the transmitter and receiver is equivalent to the timing offset. The timing offset can easily be compensated for in the decoder, thus making the modulation technique immune to the Doppler effect, useful for high speed applications [39]. Another big advantage of the large indifference to the frequency offset, which can reach up to 20% of the bandwidth without reducing the performance, is that crystals in the transmitters do not need to be extremely accurate, which reduces module costs. LoRa receivers are also able to lock onto the receiving signal's frequency, which helps to increase the receive sensitivity down to  $-136$  dBm.

LoRa employs Forward Error-correction Codes (FECs), which is used to correct errors from interference caused by Frequency Hopping Spread Spectrum (FHSS) systems. Lora outperforms other traditional modulation schemes, such as Frequency-Shift Keying (FSK) through having relatively high robustness, through having resilience to both in-band and out-of-band interference mechanisms. LoRa has 90 dB out-of-channel selectivity (compared to 50 dB of FSK), which is the max ratio of power between an interferer in a neighboring band and the LoRa signal. LoRa has a 20 dB co-channel rejection (compared to  $-6$  dB of FSK ) which is the max ratio of power between an interferer in the same channel and the LoRa signal). This co-channel rejection allows LoRa to decode signals up to 20 dB below the noise floor [40].

#### 2.4.5 LoRa parameters of the Physical layer

LoRa modulation has three main parameters which can be set by the transmitter, namely the Spreading Factor (SF), the Code Rate (CR) and the Bandwidth(BW). The effects of changing these parameters changes the effective bitrate, resilience to interference and the ease of decoding [40].

A LoRa symbol is composed of  $2^{\text{SF}}$  chips, which covers the entire channel. LoRa modulation starts at the Carrier frequency ( $f_c$ ) - half of the BW, and continues linearly



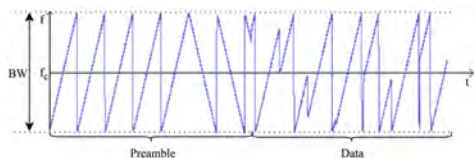


Figure 2.8: LoRa transmission frame modulation [6]

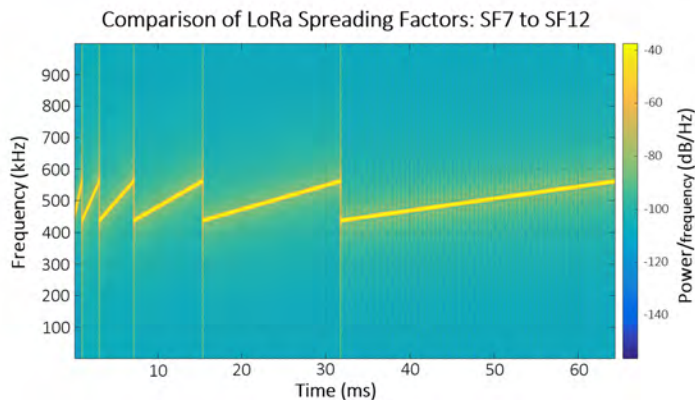


Figure 2.9: Comparison of LoRa spreading factors [5]

over time till it reaches Carrier frequency ( $f_c$ ) + half of the BW, and the starts again at the minimum frequency, as shown in Figure 2.8. The discontinuity in the frequency is what modulates the information in a LoRa signal. The Spreading factor is defined by LoRa as the log base 2 of the number of chips per symbol, for example SF 7 results in 128 chips per symbol. LoRa only utilizes six different spreading factors ranging from 7 to 12, and as there are  $2^{SF}$  chips in a symbol, a symbol can effectively encode SF bits of information [41].

The bandwidth is the important part of LoRa modulation, as it determines the max frequency variation of the symbols and the chip rate in LoRa. The chip rate is equal to the bandwidth, for example a BW of 125 kHz is equal to 125 000 chips per second. This means that if the SF increases by one the amount of chips will double, which halves the frequency span of a chip, and doubling the duration of a symbol. From Figure 2.9 the different spreading factors from 7 to 12 (left to right) can be seen on the spectrogram, which shows how the increase in the SF doubles the symbol duration, while the chirp-rate stays the same.

The symbol duration is thus dependent on the SF (amount of chips per symbol) and the chirp rate, which is dependent on the BW. Equation 2.1 shows the relationship of SF and BW to the symbol duration ( $T_S$ ).

$$T_S = \frac{2^{SF}}{BW} \quad (2.1)$$

To correlate the symbol rate to the bit rate, the included LoRa FEC code needs to be considered. The code rate (CR) is equal to  $4/(4+n)$ , with  $n \in (1,2,3,4)$ . Higher values such as 4, ( $CR = 4/8$ ) will increase tolerance towards short bursts of interference, thus reducing the packet error rate (PER), while a signal with  $CR = 4/5$  will be more susceptible to interference. As one symbol is equal to SF bits and the symbol duration can be determined from Equation 2.1, the bit rate ( $R_b$ ) can be calculated as described in Equation 2.2, with  $CR \in (1,2,3,4)$ .

$$R_b = SF \times \frac{BW}{2^{SF}} \times \frac{4}{4 + CR} \quad (2.2)$$

Example: A standard LoRa message with BW of 125kHz, SF of 7 and CR of  $4/5$  will translate into a bit rate of  $R_b = 5468$  bps.

As LoRa is intended to be a long range RF solution, it is important to keep the receiver sensitivity as high as possible in the interest of the MCL. The receiver sensitivity is a trade-off between the SF and BW. Increasing the SF and lowering the BW leads to a higher

receiver sensitivity, thus longer range. However, it does come at the price of reducing the bit rate and thus increasing the time on air which increases the power consumption. LoRAWAN supports adaptive data rates, which allows the device to select the optimal data rate in order to preserve battery and decrease airtime or increase range [42]. This feature is recommended for static device and should be disabled in situations where signal quality conditions may vary drastically. A summary of the receiver sensitivity vs the different LoRa parameters can be seen in Table 2.4.

Table 2.4: LoRa receive sensitivity vs SF and Bandwidth

Signal Bandwidth (kHz)	Spreading Factor	Sensitivity (dBm)
125	12	-137
125	7	-126
250	12	-136
250	7	-123
500	12	-134
500	7	-120

## 2.4.6 LoRaWAN security

Security in LoRaWAN is ensured through a unique 128-bit Network Session Key shared between the end-device and the network server, while a unique 128-bit Application Session Key (AppSKey) shared end-to-end at the application level. The combination of the two keys ensure authentication and integrity of packets to the network server and end-to-end encryption to the application server, which prevents radio-packet sniffing. Moreover, the addition of a frame counter, ensure that any packets received, such as a replay-attack (false messages), will be discarded if the frame counter is not within expected limits, or is lower than the current frame counter.

## 2.4.7 The Things Network

The Things Network (TTN) is a community of users who together build a network of gateways to form an open network to which LoRaWAN enabled devices can connect through to transmit messages to the Internet. These gateways form the bridge between LoRaWAN Class A devices and the TTN back-end. The gateways use broadband networks like Ethernet, Wi-Fi, Fibre or Cellular to connect to the TTN back-end. All Gateways within reach of a device will receive its messages and forward them to The Things Network. The network will keep only a single copy of the duplicate messages received by the multiple base stations. The TTN will then select the best gateway to forward any down-link messages to the device, based on the signal quality of various received packets.

The TTN platform implements a wide variety of open source components (fully compliant with the LoRaWAN 1.1 specification) used to route and handle data [43]. The two core components in the network architecture are The Things Router and The Things Handler. Packets received from the end devices are forwarded from the gateways to one or more Routers as configured by the gateway owner. The Things Gateway is pre-configured with the default router hosted by the TTN foundation, which allows plug-and-play deployment of network base stations. Routers publish the receiver packets on their built-in MQTT broker, which contains MQTT topics for both up and down-link packets. The handlers send and receive packets from routers by subscribing and publishing to their

MQTT brokers. Handlers are responsible for checking message integrity, decryption, deduplication, buffering, transformation and dispatching to application servers. Handlers are equipped with built-in data handling integrations with existing IoT cloud platforms, as well as a customizable API.

## 2.5 NB-IoT

Narrowband IoT (NB-IoT), also known as LTE Cat NB1, uses a subset of the LTE standard and is a cellular network operator supported LPWAN. NB-IoT was developed to meet the new extended coverage requirements in rural and deep indoors locations set by IoT devices, as it provides a higher link budget. NB-IoT supports a lower powered connectivity solution compared to the current GSM standard, and offers multiple years of connectivity for battery driven IoT applications [44]. NB-IoT is supported by more than 30 of the world's largest mobile network operators, who provide coverage for over 3.4 billion customers and geographically serve more than 90% of the IoT market [45]. In September 2015, the 3rd Generation Partnership Project (3GPP) announced NB-IoT as part of its Release 13, promoting the technology as the next industry general use IoT network. NB-IoT can be rolled out on most existing network infrastructure with a firmware change (some require additional hardware), thus it eases the transition for mobile network operators and fast tracks the development of the technology. Network operators have a choice of three NB-IoT deployment options, namely in-band, guard-band or stand alone deployment as can be seen in Figure 2.10. In-band deployment can be undesirable, due to capacity diversion as the 180 kHz NB-IoT spectrum is placed inside the LTE spectrum band. To solve this issue mobile network operators can place the 180 kHz NB-IoT spectrum in the guard-bands (designed to prevent interference). NB-IoT can also be deployed in a standalone band if desired. This is useful when LTE spectrum is still under development.

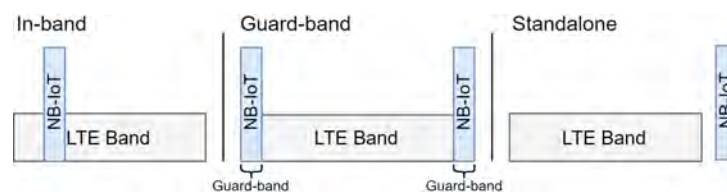


Figure 2.10: NB-IoT deployment options

NB-IoT connects devices more simply and efficiently on already established mobile networks compared to GSM, and is used to handle small amounts of fairly infrequent 2-way data, securely and reliably. NB-IoT utilizes Orthogonal Frequency-Division Multiplexing (OFDM) modulation for down-link communication and Single Carrier-Frequency Division Multiple Access (SC-FDMA) for up-link communications and limits the bandwidth to a single narrow-band of 200kHz. The use of OFDM and SC-FDMA modulation allows the advantage for a single cell to handle billions of connections and thus serving 100k-200k devices[45].

3GPP Release 13 provides the list of NB-IoT frequency supported bands: 1, 2, 3, 5, 8, 12, 13, 17, 18, 19, 20, 26, 28, 66 and Release 14 added the bands: 11, 25, 31 and 70.

Release 15 added further bands: 4, 14 and 71. A study done by GSMA [46] on the NB-IoT Forum suggests that the following bands are currently used by the different regions:

- Europe: B3 (1800), B8 (900) and B20 (800)
- Commonwealth of Independent States: B3 (1800), B8 (900) and B20 (800)
- North America: B4 (1700), B12 (700), B66 (1700), B71 (600), B26 (850)
- Asia Pacific: B1(2100), B3(1800), B5(850), B8(900), B18(850), B20(800), B26(850) and B28(700)
- Sub-Saharan Africa: B3(1800) and B8(900)
- Middle East and North Africa: B8(900) and B20(800)
- Latin America: B2(1900), B3(1800), B5(850) and B28(700)

Since NB-IoT utilizes the licensed frequency bands there is no duty cycle limitations, thus it can offer vastly greater data throughput compared to Sigfox and LoRaWAN. NB-IoT offers a down-link data rate between 0.5 to 200 kbps and an uplink data rate between 0.3 to 180 kbps depending on the network conditions [45]. The advantage of using a licensed frequency band is that output power restrictions are significantly higher compared to the ISM bands. Devices are allowed to transmit a maximum of 33 dBm for the 850/900MHz bands and 30 dBm for the 1800/1900 bands, thus the NB-IoT devices typically transmit messages at 23 dBm (200 mW). This increases the maximum coupling loss (MCL) to 164 dB, which increases coverage, penetration, and power-consumption. This is a major advantage for IoT devices located in deep coverage situations such as in manholes, underground car parks and basements. Lastly, due to the high throughput available it is possible to send Firmware Over-The-Air (FOTA) updates to IoT devices. This is a common requirement in IoT devices, and is not available on the current LoRaWAN or Sigfox networks.

NB-IoT operates in two power-saving modes, Extended Discontinuous Reception (eDRX) and Power Saving Mode (PSM), which together ensure low-power operation to allow battery-powered IoT devices as extensively discussed in [7].

In Active mode, when an NB-IoT device is connected to the network, the network periodically sends messages such as downlink data or a change of system information (paging messages) on its channels, which devices listen for and can respond to. These paging messages are also used by the network to monitor the devices connected to it and occurs quite frequently (every few seconds). These paging messages come at the price of power-consumption as the device effectively needs to be in reception mode constantly.

Extended Discontinuous Reception (eDRX) changes the need for a NB-IoT to continuously check for a paging window, by extending the interval cycle between paging windows up to nearly three hours, thus allowing the device to enter deep-sleep for longer durations. Also, this decreases power-consumption by reducing the time that the device needs to be in receiving mode, while still allowing the device to be reachable by the network when needed, as can be seen in Figure 2.11.

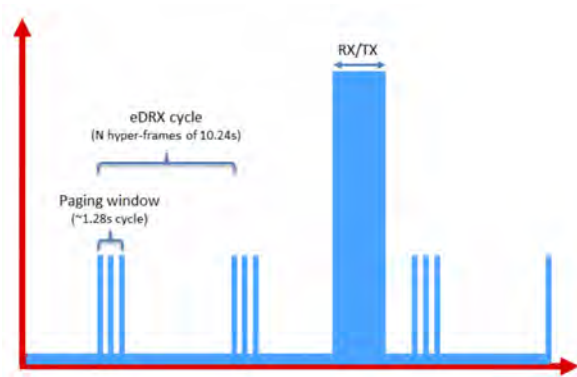


Figure 2.11: Extended Discontinuous Reception for NB-IoT [7]

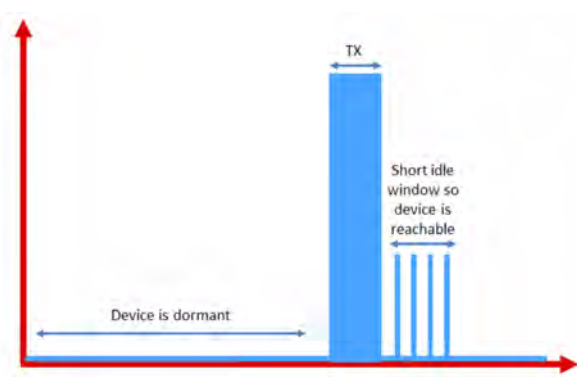


Figure 2.12: Power Saving Mode for NB-IoT [7]

To maximize power-consumption, Power Saving Mode (PSM) enables devices to enter a deep-sleep mode for up to 310 hours when not needed and only wake up to wait for a few seconds to transmit data or receive paging messages from the network, reverting back to deep-sleep mode once the paging/transmission is done, as can be seen in Figure 2.12. As NB-IoT is an evolution of LTE focused on LPWAN and set by the 3GPP standard, it inherits all of the security measures implemented in LTE. The NB-IoT SIM contains a unique key that is used to mutually authenticate the network and the device, and to generate frequently updated session keys for encrypting traffic between the device and deep within the core network.

## 2.6 Other LPWAN solutions

The different alternative LPWAN solutions available on the market today is discussed in this section. The aim is to provide a brief overview as well as investigate the complication of each of these technologies. Less focus is spent on these technologies as some of them tend to be proprietary technology, still under development or either not a viable solution in the context of the problem statement.

### 2.6.1 Weightless-P

The Weightless Special Interest Group (SIG), is a group who develops a open global standard Weightless-P technology to deliver wireless connectivity for low power, wide area networks (LPWAN) specifically designed for the Internet of Things. Weightless-P offers 100% bidirectional, fully acknowledged communications for reliability, which is optimized for the massive LPWAN IoT asynchronous up link dominated communication with short payload sizes (typically  $< 48$  bytes) [47].

Weightless-P utilizes UNB (see Sections 2.1 and 2.3) modulation in a star topology, which offers low power consumption and a typical range of 2 km in urban environments. It uses GMSK and offset-QPSK modulation schemes which deliver optimum power amplifier efficiency. Weightless, similar to LoRa and Sigfox, utilizes the ISM band in order to avoid the high cost of licensed spectrum, however it is able to operate in a variety of sub-GHz frequency bands (e.g. 138 MHz, 433 MHz, 470 MHz, 780 MHz, 868 MHz, 915 MHz, 923 MHz) in order to ensure worldwide support. The technology offers data rates between 0.625 kbps to 100 kbps at a typical transmission power of 14 dBm (up to 30 dBm). [48]

Weightless-P offers flexible 12.5kHz channel assignment to enhances network capacity by enabling frequency reuse in large scale deployments while adaptive data rates permit optimal radio resource usage to maximize network capacity. Time synchronized base stations allows for radio resource scheduling thus promoting optimal utilization. AES-128/256 encryption and authentication of both the terminal and the network guarantees data integrity. The hardware, dubbed the Weightless Ignition Pack, provides Weightless-P network connectivity (gateway and end devices) out of the box, including software protocol stack. The cost is \$1500, which is significantly higher than other solutions. No local open-source support is available for the technology in South Africa [47].

## 2.6.2 WAVIoT

WAVIoT is a Narrowband Fidelity (NB-Fi) based star topology LPWAN network which utilises the sub 1GHz ISM sub-bands. NB-Fi is a proprietary LPWAN protocol that uses DBPSK on physical layer for signal transmission. NB-Fi supports up to 1024 channels with 50 Hz bandwidth each, which translates to up to 300 nodes transmitting simultaneously to a single gateway with a low collision rate. The 50 Hz channel width NB-Fi also translates into a coverage of over 10 kilometres in an urban environment and 10+ kilometres in a rural environments. WAV-IoT supports a minimum effective bitrate of 11 bps, with a 30 seconds average uplink latency and 60 sec downlink. Devices using WAVIoT employ a low-transmit duty-cycle, with a few seconds of transmission (50mA @3.3V current draw) and then ultra-low power sleep mode. WAVIoT gateways can provide an ultra-low -154 dBm receiver sensitivity and can support up to 1 million nodes. WAVIoT gateways can be set-up as different network types: public, private, and enterprise to tailor the customers need. XTEA 256 bit key secures data from the device to server, to ensure that data stays encrypted. NB-Fi provides a full-stack solution offering software from the physical-layer (firmware) up to the application layer. WAVIoT Cloud is a web-based platform that stores all data sent to gateways by devices, which is easily available through either a web-interface or an API [49].

NB-Fi transceiver costs \$4.99, with the firmware for the NB-Fi compatible transceiver costing \$3.0. These cost along with a \$1000 per year solutions provider license (250 device licenses incl.) prohibits the large-scale deployment of this network in South-Africa. The high cost also limits the inclusion of this technology in the scope of the project [50].

## 2.6.3 N-Wave

N-Wave is based on a star-topology narrow-band LPWAN technology operating in the sub 1GHz unlicensed ISM bands. N-Wave utilized this technology to push a large scale smart-parking solution, as N-wave's nodes can cover 10km in urban environments, and 30km in rural. This long range UNB modulation is perfect for parking garages where a large link-budget is needed [25]. Limited support and deployment prevents the commercial scale availability of this network technology in South-Africa

## 2.6.4 INGENU RPMA

INGENU Random Phase Multiple Access (RPMA) INGENU utilizes the 2.4GHz spectrum band as it impose no maximum limit on duty cycle, enabling higher throughput and more capacity than other LPWAN technologies operating in sub-GHz band. Further, 100% duty cycle allows the all messages to be acknowledged, which translates in a

reliable network for critical infrastructure. RPMA allows gateways to achieve up to -142 dBm receiver sensitivity, which translates into a 168 dB MCL. Currently coverage is only available in North-America, although a temporary gateway can be rented from INGENU. Further, the Independent Communications Authority of South Africa (ICASA) limits the output power for 2.4GHz Short-Range Devices (including LPWAN technology) to 10 mW Equivalent Isotropically Radiated Power (EIRP), which is significantly lower than required by INGENU RPMA. Due to the lack of coverage and support in South-Africa, INGENU RPMA does not provide a viable LPWAN solution. [51]

### 2.6.5 Dash7

Dash7 delivers a open standard for ultra low power mid-range sensor and actuator communication known as DASH7 Alliance Protocol (D7AP). D7AP is based on active RFID standards ISO 18000-7 for 433 MHz communication, however it significantly extended. D7AP is built around a so called BLAST (Burst, Light, Asynchronous, Stealth, and Transitional) communication system which enable it to be a LPWAN competitor. D7AP is a full-stack protocol defining the complete OSI model, with support for three sub-GHz ISM bands, and three data rates (9.6 kbps, 55.55 kbps, and 166.67 kbps), as discussed above. D7AP uses the 2-(G)FSK modulation scheme [52] [53]. Dash7 offer no local coverage or support in South-Africa, with development kit starting at R4500

## 2.7 Comparison of the different solutions

The four major wide-area massive IoT networks can be partially summarised with Table 2.5, which provides a broad comparison in term of the performance of the different networks. Based on the data in Table 2.5 and the research in Sections 2.1 to 2.5, it is important to draw a direct theoretical comparison in terms of range, power-consumption, throughput, down-link latency and interference immunity.

### 2.7.1 Power-consumption

Power-Consumption in LPWAN is mostly dependent on the transmission duty cycle and network conditions, however the difference in power-consumption between the different technologies can be evaluated due to the underlying differences in modulation, transmission power and MAC-layers. GSM/GPRS is not classified as a LPWAN technology due to its poor power-consumption. GPRS requires the network to constantly page a device, which forces the end-device to be active and in receive mode which translates to decreased battery life. Transmission power can reach up to fifty times the current compared to LoRaWAN and Sigfox [54] [55] [56]. LoRaWAN's power-consumption is dependent on the SF used, as it determines the time-on-air as explained in Section 2.4.4. LoRaWAN and Sigfox perform similarly in peak current-consumption during transmission, with both technologies being able to provide 10 years battery life from a 5Wh battery (application dependent), due to the low packet-overhead. NB-IoT's power consumption is typically higher compared to LoRaWAN and Sigfox, due to infrequent but regular base station synchronization and OFDM or FDMA requires a higher transmission peak current. NB-IoT relies on a transmission power up to 23dB to enable its high link budget, compared to the 14dB limit of LoRaWAN and Sigfox.

Table 2.5: Comparison of the different wide-area massive IoT networks

Technology	LoRaWAN	Sigfox	NB-IoT	GPRS
Topology	Star	Star	Star	Star
Max data rate	27 kbps	100 bps	50 kbps UL, 60 kbps DL	115 kbps
Frequency Band	434 MHz/868 MHz	868 MHz	850 or 900 1800/ 1900 MHz	850/900/1800/ 1900 MHz
MCL	157 dB	160 dB	164 dB	148 dB
Bandwidth	125 kHz,250 kHz 500 kHz	100 Hz	192 kHz	200 kHz
Modulation Technique	Chirp-spread spectrum	BPSK	QPSK	GMSK
Nodes per gateway <sup>1</sup>	>1,000,000	>1,000,000	52,000	52,000
Proprietary	Physical layer	Physical and MAC layers	Full-Stack	Full-Stack
Message encryption	AES	Optional	3GPP (128- 256bit)	3GPP (128- 256bit)
Network operators (South-Africa)	Private (TTN), FastNet	SquidNET	MTN, Vodacom	MTN, Vodacom Cell-C, Telkom
Deployment	Early stages of deployments	Commercial	Early stages of deployments	Commercial (sun-setting)

1. Based on [25]

## 2.7.2 Range

Another major advantage of LPWAN technology is the long range which translates to fewer infrastructure needed to cover distributed devices in a large area than is required by GPRS networks. In highly networks with high end-device densities, more gateways is still needed, and devices need to limit transmission power to limit the amount of end-devices per gateway. Theoretically LoRaWAN achieves a maximum 5 to 10 km urban and 15-30 km rural range [57], Sigfox achieves maximum 10 km (urban), 40 km (rural) while NB-IoT only reaches a maximum 1 km (urban) and 10 km(rural)[20]. GSM is limited to a maximum range of 35 km due to the timing frames defined in the 3GPP technical specifications, however GSM signal is typically limited to 2-6km in urban environments [26].

## 2.7.3 Throughput

Throughput in wireless communication systems is defined as the rate of successful data delivery in a specific time period. Typically, throughput is advertised as an amount of a certain size packets that can be transmitted per time period. Throughput in LPWAN is dependent on the frequency bands used. LoRa and Sigfox utilizes the ISM frequency bands which limits the transmission time-on-air to 1% duty-cycle. This limits Sigfox's throughput to 1680 bytes per day up-link and 16 bytes per day down-link. LoRaWAN's throughput is dependent on several limiting factors; SF, bandwidth, CR and packet size. Further investigation is needed to identify the general throughput available to LoRaWAN end-devices. As NB-IoT and GSM operate in the the licensed spectrum, there are no throughput restrictions. NB-IoT and GSM end-devices' throughput is limited by their transmission speed and network-conditions. Shannon's law proposes a maximum theoretical formula to calculate the maximum theoretical throughput in a noisy environment. Shannon's law state that the maximum bit rate ( $C$ ) in bps, is dependent in the bandwidth



(BW) in Hz and the signal-to-noise ratio (S/N, not in dB), as can be seen in Equation 2.3. The maximum bit rate is highly dependent on the channel noise, thus a high density channel will result in lowered maximum throughput. Implementing Shannon's law to determine the maximum worst-case data rate of the tested IoT networks, can be seen in table 2.6.

$$C = BW \times \log_2(1 + S/N) \quad (2.3)$$

Table 2.6: Shannon maximum theoretical bit rate

Technology	Minimum SNR (dB)	Bandwidth (kHz)	Shannon max data rate (bps)
Sigfox	8 [1]	0.1	287
LoRa (SF 12)	-20 [23]	125	1794
NB-IoT	-12.6 [73]	180	15865
GSM	4 [56]	200	361470

### 2.7.4 Down link latency

In wireless communication low-latency two-way connection (end-device can send and receive packets nearly instantaneously) is often assumed. However, in LPWAN systems, the gateway to device communication is often reduced to specific time slots (increasing the latency), to reduce receive mode power consumption. Due to the asynchronous nature of LPWAN, down-link latency is dependent on the users application's transmission duty cycle, as down links typically occur after a successful transmission. GSM typically has no down link latency, as GSM requires devices to constantly listen for paging requests. NB-IoT performs the best in the LPWAN class, due to the need for infrequent but regular base station synchronizations, which allows lower (compared to LoRaWAN and Sigfox) down link latency. Although LoRaWAN class-C devices allow for no-latency and class-B for reduced latency, these classes are rarely implemented due to their higher power consumption, and not included in the scope of the comparison in this thesis.

### 2.7.5 Interference immunity

As typical LPWAN technologies operate in the ISM bands, they offer no gateway message acknowledgements and the bands contains noise from other applications. As shown in Section 2.3, Sigfox offers interference immunity through time- and frequency diversity and UNB modulation, while LoRaWAN offers interference immunity through being able to receive messages up to 20 dB below the noise-floor as explained in Section 2.4.4. LoRaWAN's LoRa modulation technique allows orthogonal demodulations, which enables packets with varying SF's to be demodulated simultaneously on the same channel. Further as both of these technologies transmits messages which is received by multiple base stations, the geographical distribution enables a higher interference immunity. NB-IoT relies on UNB modulation and along with GSM licensed spectrum to reduce the amount of noise in the channel and allow message acknowledgement.

## 2.8 Application metrics

This section investigates common metrics which typically affect the deployment of LPWAN devices in practice. The aim is to investigate these metrics to ensure a thorough

understanding of factors which might affect performance experiments. Moreover, these metrics will be practically investigated, as this will aid real world deployment of these communication technologies.

### 2.8.1 Antenna Performance

Antenna performance will play key role in evaluating the different communication technologies. To the select an appropriate antenna, radiation pattern, density and intensity, directivity, antenna gain, efficiency, bandwidth and polarization were considered. Antenna theory is vastly complex, and a basic understanding of the fundamental concepts is needed to investigate possible antennas for a wide area massive IoT network.

In practice, it is crucial to design an antenna with a quarter of a wavelength of the transmitting frequency's wave length ( $\frac{\lambda}{4}$ ), as this ensures the optimal resonance, thus increasing the antenna efficiency. An antenna with a quarter wave length should not reflect any power back to the transmitter, thus it will have a low Voltage Standing Wave Ratio (VSWR). The VSWR of an antenna can be defined as Equation 2.4, where  $V(max)/V(min)$  and is the maximum/minimum voltage along transmission line/antenna.

$$VSWR = |V(max)|/|V(min)| \quad (2.4)$$

A low VSWR (minimum VSWR is 1.0), indicates the antenna is matched to the transmission line and power delivered to the antenna is maximized.

#### 2.8.1.1 Gain and directionality

Antennas are passive components that do not contain any power sources or amplifiers. Gain can only be achieved by focusing the radiated power in a directive beam. Antennas with more gain have a narrower radiation angle, focusing the radiated power more, while low gain antennas allows for a more uniformly transmitted pattern. Receiving antennas with a high gain will add more gain than a lossless isotropic (ideal antenna that radiates its power uniformly in all directions) antennas to signals coming certain angles, while delivering minimal gain from other angles. A generalized overview of different antenna types can be seen in Table 2.7.

Table 2.7: Overview of main antenna types categories used in wide-area massive IoT solutions

Antenna type	Gain (dB)	Horizontal Beam-width (deg)	Vertical Beam-width (deg)	Ref
868 MHz Stubby	2.2	Omni	Omni	[58]
GSM Yagi	11	90	60	[59]
GSM Panel	11	120	36	[60]
Dish (5.1-5.9GHz)	30	5.8	5.8	[61]

#### 2.8.1.2 Polarisation

In order for the device or base station to receive the maximum power, the receiving antenna's polarization must be in the same orientation as the transmitting antenna's orientation. The theoretical loss due to misaligned antenna polarization can be calculated

with Equation 2.5, where  $\theta$  is the polarization mismatch angle between the antennas [62].

$$PolarizationMismatchLoss(dB) = 20\log(\cos(\theta)) \quad (2.5)$$

At a  $90^\circ$  angle (transmitter perpendicular to receiver) the receiving antenna should receive none of the transmitted power, due to the infinite polarization mismatch loss. In real world use cases, antennas used in IoT applications produces a field with polarization in more than one direction, as the end device will not be always in the correct orientation. In the case of multi-path signals; if the signals are reflected off objects that are not aligned or parallel with the polarization of the incident signal, the reflected signal will undergo a polarization shift. In general IoT use cases there will be several signals arriving at the receive node that are aligned with the polarization of the receiver antenna, even though the transmitting antenna is at a perpendicular angle, due to the reflection of the signal. A circularly polarized antenna can be used, however this will result in a constant 3dB loss, as opposed to a possible gain of a horizontally or vertically polarized antenna [62].

### 2.8.1.3 Antenna Types

Considering the antenna performance, gain, directivity and polarization, five different antennas were chosen to be tested. Dipole and Helical type antennas were chosen due to their simplicity, directionality, gain, cost and versatility. IoT devices tend to be used in a variety of situations where the devices have no guarantee in which orientations or direction it will be operated, thus a omni-directional antenna is chosen to provide the best general use results. Three different 868MHz optimized antennas were tested as well as two additional GSM-band optimized antennas. The antennas tested can be seen in Figure 2.13, which includes #1, 2.2dBi straight stubby antenna 868MHz based on a helical design, #2 3dBi 868MHz Helical stub antenna with 90deg connector, #3 3dBi Dipole 868MHz antenna, #4 0.5dBi Dipole GSM antenna and #5 3dBi GSM Helical stub antenna with 90deg connector. The corresponding antenna metrics as listed in the antenna's data sheets can be seen in Table 2.8.



Figure 2.13: Different types of antennas tested

Table 2.8: Summary of different antenna's data sheets

#	Frequency Range (MHz)	Gain (dBi)	VSWR	Polarization	Impedance ( $\Omega$ )
1	868	2.2	<2.0	Vertical	50
2	868	3	<1.5	Vertical	50
3	868	3		Vertical	50
4	790-2690	0.5		Vertical	50
5	850-1900/2100	6	<2.0	Vertical	50

To verify the theoretical performance of the chosen antennas, the antennas were tested with a network frequency analyzer to determine the optimum frequencies of the different antennas. Moreover, to determine the directivity (measure the gain in the vertical axis) of the omni-directional antennas, tests were conducted in an anechoic testing chamber. During the testing, it was found that the optimum VSWR of the antennas are not exactly at the rated frequency and that the radiation pattern of the antennas does not correlate entirely with the theoretical doughnut shape of dipole and helical antennas. The results can be seen in Appendix A.

## 2.8.2 Link budget and path loss

The link budget is a term used to describe the equation that is used to calculate expected received power. This accounts for all losses and gains between the transmitter and receiver, which includes cables, amplifiers, antennas, free-space losses, propagation losses etc. The link budget can be used to predict the the maximum coupling loss, which can be used to predict the range for a specific receiver sensitivity.

$$P_{Rx} = P_{Tx} + G_{Tx} + G_{Rx} - L_{FS} - L_{Tx} - L_{Rx} - L_M \quad (2.6)$$

Equation 2.6, describes the link budget calculation in dBm, where  $P_{Rx}$  and  $P_{Tx}$  is the received and transmitted power,  $G_{Rx}$  and  $G_{Tx}$  is the receiver and transmitter antenna gain,  $L_{Rx}$  and  $L_{Tx}$  is the receiver and transmitter losses (coax, connectors, etc.) respectively,  $L_{FS}$  the free-space path loss, and  $L_M$  the miscellaneous losses. The miscellaneous losses include refraction, reflections, diffraction, multi-path fading and obstacle attenuation. The free-space loss,  $L_{FS}$  (dB), can theoretically be calculated from Equation 2.7, where  $f$  describes the signal frequency in MHz and  $d$  the distance between transmitter and receiver in km [57].

$$L_{FS} = 34.2 + 20\log(f) + 20\log(d) \quad (2.7)$$

The free-space path loss calculation assumes a theoretical model, with no miscellaneous losses taken into account. The perfect modeling or control of path loss is impossible [63], therefore it is important to understand the variables that will influence it. The following sections provide a brief overview of different path loss variables and how to control these variables in experimental testing.

### 2.8.2.1 Refraction

Similar to light, refraction occurs in electromagnetic waves. The direction of electromagnetic wave changes while moving from one refractive index to another. The angle of incidence and the angle of refraction are linked by Snell's Law. For electromagnetic waves, a sudden change in direction due to refraction is an uncommon occurrence, however

a gradual change in direction can be expected. Weather conditions can drastically change the refractive index, thus it is important to conduct comparative tests in a controlled environment where weather conditions stay constant.

### 2.8.2.2 Reflections

Reflections caused by either man-made or natural objects (often large wet-areas or large metallic surfaces) are prone to cause a reduction in signal quality due to the effects of multi-path fading. Multi-path fading occurs in any environment where there are multiple reflections from objects, which creates multiple paths for a signal to travel between transmitter and receiver. The reflection of a horizontally polarized signals produces a  $180^\circ$  phase shift, while a vertically polarized signal's phase shift is dependent on the incident angle and reflection surface. As the signals all have different path lengths, and thus different phases, they will either add or subtract from the received signal dependent upon their relative phases. The multi-path fading effects of reflections can be mitigated in communication systems through the use of space- and frequency diversity techniques. The effects of reflections need to be kept into account when conduction signal quality experiments, thus the environment needs to be kept constant during experimental tests.

### 2.8.2.3 Diffraction

Electromagnetic waves propagate similar to light, thus the electromagnetic signals are prone to diffraction at collision with an obstacle, as proven by Huygens-Fresnel diffraction principle. At a point of diffraction (around an obstacle), every point of the wavefront is a secondary source of transmission. To determine the effect of diffraction due to an obstacle in the path of a radio-signal, the path first needs to be defined. The Fresnel Zone is the area around the visual line-of-sight that radio waves propagate into after transmission. The width of the Fresnel zone is dependent on the distance between the transmitter and receiver and frequency. Obstacles in the Fresnel zone introduces diffraction, which causes signal attenuation [64]. 20% Fresnel zone blockage introduces little signal loss, with significant signal loss occurring beyond 40% blockage. To maximize the link budget and ensure good network coverage it is ideal to install base stations on the highest point possible site as illustrated in Figure 2.14. Device 1 and 4, will suffer no significant diffraction, as there are no obstacles in the Fresnel zone, while device 2 (50% blockage) and 3(100% blockage) should experience significant diffraction losses.

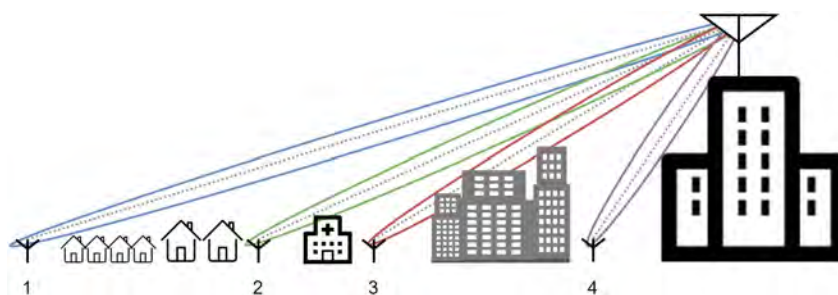


Figure 2.14: The Fresnel zone in communication systems

Tests should be conducted in environments that are clear of obstacles to minimize the diffraction losses and ensure the accuracy of the data. The diffraction losses due to an

obstacle in the Fresnel zone can be theoretically calculated, however it is beyond the scope of the work presented here.

#### 2.8.2.4 Object attenuation

Scattered objects in the immediate foreground of a transmitter, such as buildings, cars and trees, can cause a significant signal quality loss. This loss can be calculated theoretically, however this is beyond the scope of the presented work. Material penetration is highly frequency dependent operating at a lower frequency will improve link budget and range expectation [65]. In practice, signals tend to reflect from solid metal structures, while signals can pass through other types of materials with an attenuation penalty. Figure 2.15 shows typically expected attenuation values which is experienced by a GSM system at 900MHz. Obstacle attenuation needs to be considered while conducting signal quality tests and careful RF planning needs to be considered when installing devices in an indoor environment.

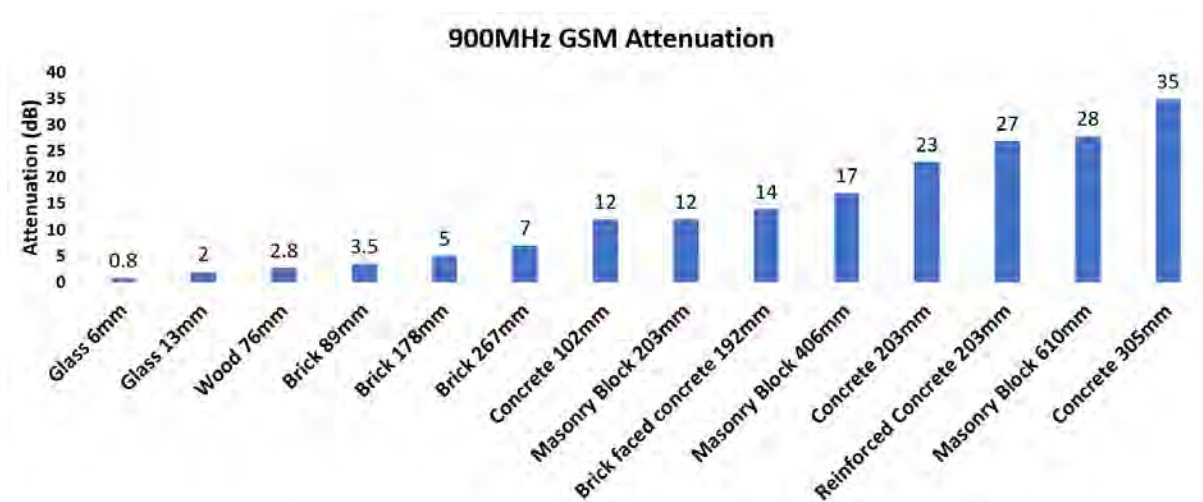


Figure 2.15: 900MHz GSM signal attenuation [8]

### 2.8.3 Near field interference

Placing an antenna of a wireless device in the reactive near-field of a large object, can cause electromagnetic coupling between the antenna and the object. The reactive near field of an antenna is defined as the region up to  $\frac{\lambda}{2\pi}$  from the antenna (5.5cm @ 868MHz). The electromagnetic coupling is able to detune an antenna, thus affecting critical antenna parameters such as impedance, efficiency, radiation and polarization characteristics, examples shown in [66]. The detuning of an antenna due to near-field interference, can cause an impedance mismatch, which will relate in a reduction of radiated power. The loss of radiated power results in a loss of link budget (therefore decreased signal performance), which can be compensated for through increasing the radiated power at the cost of battery life. An experiment by [9], can be seen in Figure 2.16, where in free-space the antenna is correctly tuned at 433MHz with a return loss of close 30dB, tested using a vector network analyser. When the antenna is then placed on the human wrist, touching the skin, the resonant frequency changes to 363MHz with almost 30dB decrease in return loss at 433MHz, representing a large impedance mismatch with a VSWR of nearly 8.

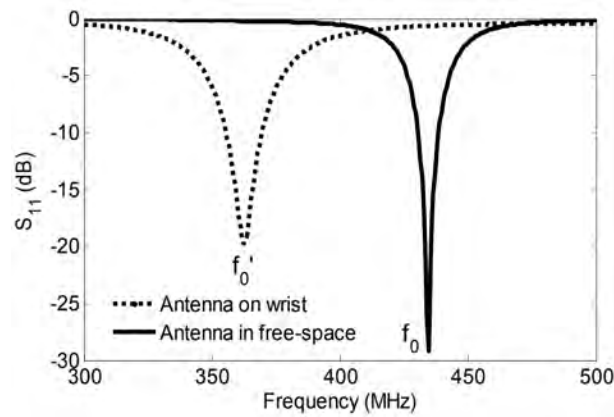


Figure 2.16: 433MHz antenna detuning [9]

### 2.8.4 Transmission power

Transmission power in wide-range massive IoT system is a trade-off between frequency-band regulation, link-budget and power consumption. A in depth analysis of transmission power vs. link budget is conducted in Chapter 4. it is important to maintain a constant maximum transmission power in RF signal quality tests in order to compare the best case scenario for each type of communication technology. In most applications (battery-life dependent) it is preferred to allow an IoT device to operate at maximum transmission power as this will maximize the link budget and therefore decrease the packet reception error margin.

## 2.9 Conclusion

Developing an IoT solution requires an in-depth investigation since the physical and protocol layers of the different solutions vary drastically. This literature study presents the theoretical advantages and drawbacks regarding the physical-layer, MAC-layer and architecture of the different wide-area massive IoT networks, since it is clear that there is no single solution for all IoT applications. To fully understand and evaluate the four major wide-area massive IoT networks, Sigfox, LoRaWAN, NB-IoT and GSM, the performance and practical application needs further practical evaluation. Using these results, recommendations can be made regarding the most applicable technology in certain use-cases. Lastly, the deployment, commercial usage and business model are also crucial factors to consider, as these devices are developed to work 10+ years, thus network sustainability needs to be viable.

# Chapter 3

## Methodology and Research Design

Wide-area massive IoT networks are used in a wide variety of applications, such as smart-parking, utility measuring, infrastructure monitoring, asset tracking *etc.* Therefore, it is crucial to develop a test system that can be used specifically to investigate the communication layer of these applications. The general testing methodology used to test the performance and application metrics is described. The methodology sets the baseline requirements for the test devices to be developed. Accordingly, the requirements and specifications of a generic communication test system are defined, which are used to investigate commercially available solutions. A final series of test devices, a back-end system and accompanying testing hardware is proposed, which can be used to investigate LoRaWAN, Sigfox, NB-IoT and GSM. Therefore, the hardware design is defined, followed by the accompanying firmware and software design.

### 3.1 Performance testing methodology

To ensure a fair and comprehensive comparison of the different communication technologies, a test methodology needs to be designed to effectively compare their performance characteristics. This section describes the general testing setup used to test the different metrics accordingly. Tests regarding LoRaWAN is done using SF7 and S12, as this shows the two extreme use cases of LoRaWAN.

#### 3.1.1 Link budget

This investigation aims to determine the maximum coupling loss of the different technologies in practice. The limit is determined by testing the packet delivery ratio (PDR) of the different technologies at different received power (RSSI) levels. Using the information analysed from this test, the practical maximum coupling loss of the different communication technologies is calculated. The maximum coupling loss can be used to compare the theoretical range of the different technologies. The major drawback of LPWAN technology is the limited bandwidth in the 868 MHz ISM band due to the 1% duty cycle limitation. Acknowledgements of uplink messages is thus extremely limited. Therefore, the packet delivery ratio and maximum coupling loss of each technology is of utmost importance when implementing these solutions. In the experiment, 50 12-byte messages are transmitted by the various devices at 7 different RSSI levels, ranging from -90 dB to -150 dB in -10 dB increments. The devices are placed at different locations relative to the base stations to ensure a variation in the RSSI levels. Pre-test messages are sent



to ensure that the device is operated at the correct RSSI level and that the RSSI level stay within 2% accuracy. The messages are sent every 20 seconds and the antenna and test devices stays consistent for all measurements. The results are analysed to ensure a consistent RSSI level during the test.

### 3.1.2 Power-consumption

The power-consumption of the different communication technologies vary drastically, therefore various measurement approaches are used. Practical testing based on measuring the battery life duration of each test system is considered. However, due to the battery capacity, regulator efficiency and battery discharge rate variables which are difficult to control, this testing method is not practically possible. Therefore, the aim is to determine the transmission, receive, idle and sleep-mode power-consumption profiles of the different modems in general IoT use cases. This is done through the development of a high resolution and high sampling rate power-consumption profile logger that is discussed in Section 3.7. The practical results are used to predict battery life duration on an ideal battery. The power measurements and modelled ideal battery life is compared to the theoretical power consumption in Chapter 4.

### 3.1.3 Throughput

To compare the different throughputs available to the different technologies, a test is designed to measure the number of bytes that can be transmitted per day. To measure the throughput of LoRaWAN, the different SFs, packet-sizes and the receive window times needs to be measured. Using the measured data, the throughput per 24h time period with regards to the duty-cycle limitation can be calculated. As Sigfox has a set throughput per 24h time period, the maximum sequential throughput need to be calculated by measuring the data-rate. Since NB-IoT and GPRS's throughput is only dependent on the transmission data-rate and network conditions, throughput tests will be based on the maximum sequential transmission rate. NB-IoT's throughput will be measured by measuring the transmission time of the modem per sent data packet. Although this test, does not signify the maximum data-rate, it determines the practically implemented maximum throughput of the technology.

### 3.1.4 Scalability

Due to the drastic differences between the medium access (MAC) layers used by various radio communication technologies, different approaches are used to determine the scalability of the technologies.

#### 3.1.4.1 NB-IoT and GSM scalability

Since NB-IoT uses OFDM and SC-FDMA modulation and GSM is based on CDMA technology, modelling or testing the scalability of a cell is beyond the scope of this project. The scalability of a NB-IoT cell is based on theoretical research, which estimates a single base station can support up to 55000 end-devices per cell [21]. Similarly, current literature estimates GPRS technology can support up to 52000 end-devices per base station.

### 3.1.4.2 LoRaWAN scalability

Currently, LoRaWAN and Sigfox devices can transmit asynchronously, since no listen-before-talk (Asian and Korean bands do however support this feature) or multiple access scheduling methods are implemented. However, these devices are duty-cycle limited, which allows the channels to be free for use by other end-devices, therefore enabling scalability. Practically testing the scalability is not feasible, as the number of sequentially transmission scheduled devices needed to saturate channels would be more than 100 devices (1% duty cycle limitation per device). A study by Adelantado et al. in [24], models the PDR of a varying number of LoRaWAN nodes transmitted packet per hour per node vs. the received packets/hour per node. The study concluded that scalability in a LoRaWAN network is relatively low, with a PDR of 14.01% for 250 end devices transmitting 2620 10 byte packets per hour each, and suggested implementing TDMA in a LoRaWAN network. However, the study does not clearly define the PDR at different spreading factors. The study by Bor et al. in [67], uses experiments to develop models describing LoRa communication behaviour. These models are used to parameterise a LoRa simulation to study scalability. The study concluded that with a typical LoRaWAN setup (SF12, 125 kHz bandwidth, CR 4/5), with each node transmitting a 20 byte packet every 1000s and a PDR of greater than 90% required, a single gateway can support 120 devices.

A theoretical scalability estimate can be calculated based on the literature review. A LoRaWAN device is allowed to transmit at a 1% duty cycle, therefore the probability of a single device transmitting on any channel,  $P_{trans}$  is given by Equation 3.1. The probability of any number,  $N$ , of device transmitting at any give time,  $P_n$ , is given by Equation 3.2.

$$P_{trans} = 0.01 \quad (3.1)$$

$$P_n = N \times P_{trans} \quad (3.2)$$

As LoRaWAN allows devices to transmit randomly on up to any of the 8 available channels, the probability of any number of devices transmitting at any given time,  $P_{nc}$ , on a single channel (with  $C$  as number of channels) is given by Equation 3.3. As the LoRaWAN network is based on the pure unslotted ALOHA protocol [24](whenever a device has a frame to send, it simply transmits), the packet error probability,  $P_{err}(N)$ , for  $N$  devices can be calculated using Equation 3.4.

$$P_{nc} = \frac{N \times P_{trans}}{C} \quad (3.3)$$

$$P_{pdr}(N) = e^{-2\frac{N \times P_{trans}}{C}} \quad (3.4)$$

To validate Equation 3.4 a python LoRaWAN simulation model is developed to predict the number of packet errors depending on the network's density. The simulation is used to model a single LoRaWAN gateway supporting a various number of up-link centric nodes. The base station can receive multiple packet concurrently on different channels, and it is assumed that the base station does not transmit any message acknowledgements or down-link messages. The model simulates a defined number of devices' transmissions with random transmission start-times, a constant transmission duration and random channel selection. The model then counts the number of packet collisions occurring. In any packet overlap cases the both packets are regarded as a missed packets. In practice, packets overlaps might not result in packet loss, as the co-channel rejection and capturing

effect is not calculated in this simulation. The results, seen in Figures 3.1 and 3.2, verifies the accuracy of Equation 3.4.

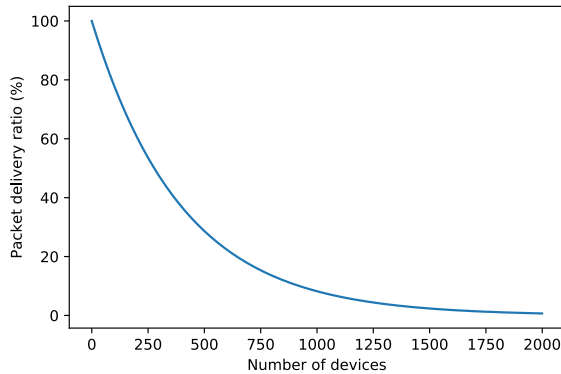


Figure 3.1: LoRaWAN packet error rate at 1% duty cycle transmitting on 8 channels, theoretically calculated from Equation 3.4

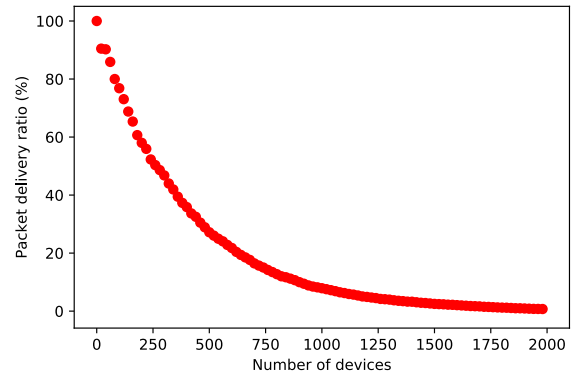


Figure 3.2: LoRaWAN packet error rate at 1% duty cycle transmitting on 8 channels, practically simulated

Figures 3.1 and 3.2 indicates a relatively low scalability of a LoRaWAN system transmitting at its full 1% duty cycle. To adapt the Python model to typical real world applications, the simulation is adapted. The real-world simulation assumes each device transmits a single 12-byte packet at a random time in the simulation at a constant SF. The transmission start time of the devices are randomly uniformly distributed between 0 and 1000 seconds. Each device is allocated a random RSSI level, simulating devices' received power in real world use cases. Practical testing indicated that the devices transmit the packets on a random channel, with 3 channels allocated to SF7 and 8 channels allocated to SF12. The simulation assumes devices follow the same channel selection behaviour. The real-world simulation assumes at a collision, the packet with the lower RSSI value is lost. The simulation is repeated 5 times to average the error values.

### 3.1.4.3 Sigfox scalability

Currently, there is no literature available that specifically focus on the scalability of a single Sigfox base station. According to Sigfox in [1], a single base station can support 270 devices transmitting concurrently, while ensuring a PDR of 99.9%. As Sigfox uses UNB modulation, it allows devices to transmit in 100 Hz channels uniformly distributed in its 200 kHz spectrum. This enables a vast number of devices to transmit concurrently, without transmitting on the same frequency channel. The addition of three frequency diverse frames to transmit a single message further increases the scalability, as shown in Figure 3.3. A simulation is designed to calculate the number of Sigfox devices transmitting concurrently. The simulation assumes the devices are transmitting at the maximum allowed 12-byte message length. The simulation further assumes that all devices transmits the single messages at a random time uniformly distributed between 0 and 1000 seconds. As a Sigfox packet is required to be at least 8dB higher than the noise around it to be received, a sufficient guard band is needed between two signals, to prevent interference. This is not considered in the simulation, as an ideal situation, with no power beyond

the 100Hz UNB, is assumed. The simulation aims to indicate the maximum number of devices supported by a single gateway while still ensuring a PDR of 99.9%. 70000 devices are simulated to calculate the average number of Sigfox devices transmitting concurrently for varying number of devices.

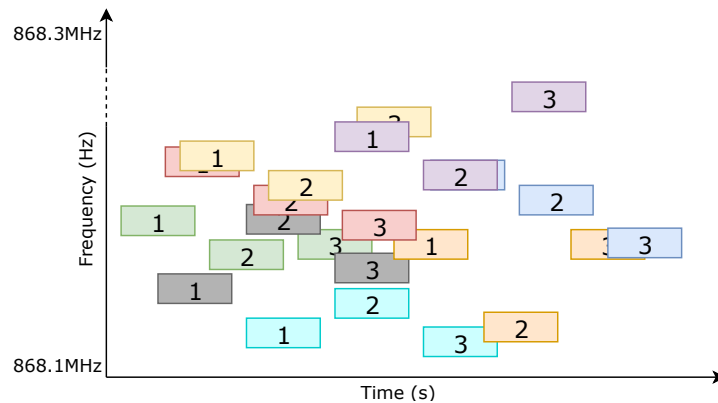


Figure 3.3: Sigfox devices transmitting three frames with frequency and time diversity

## 3.2 Application testing methodology

This section describes the methodologies used to evaluate the metrics that influences the performance of end devices in real world use cases. Through examining these metrics, recommendation can be made on how to design and deploy IoT devices which utilizes the different technologies.

### 3.2.1 Antenna

A theoretical overview of the different antennas that will be evaluated is provided in Section 2.8.1 along with the discrete antenna tests provided in Appendix A. As Sigfox and LoRaWAN operate in the ISM band and GSM and NB-IoT operate in the licensed cellular bands, the frequency variation should correlate to the antenna's designed optimum frequency. To compare the different antennas, an experiment is used, in which devices are kept in a constant base station line of sight signal environment. The antennas of the different devices are changed and measurements of the RSSI of each antenna is recorded. This practical testing will then be compared to discrete antenna tests to evaluate an ideal antenna for each technology. Tests are performed in a line of sight environment, 200m away from the LoRa and Sigfox base station and 2km away from the NB-IoT base station, in order to minimize external factors, such as far field interference, to affect the performance of the devices. As the Sqwidnet network offers several base stations around the testing area, the average RSSI to different gateways at different distances is measured, as this helps to highlight the effect of the antennas. GSM test are performed in a random outdoor environment, since access to the coordinates of GSM base station locations is impossible. In order to ensure accuracy five, 12-byte messages will be sent and the average RSSI level calculated. All measurements are recorded with the antennas in the same vertical orientation to eliminate the effects of polarization and exactly the same position to ensure the accuracy of the test.

### 3.2.2 Polarisation

Since effects of a polarisation mismatch is reflected in the drop of signal quality, tests are conducted practically. Tests of the different technologies needs to be done line of sight in order to reduce the effects of multi-path fading. A baseline signal quality measurement is done with an omni-directional antenna. The same measurement is done, however, the device is rotated 90 degrees perpendicular to the receiving antenna. The results is then compared to determine if the polarization effect is as large as theoretically calculated. The effects of polarisation were tested through transmitting 20 messages from each type of communication technology (except GSM) in a controlled environment for parallel and perpendicular antenna orientation. An average baseline (parallel) RSSI value was recorded for each type of technology within an environment where the objects between the transmitter and receiver stayed constant (keep multi-path interference constant). A vertically polarized 3 dBi dipole 868 MHz omni-directional antenna is used. As Sigfox, LoRaWAN and NB-IoT have gateways in the same location, it is a fair comparison of the different types of technologies in terms of polarization as multi-path interference stayed constant. The GSM base station location is not known, therefore GSM is not included, as multi-path interference will affect the test. The tests were then repeated for perpendicular polarisation in the same environment and with the same antenna.

### 3.2.3 Near-field interference

LPWAN and GSM modules are prone to be used in various operating conditions, mounted in water and dust proof casings in non-ideal locations. The mounting of these devices tend to influence the RSSI level, due to interference caused in the near-field as indicated in Section 2.8.3. Effects of near-field interference is tested by conducting a base-line test in a controlled environment and then adding different objects directly against the antenna, causing near-field interference. The testing environment is kept constant during the complete experiment, and the interfering object is placed out of the line-of-sight to test the effects of antenna detuning and not interference in the line of sight. Theoretically, there should be no difference between the different technologies, as the antenna-detuning will only increase the amount of transmitted power reflected to the transmitting module (changing the VSWR). To simulate the devices being used as a wearable, a human wrist is placed directly against the antenna, similar to a smart watch. Further, a 5x5x1cm wood and metal plate is also introduced independently to test the effect of placing an antenna close to the different types of materials. Lastly, the effect of placing the antenna directly against a commonly used 5x10x4cm PVC plastic enclosure was tested, as this simulates the most common type of near-field interference affecting the devices. The 3 dBi Dipole 868 MHz antenna is used in the tests, as the anechoic testing chamber indicated that it provided the optimum omni-directional spreading pattern.

### 3.2.4 Transmission power

Testing the effects of varying the transmission power of the devices, consists of two parts; testing the transmitted power vs. the received power and measuring the transmission currents at different transmitted powers. Testing the transmitted power vs. the received power is achieved by placing the devices in a constant signal environment and changing the transmitted power and measuring the received power by the base stations. GSM and NB-IoT are excluded from this test, as their transmission power is variable and set by the

the network, depending on the current received signal quality. The power-consumption of LoRaWAN and Sigfox is measured at varying transmitted powers, following the same procedure as described in Section 3.1.2. Using these results together with the performance results will allow IoT device manufacturers to better optimize end-devices for battery driven applications.

### 3.2.5 Path-loss

Path-loss prediction is a critical component of LPWAN technologies. An experiment is conducted to measure and model path-loss in a semi-urban environment. Specifically, LoRaWAN and Sigfox is modelled as these technologies offer no message reception acknowledgement, therefore a theoretical path loss calculation could prove useful in base-station/device placement planning. To accurately model the theoretical path loss for the different communication technologies, the theoretical free-space path loss model is compared with practical path-loss results. Comparing the measured path loss to the theoretical free-space path loss, should provide a relative off-set value. Theoretically, this off-set value can then be used to model the actual path-loss. The practically measured path loss is calculated with the link budget equation, with miscellaneous losses assumed to be 0dB, and the receiving antenna's gain as 2dB. Practical path loss measurement tests will be performed using a test device equipped with a omni-directional 3 dBi dipole 868 MHz antenna mounted vertically on a car's roof rack. The device will be driven around in the Stellenbosch semi-urban environment and the GPS and RSSI for each specific testing point needs to be logged to a database. Devices' transmission power was kept constant at 14dBm. The RSSI measurements for each coordinate will be deducted from the RSSI level of the transmitted coordinate packet, measured by the receiver.

### 3.2.6 Coverage

A coverage map of the testing area for various communication technologies will examine the state of network deployment. Although this test will not be representative of network deployment globally, it should highlight the deployment status in Stellenbosch. The coverage map along with the expected PDR (investigated in Section 4.1.1) can also give the user an idea of what outage probability they might expect. Mapping the coverage of the testing area is achieved by following a set route and mapping the signal quality of the various communication technologies at several coordinates.

To plot the coverage maps of the different technologies, sample test messages were sent at random locations across the semi-urban town of Stellenbosch. The GPS coordinates and signal strength of the messages was then saved and logged to the coverage maps. As Sigfox coverage is provided by Sqwidnet South-Africa, there are several base stations covering the testing area, however the locations of the base stations are confidential. LoRa coverage is only provided by two DIY base stations, one located in the centre of the testing area while the other is 3.3km outside of the main focus area. GSM coverage is provided by the local cellular network operator MTN who owns an undisclosed number of cellular base stations at unknown locations. NB-IoT coverage is provided by MTN, with a single base station in the centre of the testing are.

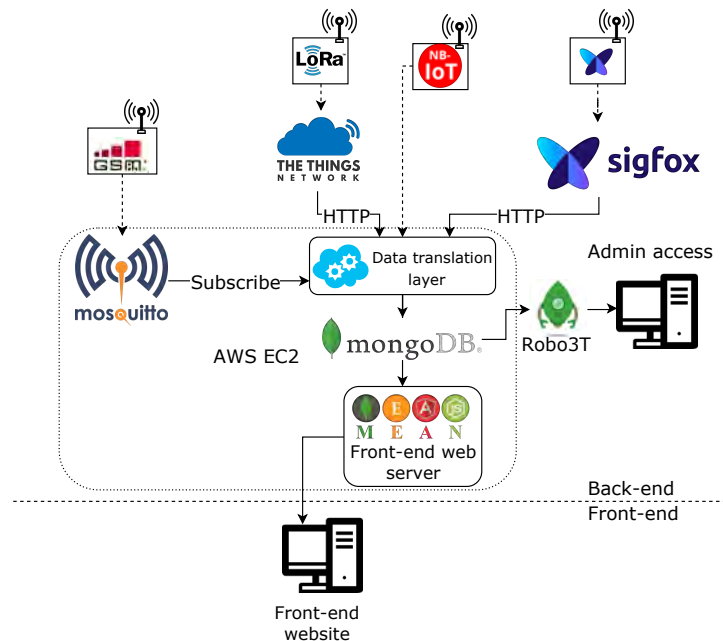


Figure 3.4: Complete system architecture overview

### 3.3 Conceptual test system overview

To implement a test system which can be used in the methodology listed in Section 3.1 and 3.2, an overall design needs to be defined, which will enable the different components to work collectively. Figure 3.4 illustrates a complete overview of how the different sections interact to complete the testing system. Each of the different sections (device hardware, device firmware, base stations and back end system) will be discussed in the following sections. To implement a generic testing device, which can be used to effectively evaluate the performance and application metrics, the following requirements is needed in the test system:

- A low power micro-controller unit (MCU) shall be implemented, as opposed to a UART-USB controller or micro-processor. The MCU is needed as the devices are required to be used in stand-alone situations where power consumption is critical.
- Four different communication modems shall be implemented on different testing devices for each type of technology, as opposed to one complete test device. This design decision is done to eliminate the the deep-sleep currents of other communication modules when tests are performed on a single technology and reduces the risk of cross Electromagnetic interference (EMI) interference on the PCB.
- A low-noise DC-DC regulator shall be implemented, which will enable battery-driven applications and reduce the EMI of the system.
- Peripherals, such as a GPS socket, GPIO, buttons and debugging LEDs shall be implemented, as they will allow the the testing device to be used in a variety of battery driven applications and enable the device to be used effectively in performance and application testing.
- A SubMiniature version A (SMA) RF connector shall be implemented on all testing devices. This will allow the testing devices to be used to evaluate the effectiveness

of various antennas. A 50 Ohm impedance transmission line should connect the modem to the SMA socket, as this will ensure that the complete antenna circuit is matched at 50 Ohm impedance.

Figure 3.5, shows the general layout of a test device which will be implemented in the testing system.

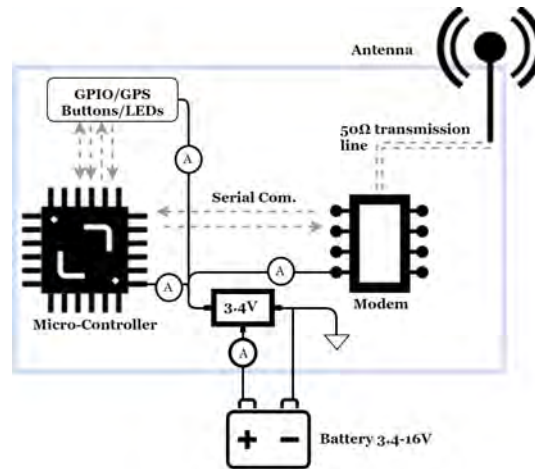


Figure 3.5: Generic testing device

### 3.4 Test device firmware requirements

Based on the requirements of the methodology, the following list of test device firmware requirements were deduced. Table 3.1 lists the function requirements of the four test systems, each with the accompanying communication specifications as listed in 1-4, and the general firmware requirements is listed in 5. Further the firmware function requirements limits the scope of the test system design process to the the requirements mentioned in Table 3.1, as the possible firmware of the test systems are nearly limitless.

#### 1 The GSM test system shall be able to perform the following functions:

- 1.1 Connect to a cellular service provider tower.
- 1.2 Set packet-session-data (PSD) context (APN)
- 1.3 Connect via a PDP connection
- 1.4 Create a local TCP socket
- 1.5 Connect to a server with specified IP address /domain name and port number
- 1.6 Transmit data via a chosen protocol
- 1.7 Receive data via a chosen protocol
- 1.8 Turn on deep-sleep function
- 1.9 Determine signal quality and signal enviroment
- 1.10 Wake-Up GSM modem

#### 2 The Sigfox test system shall be able to perform the following functions:

- 2.1 Adjust transmission power
- 2.2 Send data in byte format with no down-link expected
- 2.3 Send data in byte format with down-link expected
- 2.4 Receive data in byte format
- 2.5 Turn on deep-sleep function



2.6 Wake-Up Sigfox modem

**3 The LoRaWAN test system shall be able to perform the following functions:**

- 
- 3.1 Determine modem firmware
  - 3.2 Determine the modem (hardware) EUI (OTAA)
  - 3.3 Set the Network session key (ABP)
  - 3.4 Set the Application session key (ABP)
  - 3.5 Set the Device address (ABP)
  - 3.6 Set the Application EUI (OTAA)
  - 3.7 Set the Application key (OTAA)
  - 3.8 Activate/Deactivate active data rate setting (required by TTN)
  - 3.9 Adjust the desired data rate
  - 3.10 Adjust the desired power-level
  - 3.11 Join LoRaWAN network through ABP/OTAA
  - 3.12 Send data in byte format with no down-link expected
  - 3.13 Send data in byte format with down-link expected
  - 3.14 Receive data in byte format
  - 3.15 Turn on deep-sleep function
  - 3.16 Wake-Up LoRa modem

**4 The NB-IoT test system shall be able to perform the following functions:**

- 
- 4.1 Connect to a NB-IoT network operator
  - 4.2 Determine network registration status
  - 4.3 Determine signal quality and signal environment
  - 4.4 Set packet-session-data (PSD) context (APN)
  - 4.5 Send data via a UDP message
  - 4.6 Receive data via a UDP message
  - 4.7 Ping a certain IP address
  - 4.8 Turn on deep-sleep function
  - 4.9 Wake-Up NB-IoT modem

**5 The test system shall have the following peripheral features:**

- 
- 5.1 GPIO input is needed to connect various applications
  - 5.2 Two interrupt pins is needed to connect pulse-counter applications
  - 5.3 Generic interface needed to connect to applications such as GPS/Accelerometer
  - 5.4 Generic input button for various applications
  - 5.5 Reset button to restart device
  - 5.6 Debugging LED

Table 3.1: Test device firmware design specifications

### 3.5 Generic testing devices available

Certain generic development boards were considered and evaluated. Off the shelf solution would reduce development time, however there are certain trade-offs. A summary of these devices can be seen below, along with the drawbacks.

### 3.5.1 FiPy and LoPy

The FiPy and LoPy are devices developed by PiCOM and offer a all-in-one IoT connectivity solution. The FiPy offers WiFi, Bluetooth, LoRa, Sigfox and dual LTE-M (CAT M1 and NB-IoT), while the LoPy offers Bluetooth-LE, WiFi and LoRa. The communication modules are connected to a powerful ESP32 microprocessor, which utilizes MicroPython (a software implementation of the Python 3 programming language, written in C, that is optimized to run on a micro controller) to perform functions. Due to the FiPy and LoPy's combination of both Wi-Fi and LoRa, the devices can be used as a LoRaWAN Gateway, however this limits the Gateway to only single channel reception. Due to the wide variety of communication technology available in the Fi-Py and the low-power consumption of the ESP32 micro controller the device was a serious test bench competitor. The Fi-Py was however not chosen as it lacks support for GSM, individual component power-consumption measurement and high cost.

### 3.5.2 Telit 868s Sigfox development board

The Telit 868s Sigfox development kit offers a single Sigfox modem in conjunction with a UART-USB controller, battery clip with regulator, a power-consumption circuit and debugging LEDs and switches. The development kit was not chosen as it lacks a micro-controller to enable continuous transmission, lack of availability and high cost.

### 3.5.3 The Things Uno

The Things Uno is a development board offered by TTN, which offers a Arduino Uno in conjunction with a Mircochip RN2483 on a single compact unit. The Things Uno offer a perfect development unit, as it offers a complete MCU, modem and regulator unit, however the lack of individual component power-consumption measurement, availability and high cost limits this development kit.

## 3.6 Test device hardware design

In Section 3.3 a test system is proposed that allows thorough comparative testing of the different LPWAN standards; LoRaWAN, Sigfox and NB-IoT vs. the current GPRS standard. The test system is designed according to the system specifications listed in section 3.4, to allow performance- and operation metrics to be tested. The following chapter describes the communication modules, micro-controller and other hardware available, as well as functionality, constraints and motivation behind major test-system hardware-design choices. The test system needs to be kept fair and comparable between the different communication technologies. Four different test devices are built, which reduces the chances of cross-interference between the different components during testing. Moreover, it enables modular test-systems which can be used in real-world situations.

### 3.6.1 General test device hardware design

The basis of the test system (MCU, board-layout, current-measurements and peripherals), stays consistent throughout the four devices, with only the communication module and required voltage regulator varying. Figure 3.5 shows the general test device layout, with the following section describing the component choices available and design choices made.

### 3.6.1.1 GPRS modem

Two quad-band 850/900/1800/1900 MHz GPRS modules, commonly available and used in several IoT applications [68] [69] were considered in the GPRS test bench. The U-Blox Leon-G100 [56] and SIMCom SIM800C [70] feature a standby power consumption of <1 mA, a maximum GPRS data down-link/up-link transfer rate of 85.6 kbps and supports standard AT commands according to 3GPP standard. Both modules are class B GPRS modems and offer transmission power up to 2 W at 850/900 MHz and 1 W at 1800/1900 MHz. The two GSM units compare similar in terms of usability and performance, therefore the U-Blox Leon-G100 was chosen due to availability and familiarity.

### 3.6.1.2 Sigfox modem

Two different Sigfox modems were evaluated and tested, the Wisol SFM10R [71] and the Telit LE81-868S [54]. Both modules offered similar RF and current consumption performance, however the Wisol module was chosen due to its extremely low cost (R35), availability and regular industry usage.

### 3.6.1.3 LoRaWAN modem

LoRa modules are currently offered with two types of radio technology: LoRa and LoRaWAN, both of which were evaluated and tested. LoRa modules only contain the physical LoRa modulation link layer. It is ideally suited for point-to-point communication systems and is relatively cheaper than LoRaWAN modules. LoRaWAN modules contain both the physical LoRa modulation link layer and the application control layer used to communicate in a LoRaWAN network.

A LoRa modem, The HopeRf RFM95 [72], was considered as it provides a high receive sensitivity (down to -148 dBm) combined with variable transmission power of up to +20 dBm and low cost. The popular Microchip RN2483 [55], used in a variety of LoRaWAN products such as The Things Uno, was chosen as a LoRaWAN modem due to its low-power consumption, industry usage and flexible command Application Programming Interface (API). Ultimately, the full LoRaWAN-stack modem is implemented as it simplifies the firmware design process described in Chapter 3.9.

### 3.6.1.4 NB-IoT modem

As NB-IoT technology is still a relatively new development, the only NB-IoT module commercially available is the Ublox Sara-N200 [73]. The Ublox Sara-N200 offers a cost efficient solution with NB-IoT band 8 support, which is currently the band utilized by mobile network operators in South-Africa. The Ublox Sara-N200 utilizes the current AT command standard used by GSM with protocol support for IPv4, embedded UDP/IP, generic Constrained Application Protocol (CoAP).

### 3.6.1.5 Micro-controller

A micro controller (MCU) implemented in the test bed devices, allows continuous autonomous transmission over long time-periods, contrary to a USB-to-UART IC, which would send modem commands directly from a PC. The inclusion of a micro-controller further allows the testing of the communication technology in general use cases, such as a temperature sensor, pulse-counters or GPS loggers, where different peripherals such

as ADC, DAC, I2C, UART, SPI and GPIO are needed. Two 8-bit AVR MCUs, the ATXmega128-A4U [74] and ATMEGA328P-A4U [75] were evaluated and tested. The comparison between the two different MCUs is primarily based on power-consumption and peripherals. Existing IoT solutions such as smart geyser controllers [76], smart water meters and IoT card readers developed utilized the ATXmega128-A4U, due to its vast number of peripherals, usability and low-power consumption. The ATMEGA328P-A4U was chosen due to its ultra-low power consumption and familiarity with the AVR firmware development environment. The ATMEGA328P-A4U provides a single UART connection which is utilized by all the IoT modems. Moreover, it provides sufficient GPIO-pins for modem reset and control features, buttons and LEDs, ADCs which can be utilized for battery level monitoring or temperature readings and a SPI interface which is used to program the MCU via a ATMEL-ICE programming device.

### 3.6.1.6 Voltage regulator and batteries

The design of ultra-efficient voltage regulators for battery-driven projects is beyond the scope of the project, as the aim is to evaluate the different communication technologies. The voltage regulator should provide a common voltage level that is sufficient for all components, provide a sufficient maximum current to supply the different components and as far as possible reduce the regulator noise to improve the power-consumption measurements. A low-dropout voltage linear regulator (LDO) is chosen for the Sigfox and LoRaWAN test devices. These devices require a 60mA max current while transmitting with the debug LED on. 3.3V suits all the components optimum operating voltages. Further, the LDO provides low voltage output ripple, low design complexity, low cost, high power efficiency when the battery choice is chosen to minimize  $V_{in} - V_{out}$ , low noise and low EMI. LDO regulators are also a viable GSM and NB-IoT option, however since GSM solutions typically tend to be used in conjunction with a AC-DC mains power converter, the input voltage range needs to be wider. Thus a switch-mode power supply (SMPS) is preferred. The SMPS supply also satisfies the higher current required by GSM and NB-IoT. A SMPS design was implemented based on the hardware recommendation of the Leon-G100 [77]. The SMPS design utilizes a L5987 module [78], which is altered to allow a 3.4V output voltage (based on the components optimum operating voltages) with low output voltage ripple.

Due to the extremely low power consumption of LPWAN technology, the battery chosen for each application needs to be carefully considered with regard to capacity, space-available, operating voltage, cut-off voltage, operating temperature conditions and self-discharge rate of battery technology. Batteries for GSM applications require a discharge rate that can deliver 2.5A peak currents and have a DC series resistance to avoid a VCC voltage drop greater than 400 mV during 2.5A transmit bursts [77]. Although the different battery technologies available are important, they are not evaluated in this dissertation, due to the wide variety of IoT applications with different power requirements available.

### 3.6.1.7 Antenna track

In order to minimize losses and reflections in the microwave transmission line, which connects the modem to an antenna, it needs to be designed to achieve optimum performance. There are two major types of microwave transmission lines namely Coplanar wave guide (CPW) and Microstrip lines.

Microstrip microwave transmission lines, shown in Figure 3.6, are designed with a thin

transmission line track (red) on top of a PCB (grey), and ground planes (yellow) surrounding the transmission line track. The design of a Microstrip line is affected by a number of factors. The major factors are the thickness of the dielectric material, the dielectric constant and the width of the track.

CPW microwave transmission lines are designed similar to a normal micro-strip transmission line with the addition of ground planes on either sides of the PCB. This changes the E-field of the transmission line. In addition to the above mentioned factors, the gap between the transmission line and the top ground plane will also affect the impedance of the line.

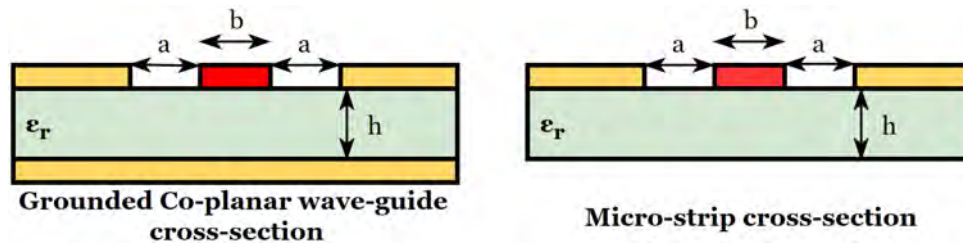


Figure 3.6: Coplanar Waveguide transmission line (Left) vs design Micro-strip (Right) [10]

The choice was made to use a CPW transmission lines as a ground plane would be required for other components on the top and bottom layer. The dimensions of the CPW were calculated with the help of a calculator which can be found at [79], which is based on the Equations B.1 to B.5 (see Appendix B) described in [80]. The CPW transmission line was designed for  $50\Omega$ , as this matches the requirements of all four communication modules, as well as the SMA connector impedance and the antenna's impedance listed in Section 2.8.1. The board thickness  $h$ , was selected as 1.6mm, the trace gap width ( $a$ ) as 0.15mm, trace width ( $b$ ) as 1mm and the substrate consists of FR4 PCB board which has a dielectric constant of 4.5.

### 3.6.1.8 Current measurement

All four devices are equipped with a bridge in the  $V_{cc}$  line, between which a current measurement device can be placed to measure current flow to either the GPIO, Modem, MCU or to the complete device. Figure 3.5 highlights this feature, while the exact circuit design can be seen in Figures B.2 to B.6.

## 3.6.2 Test device hardware summary

The designed test devices can be seen in Figure 3.7, with the accompanying design in Appendix B, which shows a complete integration of the components listed in the sections above. The test devices performed as expected on a hardware level, with the addition of a single LED, which was used during debugging, along with one MCU reset button and a general purpose input button. Two MCU interrupt pins are available as pulse counters along with a GPS hardware interface, which allows a UBLOX NEO-7N GPS module to be attached in order to do network coverage testing.

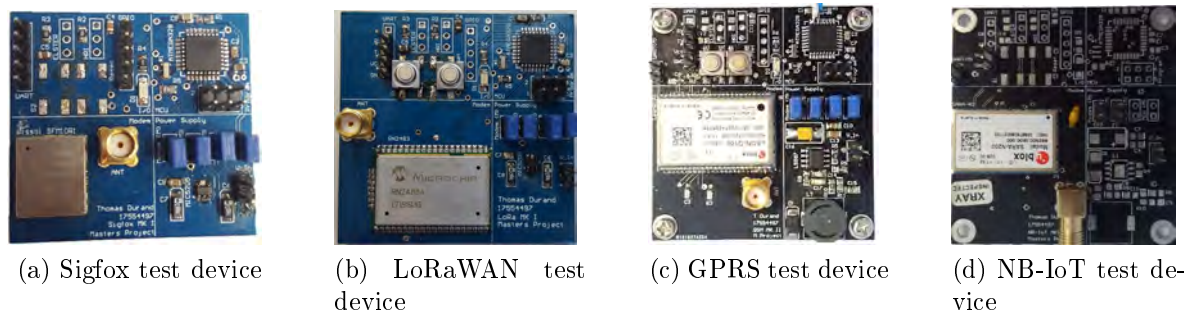


Figure 3.7: Designed test devices

### 3.7 Power-consumption measurement

Accurate measurement of the different technologies' power-consumption during transmission, reception, idle and sleep-modes is required. The systems operate at a constant voltage, which can be measured by an oscilloscope, therefore only current-measurement solution needs to be developed. Commonly current measurement is done with a multimeter, however due to the high cost of digital multimeter which is able to log data a custom solution is designed. Two common solutions to current measurements are applied in practice, either through a shunt resistor or through magnetic field sensors, such as Hall effect sensors. In this application, currents between a few micro-ampere and a maximum of three amperes need to be measured, thus a shunt resistor is used.

Shunt-resistor based current measurement is achieved by placing a low-value sense resistors in series with the supply and load, measuring the voltage drop across the shunt resistor. The current sense resistor can either be placed between the load and ground (low-side current measurement) or between the voltage supply and the load (high-side current measurement). High-side current measurement is chosen for this specific application, as the monitoring of multiple loads (MCU, Modem, GPIO and Input) is required. High-side current measurement reduces the potential for ground loops, as opposed to implementing low-side current measurement and is more reliable as a common stable voltage source is used as reference [81].

The voltage drop across the shunt resistor is intentionally very low, as it should not affect the power supplied to the test circuit, therefore the voltage needs to be amplified by an op-amp circuit. The amplified current measurement voltage needs to be logged by an application in order to measure current-flow over a time period. The sampling rate of the current measurement device is a critical factor, as transmission current peaks needs to be logged in order to fully evaluate the communication technology. GSM requires the highest sampling rate as a standard GSM frame consists of 8 equal size 576  $\mu$ s transmit, receive or idle slots. Therefore, a sampling rate of at least 3.466kHz is required to provide at least two samples per slot (Nyquist rate). A proposed solution is to use a 16 MHz Arduino's ADC, where the A/D prescaler factor is set to 128, therefore  $16 \text{ MHz}/128 = 125 \text{ KHz}$ . Each conversion in AVR takes 13 ADC clocks so  $125 \text{ KHz}/13 = 9615 \text{ Hz}$ . As the Arduino enables a high enough sampling rate, a high-side current measurement Arduino breakout board solution was designed, simulated and tested as shown in Figure 3.8. The current-measurement device consists of a 0.01, 1 or 10  $\Omega$  variable high-side shunt resistors, two input buffering op-amp circuits and a 100 times gain differential op-amp circuit. The op-amps are powered by the 5V Arduino regulator, which enables a high output voltage swing used to amplify the shunt resistor voltage.

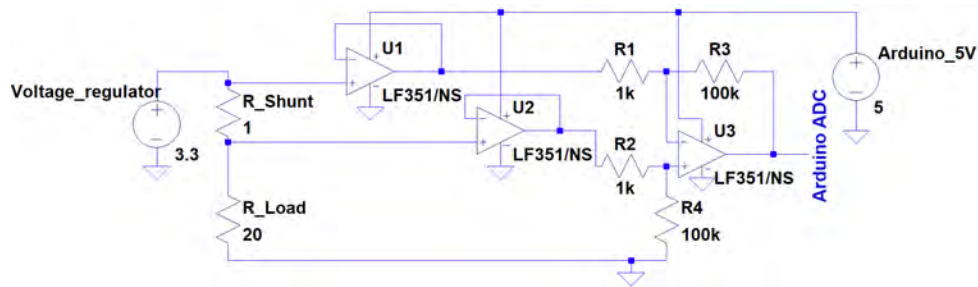


Figure 3.8: Spice model of current measurement solution mk I

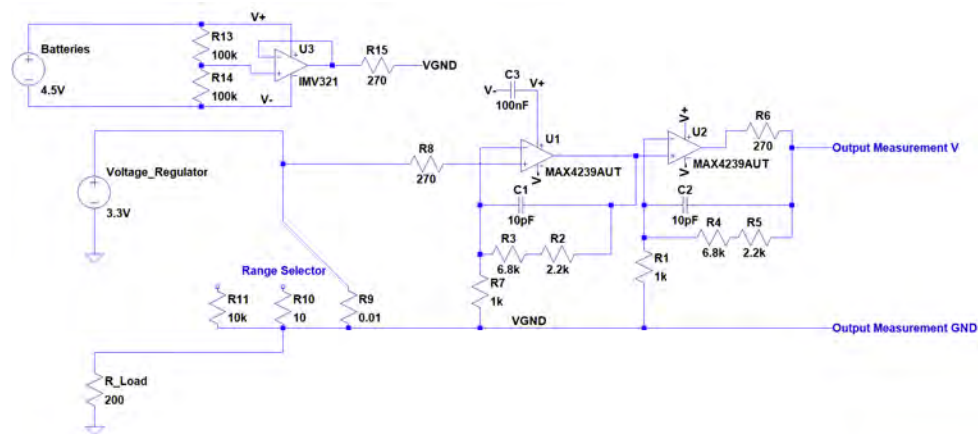


Figure 3.9: Spice model of current measurement solution mk II

Simulation and testing identified flaws in the design. The op-amps chosen has a high voltage off-set, which led to inaccurate measurements. Further, the Arduino failed to provide the theoretical ADC sampling rate, as measurements first need to be stored and sent via serial to a computer, which increased the processing overhead, reducing the sampling rate.

To address the voltage-off-set issue, an existing open-source hardware design, the uCurrent gold is utilized [82]. The uCurrent circuit design provides  $<+/-0.05\%$  measurement accuracy on  $\mu\text{A}$  and  $\text{nA}$  ranges and  $<+/-0.1\%$  in the  $\text{mA}$  range, due to the extremely low system op-amp voltage offset of  $<50\ \mu\text{V}$ .

The current measurement device mk II uses an extremely low voltage offset MAX4239AUT op-amp in a two stage non-inverting op-amp gain configuration to achieve a 100 times shunt resistor voltage gain. This output-voltage can be measured by any voltage measuring devices. To log the current consumption data, a digital oscilloscope, Tektronix TBS1032B, is used, due to its high sampling rate and accuracy. A similar shunt resistor variety is used in order to switch between different current measurement ranges, which can be seen in Table 3.2. To allow a voltage offset from the received input voltage from the measured device, three AAA batteries in series are used along with a op-amp voltage divider circuit. The complete circuit design can be seen in Figure 3.9.

Table 3.2: Current measurement solution mk II measurement range

Measurement Range	Shunt Resistor ( $\Omega$ )	Output Voltage Unit	Measurement Range	Max current through shunt resistors (mA)
nA	10 000	1 mV/nA	0-2250 nA	3.16
$\mu$ A	10	1 mV/ $\mu$ A	0-2250 $\mu$ A	111.8
mA	0.01	1 mV/mA	0-2250 mA	10 000

To confirm the implemented design, the current measurement devices is practically evaluated trough varying the voltage across an  $8\Omega$  load. This measurements is compared to the theoretically expected results, shown in Figure 3.10, which verifies the low offset-voltage op-amp circuit design.

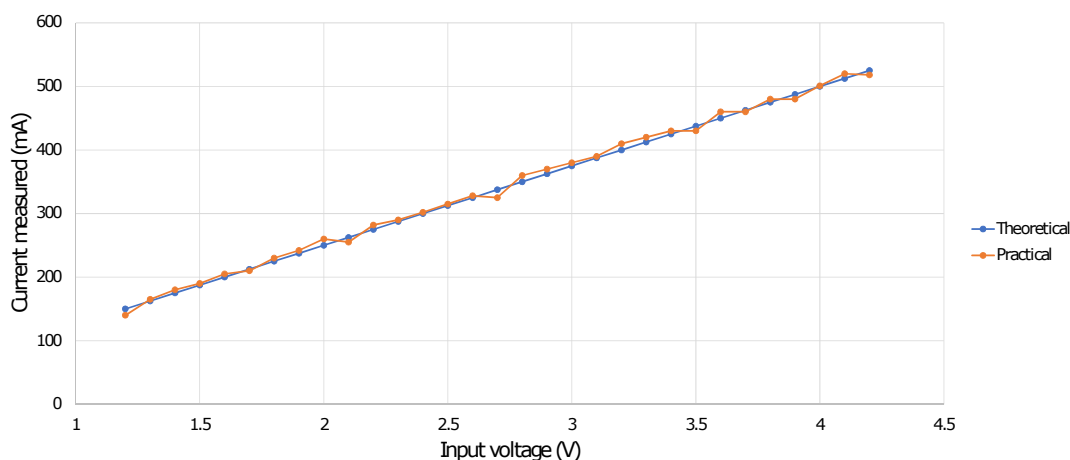


Figure 3.10: Current measurement solution mk II validation

## 3.8 Network base stations

The tested LPWAN technologies and GPRS rely on a star-network topology network. This reduces the number of hops from source to destination, overall complexity, minimizes delay and improves stability. The different base stations available need to be surveyed and analysed.

### 3.8.1 GSM and NB-IoT base stations

The GSM infrastructure in South-Africa is quite prominent as there are four major mobile network-operators who provide GPRS coverage in South-Africa. GPRS gateways are built and maintained by the mobile network-operators with base station information remaining propitiatory, therefore no investigation is possible. NB-IoT coverage is provided by mobile network-operators aswell, however currently only MTN and Vodacom have launched commercial scale trial NB-IoT network base stations. Trials for the NB-IoT base stations are focused in Gauteng, South-Africa. However, with the help of MTN and ZTE a single GSM base station in Stellenbosch, Western-Cape, South-Africa was upgraded to support NB-IoT. Vodacom, has seven NB-IoT base stations in Western-Cape, South-Africa, however a lack of contracted Vodacom SIMs with M2M Lite or Narrowband Lite functionality activated hinders the development of NB-IoT.



### 3.8.2 Sigfox base stations

Sigfox network coverage is provided by Sqwidnet South-Africa, with several gateways providing coverage for the Western-Cape. Although base stations aren't as densely populated as GSM, sufficient coverage is provided in major centers. Due to the combination of indoor interference and long distances to base stations, deep-indoors applications might suffer significant signal loss. Continuous roll-out of Sigfox base stations will solve this issue and will increase redundancy resulting in increased reliability.

### 3.8.3 LoRaWAN TTN base stations

Due to a lack of TTN coverage in the testing area a TTN base station needs to be designed, built and deployed to complete a fair network evaluation. The following available solutions need to be evaluated and possibly implemented.

- **The Things Gateway (R5370 approx.)[83]:** This prebuilt base station supplied by The Things Network offers coverage range up to 10km, however it is typically meant to provide indoor coverage and does not offer any Power-over-Ethernet (PoE) setup support.
- **Lorrier LR2 (R10400 approx.)[84]:** The LR2 is a carrier grade base station intended for building large scale IoT networks based on the LoRaWAN protocol. The base station is more complex as it can be used in a variety of applications.
- **RPI + RAK831 (R5000 approx.)[85]:** This self-built base station relies on a RAK831 LoRa concentrator board connected to a Raspberry Pi (RPI) via an adapter board. The complete design needs to be enclosed in an external case with an omni-directional 868 MHz antenna added.
- **RPI + IMST 880A concentrator board (R6000 approx)[86]:** Although similar to the RPI + RAK831, this base station relies on an IMST 880A LoRa concentrator board to handle the LoRa modulation.

Due to parts availability, cost and functionality, the raspberry pi along with the IMST 880A concentrator board solution was chosen. An overview of the planned network base station, based on the design guide provided by TTN can be seen in Figure 3.11.

The IMST iC880A is able to receive up to 8 LoRa packets simultaneously sent with different spreading factors on different channels [87]. This allows the LoRaWAN gateway to scale to accommodate a large number of end-devices. This use of a PoE setup simplifies the base station setup and further ensures that the LTE Router can be placed away from the concentrator board to reduce EMI. A 4 dBi omni-directional antenna is used by the gateway to ensure that the signals can be received uniformly from all directions. The gain of the receiving antenna is a trade-off between the receiving-antennas gain (which increases the link-budget) and the gain directionality of the antenna. The RPI is formatted to use ResinOS, a bare-bone, Yocto Linux based host OS. This enables the remote management and diagnosis of the packet-forwarding application which sends the data from the concentrator board to TTN's servers. The gateway is made publicly available for any developers to use and has received 540 856 and transmitted 246 messages (measured 07/07/2018) since its construction in Aug 2017. This verifies the up-link centric nature of LPWAN technology. The gateway coverage can be seen in Figure 3.12,

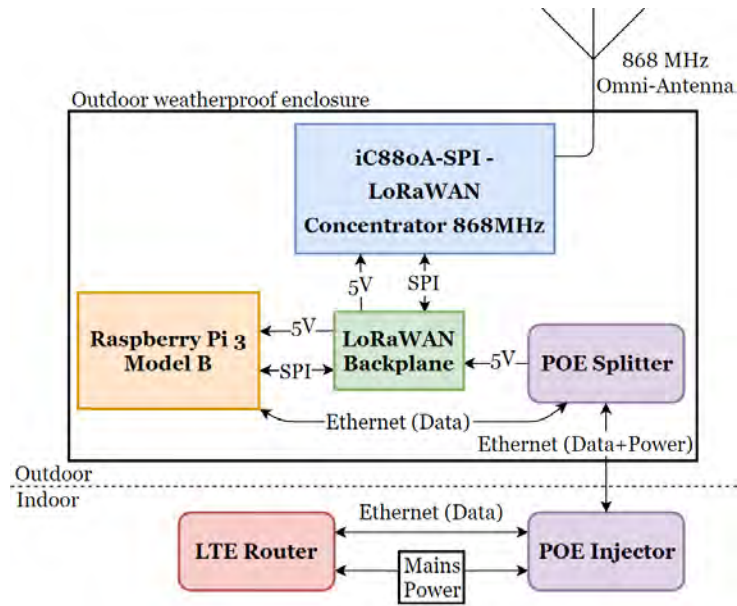


Figure 3.11: LoRaWAN The Things Network base station overview

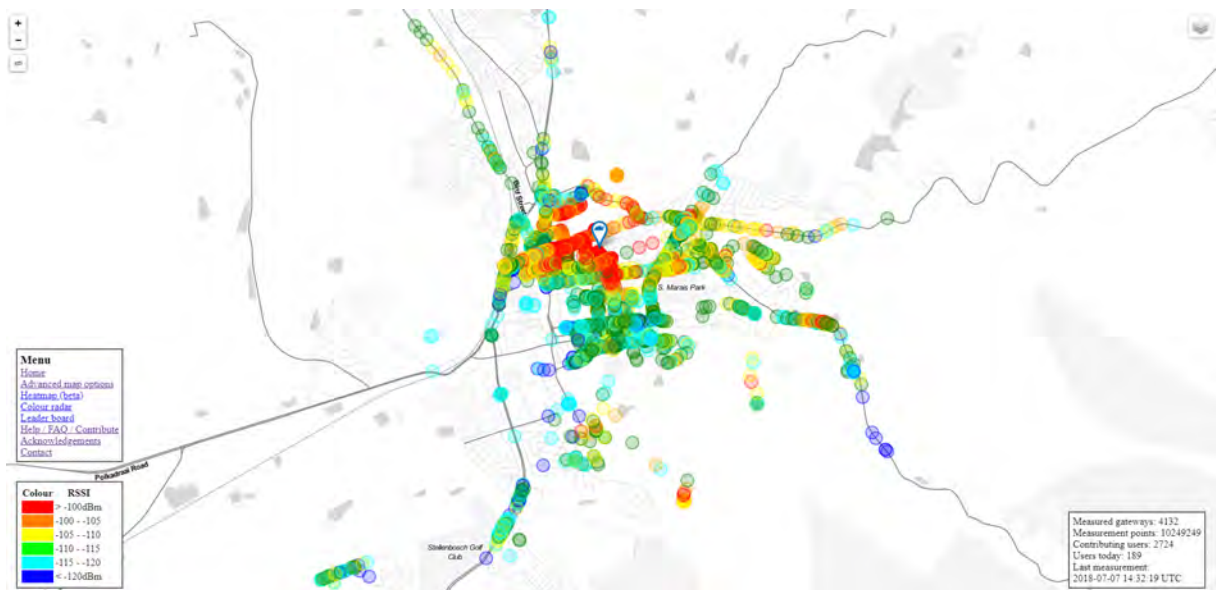


Figure 3.12: LoRaWAN TTN base station coverage [11]

as measured by a community of LoRaWAN TTN developers using the TTN Mapper platform developed by JP Meijers [11].

### 3.9 Firmware and back-end architecture

Integrating the hardware systems described in Chapter 3.6, requires various software components to enable functionality of the testing-devices. The first section of this chapter presents a high-level overview of the general firmware architecture and the communication stack drivers used in the different testing-devices. The generalized firmware architecture described enables sleep-modes, serial-drivers, modem-drivers, peripheral control and GPS functionality.

The different transmission protocol's data-link and network layers are addressed through the firmware design regarding modem-commands. GPRS varies drastically in complexity from the other LPWAN technologies. Only a brief overview of the GPRS basic firmware design choices that enables a functional testing-device is provided with functions such as firmware-over-the-air omitted.

The different technologies utilize various APIs to allow data access. An overview is provided of the rudimentary back-end data storage solution. This allows data gathered by the different testing devices to be stored for performance- and operation data analysis.

### 3.9.1 Firmware architecture

The embedded firmware should be minimalistic, efficient, real-time and stable in order to allow accurate and repeatable experimental testing. The firmware design utilized in the test-benches relies on a commonly used unobstructed infinite loop. It is used to schedule synchronous processes and react to asynchronous events. The use of an unobstructed infinite loop allows efficient system-time management. This enables accurately scheduled transmissions which is a specific requirement of duty-cycle limited systems. The test-systems are not designed with a specific use case in mind, however provision needs to be made for both asynchronous events, such as a pulse-counters, and synchronous events, such as ADC measurements. A broad overview of an up-link centric testing device's firmware can be seen in Figure 3.13.

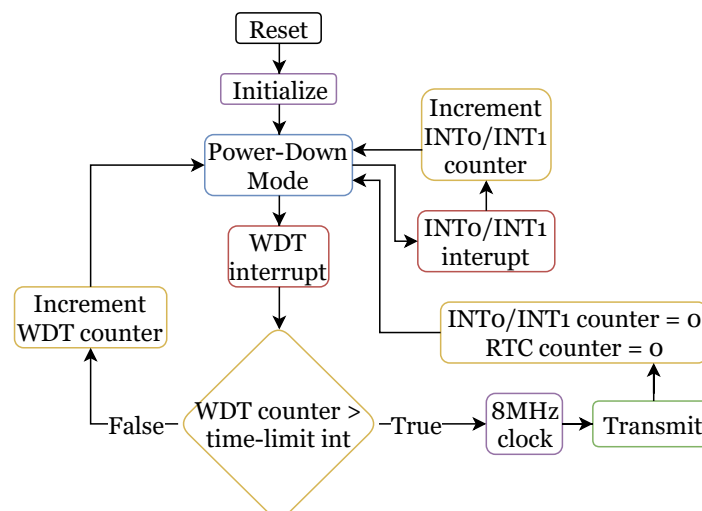


Figure 3.13: Up-link centric device firmware overview

As power-consumption in LPWAN technologies is of the utmost importance, the AT-Mega328P MCU utilizes power-down mode to save-power and a watch dog time (WDT) to enable accurate synchronous time keeping. The internal 8MHz oscillator is only utilized to perform normal operations (UART, ADC, DAC etc). The WDT (along with the reset-signals and two interrupt-signals) is the only clock signal able to wake the AT-Mega328P from power-down mode and is configured to interrupt every 8 seconds (max WDT duration). It is important to note that interrupts need to be kept as short as possible. Interrupts should only be used to increment a counter or set a flag, as this will increase time keeping accuracy and reliability.

In order for the MCU/Application to transmit or receive a message, modem driver firmware is needed. A basic OSI model of the transmit/receive firmware is demonstrated in Figure 3.14. The modem firmware differs drastically for the different technologies, however GSM, NB-IoT and Sigfox all utilize the Hayes ATtention (AT) command set. The LoRaWAN RN2483 uses a MAC command library. AT commands always has "AT" as the first two characters of any command and are terminated with a carriage return (cr), example "AT+COPS=0\r". Similar to the AT command set the MAC library always has "MAC" as the first three characters of any command and is terminated with a cr along with a new line character (n), for example "mac set adr off\r\n". Although GSM, NB-IoT and Sigfox all use the AT command set, the Network/Transport/Session layers differ. Therefore a different AT command library is needed for each modem which is discussed in the Sections 3.9.1.1 to 3.9.1.4.

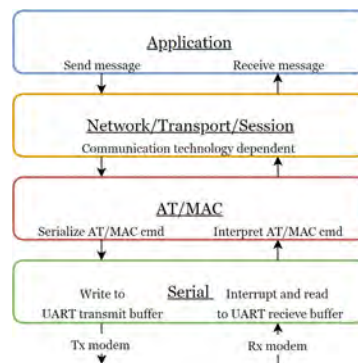


Figure 3.14: Basic overview of the communication modem firmware sections

The serial communication to the modems utilizes UART at varying baud-rates. An interrupt is set to trigger once data is received from the modem as in the case of a received packet. The received data is stored in a receive-buffer, while data which needs to be sent to the modem is first read into a transmit buffer and then sent to the modem.

As the general application layout, AT/MAC commands and serial layer has been discussed, it is important to investigate the different network/transport/session layers of the different communication technologies.

### 3.9.1.1 GSM modem drivers

GPRS consists of a complex integration of the network/transport/session layers. Therefore this section will be divided into an operator selection and packet switched data section, TCP section and the application protocol section. In Figure 3.15, the general purpose GPRS firmware provides a clear overview of how the different sections follow and cooperate with each other.

**Operator selection and packet switched data** Connecting to a mobile network operator is achieved through automatic selection or a specified mobile network operator can be selected (useful for global devices, example shipping container tracking). Automatic selections is chosen through specifying operator selection (COPS) as 0 where the network is chosen based on the SIM card connected to the modem. Manual selection is achieved by specifying COPS as 1 along with the operator Mobile Country Codes (MCC) and Mobile Network Codes (MNC).

Packet-switched data (GPRS) is enabled through establishing a packet-data protocol session (PDP). This can be achieved by using one of three different modes: (1) dial-up mode, (2) opaque command mode, or (3) transparent transmission mode, depending on the requirements of different user applications. The different modes vary drastically with dial-up mode requiring the IP-stack to be managed by the MCU, opaque command mode allowing the IP-stack to be managed by the modem (however the TCP connection needs to be managed by the MCU) and the transparent transmission mode integrating both the IP-stack and TCP protocol [88]. Dial-up mode is disregarded as it would increase the modem firmware complexity requirements drastically and requires the complete IP-stack to be integrated. Transparent transmission mode does not allow ASCII characters, which limits the use of lightweight application protocols such as MQTT. Therefore, opaque command mode is chosen to be integrated into the system.

To establish a valid PDP session an IP version and Access Point Name (APN), used to select the external packet data network (PDN) to be connected to, needs to be configured. After the PDP profile has been set the PDP connection can be activated and a Transmission Control Protocol (TCP) socket can be configured.

**TCP socket** TCP is a standard that defines how to establish and maintain a network connection through which data can be exchanged. TCP works with the IP-stack to enable communication from device to a remote network server with a IP address. In the context of this application the TCP socket is created, connected and used to transmit/receive data. To create a TCP socket the IP address and port to connect first need to be defined. The specific IP address of a website can be identified through a Domain Name System (DNS) lookup by using the "AT+UDNSRN=0,<web-address>" command. The modem will respond with the web address's IP address. Once the TCP socket create command is sent, the modem will respond with the local port number to which TCP data can be sent to (up to 7 local TCP ports can be defined). The next step is to connect to an external IP address and port number. This allows the modem to send data through the TCP socket directly to the specified IP address and port number. Data can now be transmitted through the TCP socket, and a notification will be sent to the MCU when data is received via the TCP socket. Once the modem is shut-down, the TCP socket will automatically close. Once TCP socket is created, an application protocol needs to be used in order to transmit and manage data in an efficient manner.

**Application protocol** Various application protocols exist which can be used in conjunction with GPRS. Two main industry variates were considered, Message Queuing Telemetry Transport (MQTT) and the Constrained Application Protocol (CoAP) (lightweight Alternative to HTTP) in the context of the application requirements.

The MQTT protocol is an extremely light weight, flexible and scalable IoT solution . MQTT relies on a publish-subscribe protocol, which utilizes topics ordered by different levels, which are separated by "/" characters. A central server, called the broker, with a web-address or fixed IP address, allows clients to connect to and publish messages to the topics. The broker will then forward the messages to any clients who are subscribed to the specific topic. The responsibility lies on the system architecture designer to design **and** implement the MQTT architecture correctly as devices can not be contacted directly as they possess no specified address. No data storage is natively implemented in the MQTT broker, therefore a data gathering node needs to be added which is subscribed to the various topics to store the data.

The CoAP protocol is based on the request-response communication model and is a lightweight version on the highly popular web HTTP protocol in terms of the REST model

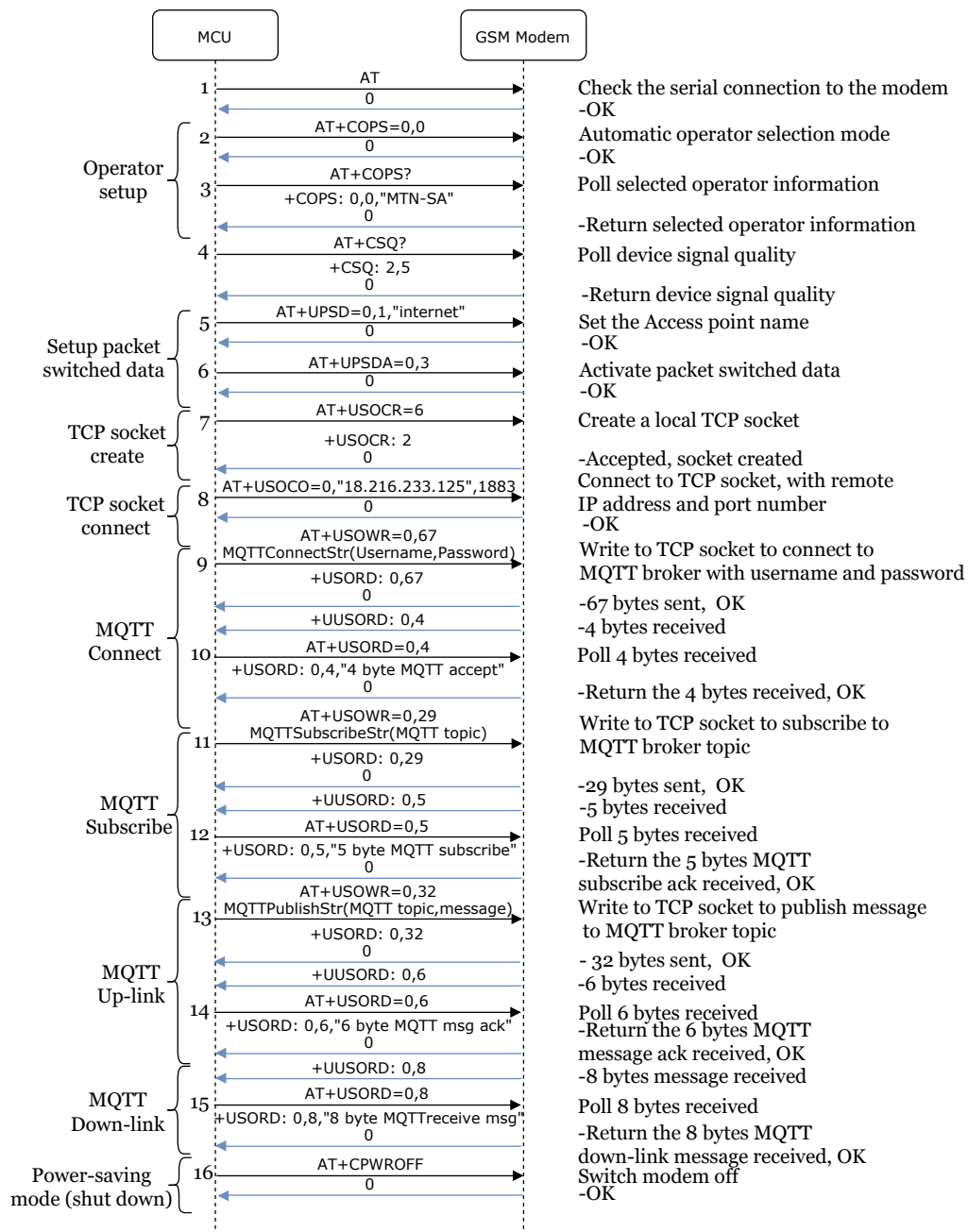


Figure 3.15: GSM MCU-communication sequence diagram

with GET, POST, PUT and DELETE (CRUD) methods. Critically, CoAP extended the HTTP GET method to include a "subscribe" feature, which allows the publish-subscribe feature. The binary headers is set to a fixed 4 bytes limit which reduces overhead, enabling the use of this application protocol in battery-powered solutions.

Both CoAP and MQTT application protocols offer similar excellent lightweight performance, however due to the popularity of MQTT, the protocol is chosen in this specific case.

### 3.9.1.2 Sigfox modem drivers

The Sigfox modem firmware design is extremely simplified, and provides a nearly "plug and play" solution, as can be seen in Figure 3.16. The simplified design enables true low

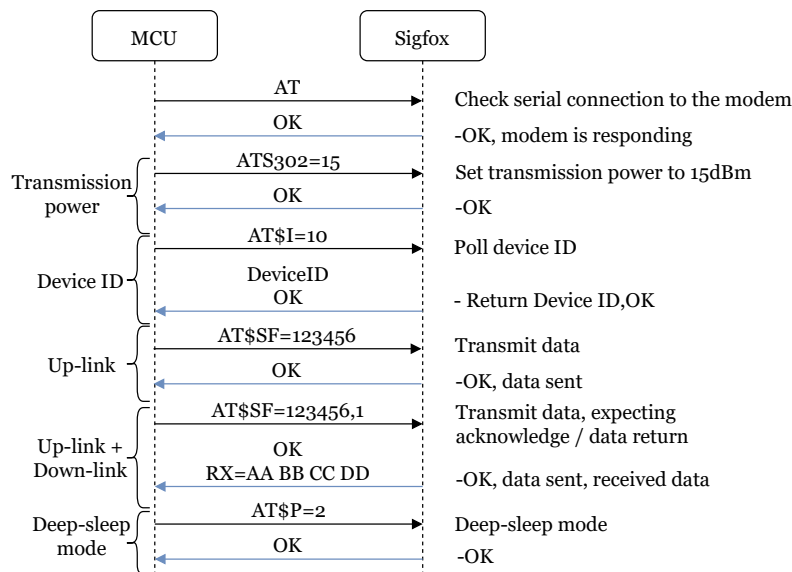


Figure 3.16: Sigfox MCU-communication sequence diagram

cost devices, as MCU with less EPROM memory is required therefore reducing the overall cost. The modem has a choice between sleep-mode or deep-sleep-mode, and can return to active mode from deep-sleep mode by toggling the modem reset line or from sleep mode by sending a UART-break. The management of Sigfox devices is done on the Sigfox back-end, with each modem's Device ID and PAC number required. The Device ID and PAC number can be obtained from the modem through the "AT\$I=10" and "AT\$I=11" commands respectively. Care should be placed in the firmware design not to surpass the up-link and down-link message allocation limits as mass-production of Sigfox devices needs to go through a Sigfox firmware certification test in order to comply to the "Sigfox ready" standard.

### 3.9.1.3 LoRaWAN modem drivers

Due to the versatility of the LoRaWAN technology, there are several LoRa modulation settings which needs to be set before a device can join a LoRaWAN network, as can be seen in Figure 3.17. The system information stage of the firmware design is used to check modem responsiveness and with verifying the important hardware Extended Unique Identifier (EUI). The LoRaWAN key settings is dependent on which LoRaWAN access method used ABP/OTAA as discussed in Section 2.4.3. Various LoRa modulation settings can be adjusted, however there are four important settings which need to be adjusted to connect to TTN. Firstly, the adaptive data rate (ADR) needs to be disable to keep the SF constant throughout tests. Thereafter, the transmission output power and spreading factor is adjusted. Lastly, the automatic reply function which automatically transmits a empty frame upon a successful down-link message or when the frame pending bit has been set by the server needs to be disabled as required by TTN.

The settings are now saved to the device's EEPROM, and the modem is able to connect to the LoRaWAN network through either of the preferred join procedures. The LoRaWAN device can now send up-link messages, with the option to send confirmed up-link messages or receive down-link messages. Sleep mode is enabled by sending the system sleep command with a specified sleep duration in milliseconds. However, the modem can be prematurely woken through toggling the modem reset line or sending a UART break

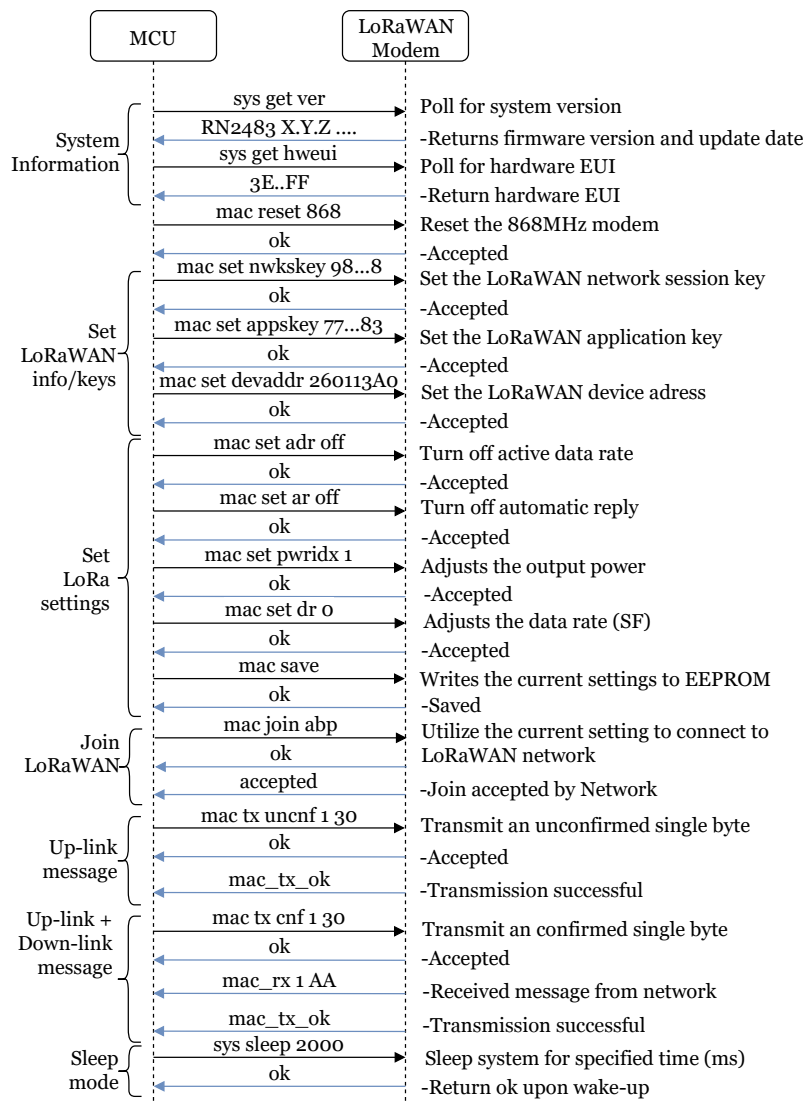


Figure 3.17: LoRaWAN MCU-communication sequence diagram

followed by a '0x55' char at the preferred baud rate. The complete LoRaWAN firmware is relatively simple as there are no complex operator selection procedure as with GSM and NB-IoT. Care should be placed on selecting the correct join procedure, as OTAA is typically advised. The use of a LoRa module that incorporates the complete LoRaWAN stack is advised as it significantly reduces the modem firmware design and enables a lower cost MCU to be used as less EEPROM is required to store modem commands.

#### 3.9.1.4 NB-IoT modem drivers

NB-IoT requires two stages of network configuration to enable communication to a network. The first section is mobile network operator specific settings which allows the device to connect to the base stations as can be seen in Figure 3.18. In the second stage, the NB-IoT follows the same manual network-operator selection procedure as described in Section 3.9.1.1. The "CEREG?" AT command is important, as the MCU needs to ensure that the modem is correctly connected to the NB-IoT capable base station before any data can be transmitted. Once the modem is correctly connected, data can be sent and received through User Datagram Protocol (UDP) datagrams, by selecting a IP address



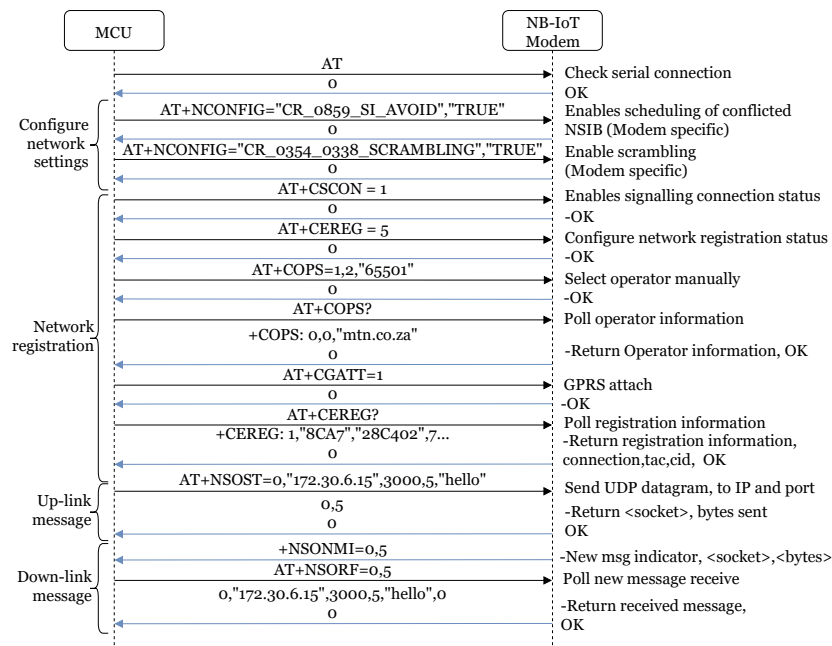


Figure 3.18: NB-IoT MCU-communication sequence diagram

and port number. At this point, an application protocol which supports UDP messages such as CoAP can be implemented. CoAP is however not implemented in this thesis due to NB-IoT network access time constraints. Instead predefined UDP echo servers provided by Vodacom for testing purposes are used to enable the testing required by Chapter 4.

### 3.9.2 Back-end architecture

The variety and scale of data produced by the different communication technologies requires a centralized data gathering solution. The complete system can be seen in Figure 3.4, and consists of various components which will be discussed below. The complete back-end system stores Sigfox, LoRaWAN and GSM data, however since the CoAP application protocol is not implemented NB-IoT is not officially supported. NB-IoT devices should be easy to include as the data translation layer discussed below supports the more complex version of the lightweight CoAP application protocol standard (HTTP).

**AWS EC2:** The core development of the centralized data gathering solution is hosted on an Amazon web services (AWS) Elastic Compute Cloud (EC2) instance to simplify the overall design and ensure stability. Security on the AWS EC2 instance is strictly controlled through white-listing certain IP addresses on ports and closing all unused ports, as ransomware attacks on open ports is a common occurrence. In order to manage the AWS EC2 instance through a Secure Socket Shell (SSH) connection, a unique Private Key Pair is required, which is used to improve security.

**Sigfox back-end:** The Sigfox back-end is maintained by the international Sigfox group, and allows access to data transmitted by nodes through the local Sigfox network. The Sigfox back-end allows a variety of device management features including: registering new devices, data access, call-back setups, device monitoring, registration status, service map, signal RSSI and SNR monitoring, device tracking and received gateway information. An example of the Sigfox back-end can be seen in Figure C.2. The back-end allows Sigfox messages to be forwarded to a custom back-end through the use of the HTTP Post

function. Down-link message is received from the user's custom back-end by the Sigfox back-end through a HTTP Get function, which is then forwarded to the specified device.

**TTN back-end:** The TTN's back-end system is maintained through the TTN industries and is similar to the Sigfox back-end. The back-end allows device management, device and application key management, data access, call-back setups, device monitoring, registration status, signal RSSI and SNR monitoring and received gateway information. Since the network is built by the community, back-end access to owned gateways is also available on the TTN back-end. Data can be accessed through a variety of integrations ranging from HTTP access to IFTTT integration. To simplify the data storage solution designed in this work, data is accessed similarly to the Sigfox back-end, through HTTP.

**Mosquitto MQTT broker:** Mosquitto offers an open-source MQTT protocol versions 3.1 and 3.1.1 broker implementation, allowing MQTT devices to publish/subscribe to various topics. Security regarding the MQTT broker is managed through a username and password required to publish/subscribe to the MQTT broker. Data is securely transferred from the broker to the data translation layer through the inherent quality of service offered by MQTT. All messages sent to subscribers need to be acknowledged by the recipient (data translation layer in this case). The MQTT broker is hosted on an AWS EC2 instance, which allows the broker to maintain a static IP address, which simplifies the overall design complexity. As the MQTT broker is hosted on an AWS EC2 instance, it ensures that the broker will be constantly on-line regardless of power-outages or network outages, which increases data reliability.

**MongoDB:** MongoDB offers a free and open-source Non-Structured Query Language (NoSQL) database, which stores data in flexible JSON-like documents, allowing the data structure to be changed over time. The unstructured nature of NoSQL allows multiple random fields to be defined to store the varying nature of data that is generated by the different devices and communication technologies. A major advantage of MongoDB is it offers the ease of integration into a common industry utilized MEAN-stack front-end web-site. Further, it allows direct access to the database to do back-end device administration through applications such as Robo 3T.

**Data translation layer:** The data translation layer (DTL) forms the core of the system architecture and is used to link the different system components together. However, the DTL is not the main focus of this thesis, therefore only a broad overview of the work done will be presented, with the general DTL structure seen in Figure C.4. The DTL is a python3 script that is launched on the AWS EC2 instance and has three major components; an HTTP request handler, MQTT subscription client and a MongoDB client. The HTTP request handler listens on port 8080 for any incoming traffic, verifies the data with a password and serializes the x-www-form-urlencoded data message. The HTTP request handler is used to store all the data received from the Sigfox and TTN back-ends. The MQTT subscription client which is used to store data received from GSM devices, connects to the MQTT broker with the predefined user name and password through the 'localhost' (same AWS EC2 instance) IP address on port 27017. After successful connection to the MQTT broker, the MQTT subscription client subscribes to the MQTT topic used by the GSM devices and forwards the received messages to the MongoDB client. The MongoDB client connects to the MongoDB hosted on the same AWS EC2 instance, and writes all the data received directly to the database. This can be accessed through the Robo3T user-interface by the administrator.

**MEAN-stack:** The java-script MEAN-stack is a full-stack solution which enables building fast and robust web applications using MongoDB, Express, AngularJS, and

Node.js. The front-end web development is a critical component in commercially deployed IoT solutions, however it is not a critical component of this thesis. Therefore, only a proof of concept MEAN-stack website was developed as can be seen in Figure C.3.

### **3.9.3 Closing remarks on the firmware and back-end architecture**

The firmware and back-end architecture designed in this chapter serves as the basis for experimental testing. Certain parts of the firmware differs depending on the situational testing, for example the addition of a GPS requires GPS-drivers and the use of pulse-counters requires the addition of interrupts. All parts of the firmware and back-end systems worked as required, and the modular design enables a wide variety of applications to apply the communication systems.

# Chapter 4

## Results

Utilising the developed test system a fundamental comparison of the different communication technologies can be achieved by analyses of the performance data collected. Section 4.1 describes the performance comparison of the different communication technologies. This compares the fundamental performance of the different communication technologies, regardless of how they are employed. Section 4.2 compares the real world usage of the different technologies, which is useful to enhance the performance in application. To verify the performance of LoRaWAN and Sigfox, Section 4.3 describes the practical results of using these communication technologies in real world applications.

### 4.1 Performance results analysis

This section validates the theoretical performance of the different communication technologies through practical testing. Tests are performed using the mk III iteration of the test devices, and the individual test setups are explained accordingly. Any firmware adjustments from the base design in Section 3.9.1 made for specific experiments will be stated accordingly in the section. The major aim of this section is that test needs to prove consistent and repeatable, thus test were performed several time (experimental test-setup dependent) to ensure that results obtained stayed consistent.

#### 4.1.1 Link budget

The results of the packet delivery ratio at different RSSI levels shown in Figure 4.1, can be used to determine the maximum coupling loss of each communication technology (according to Equation 2.6), as show in Table 4.1. As the antennas used by the GSM, NB-IoT and Sigfox's base stations are not known, a 2dBi receiver antenna gain is assumed, this is the typical value of omni-directional antennas. Transmitter and receiver losses is assumed to be 0 dB. The maximum coupling loss measured for the different technologies correlate to the theoretical maximum coupling loss listed in Table 2.5.

Comparing the measured link budgets, it is clear that the extra overhead available in the LPWAN solutions, Sigfox, LoRaWAN and NB-IoT will allow for better indoor coverage. This allows the LPWAN devices to be used in less than optimal operating conditions.

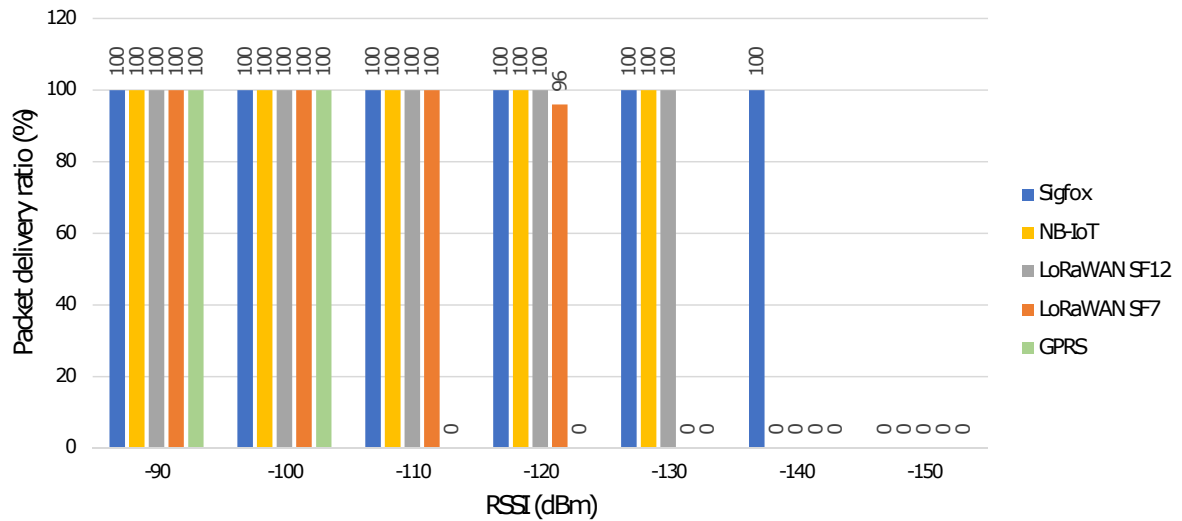


Figure 4.1: Packet delivery ratio of different communication technologies in different field test conditions

Table 4.1: Measured link-budget of different communication technologies

	Received power limit (dBm)	Transmitted Power (dBm)	Antenna Gain (db)	Maximum coupling loss (dB)
Sigfox	-140	14	5	159
NB-IoT	-130	23	5	158
LoRaWAN SF12	-130	14	5	149
LoRaWAN SF7	-120	14	5	139
GPRS	-100	23	5	128

## 4.1.2 Power-Consumption

Power consumption of the different devices is measured using the current logging device described in Section 3.7.

### 4.1.2.1 LoRaWAN, Sigfox and NB-IoT

Figures 4.2 to 4.4 show the current consumption of a 12 byte message at 3.3V for Sigfox and LoRaWAN, excluding the micro controller. It is important to note the peak currents drawn from each technology, as well as the current consumption profile. From Figures 4.2 to 4.4, it is clear that LoRaWAN at SF7 consumes drastically less power than LoRaWAN at SF12, due to the high transmission rate at SF7. It is also worthy to note the 2.8 mA idle current of the LoRaWAN modem, which can be reduced by switching the modem to sleep mode. Due to the three transmission repetitions of Sigfox, the the current consumption is drastically more than LoRaWAN at both spreading factors.

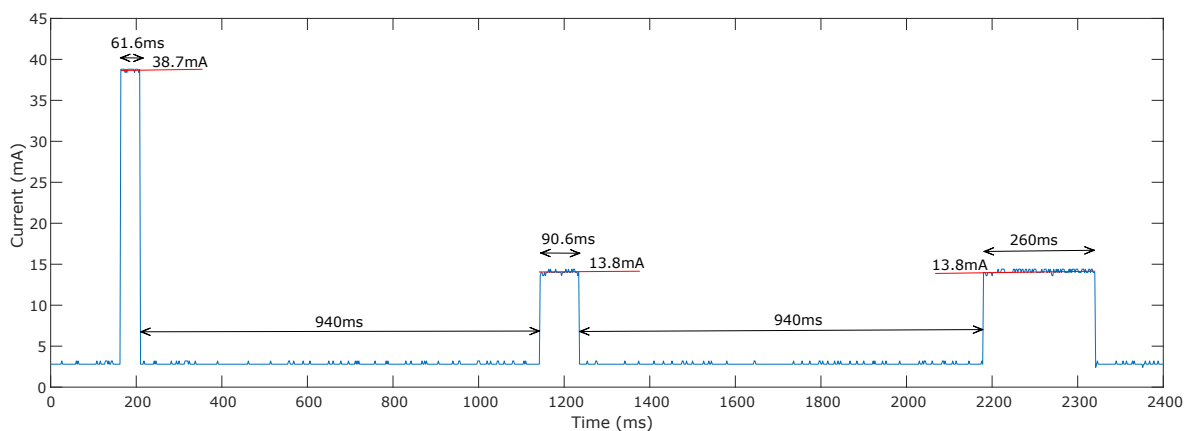


Figure 4.2: LoRaWAN SF 7 (RN2483) 12 byte transmission current-consumption at 3.3V

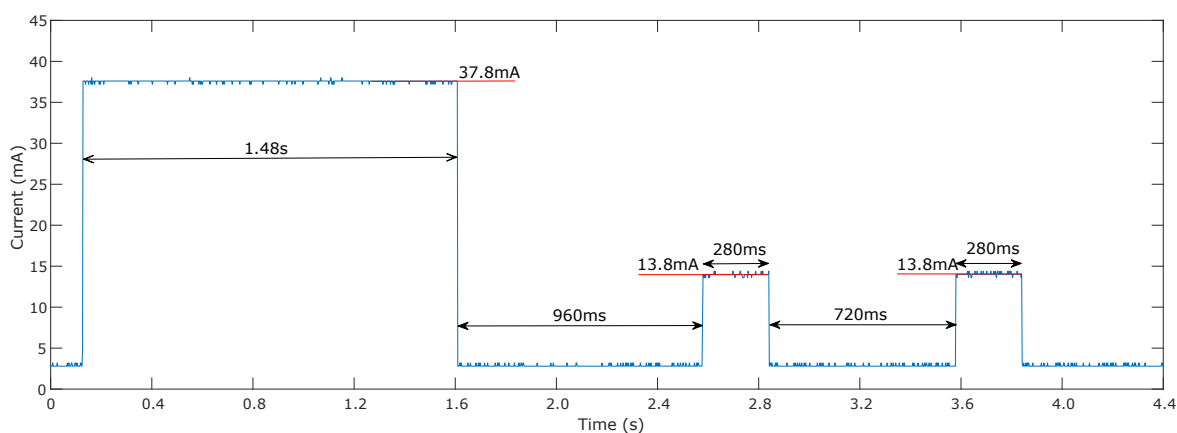


Figure 4.3: LoRaWAN SF 12 (RN2483) 12 byte transmission current-consumption at 3.3V

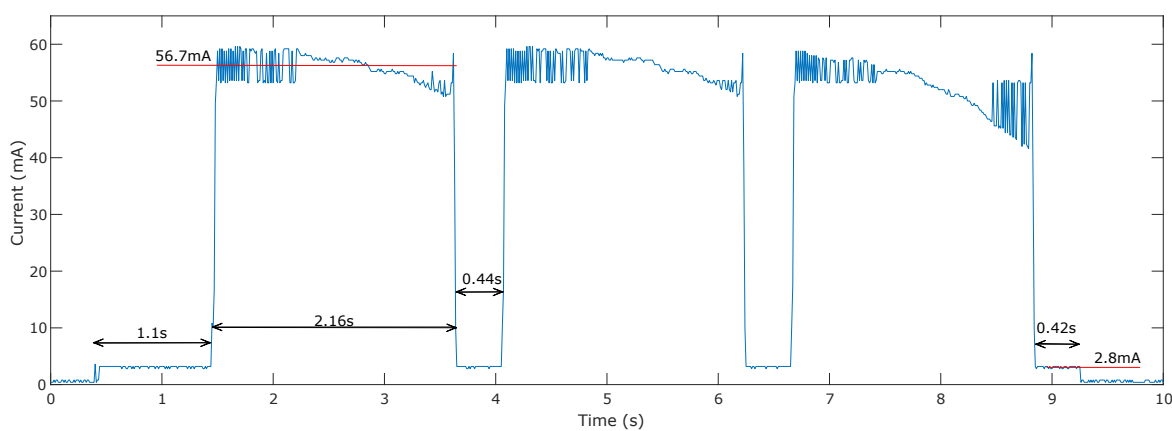


Figure 4.4: Sigfox (Sfm10r1) 12 byte transmission current-consumption at 3.3V

Measuring the power-consumption of NB-IoT requires measuring the different phases of the the current-consumption profile. The transmission current of a single transmission frame used to send a section of a 12-byte packet at 23dB is shown in Figure 4.5. To calculate the complete transmission time, the "AT+NEUSTATS" command is used

to measure the milliseconds the modem spent in transmission mode. The transmission current is significantly higher compared to LoRaWAN and Sigfox, due to the higher transmission output power.

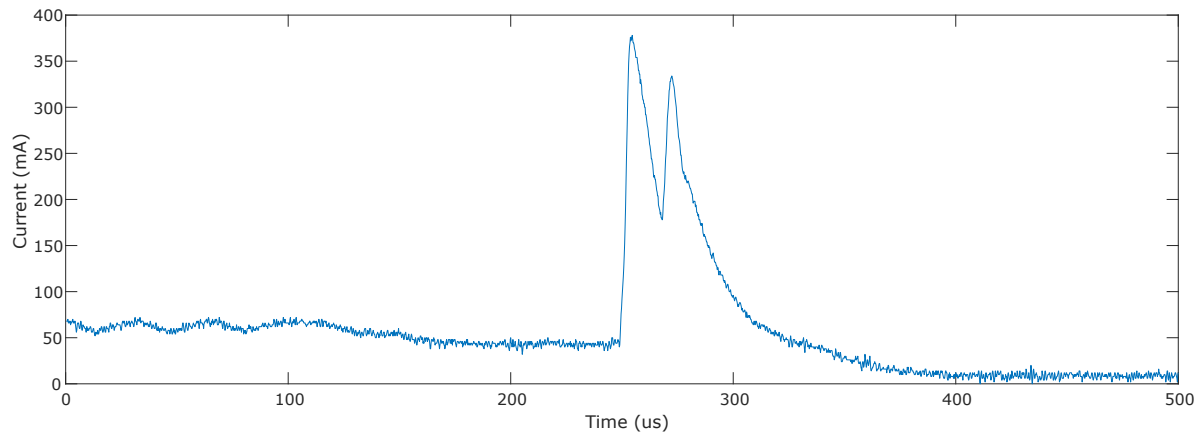


Figure 4.5: NB-IoT 12-byte transmission current-consumption profile at 3.4V

Figure 4.6 shows the complete power consumption profile of a single 12-byte packet. The modem moves from RRC-idle state to transmission state. Thereafter, the modem continues to be in RRC-idle state for 250s. This RRC connection phase is completely network operator dependent. The current consumption profile of the RRC-connection phase can be seen in Figures 4.7 and 4.8. A single RRC window consists of a receive frame with a current consumption of about 80mA at 3.4V and 10 ms duration.

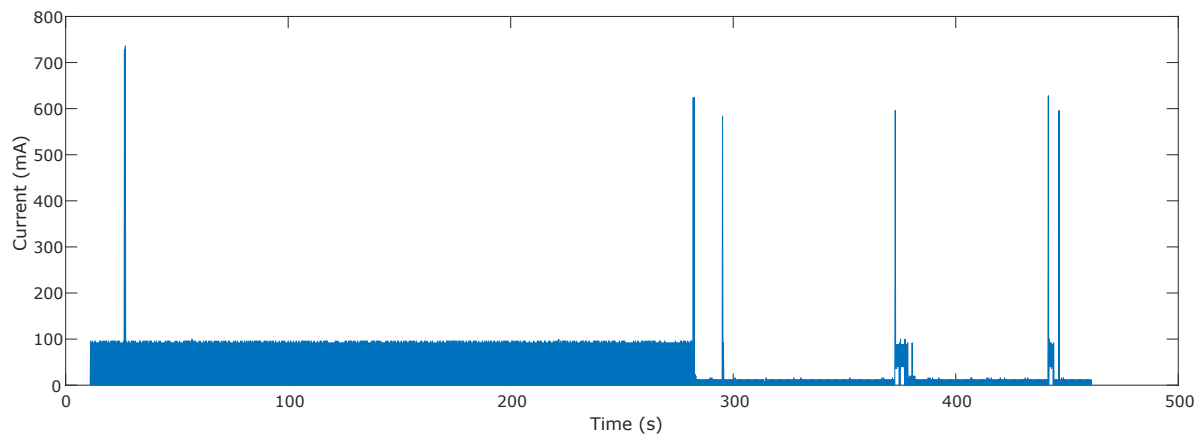


Figure 4.6: NB-IoT 12 byte transmission and RCC connection release current-consumption profile at 3.4V

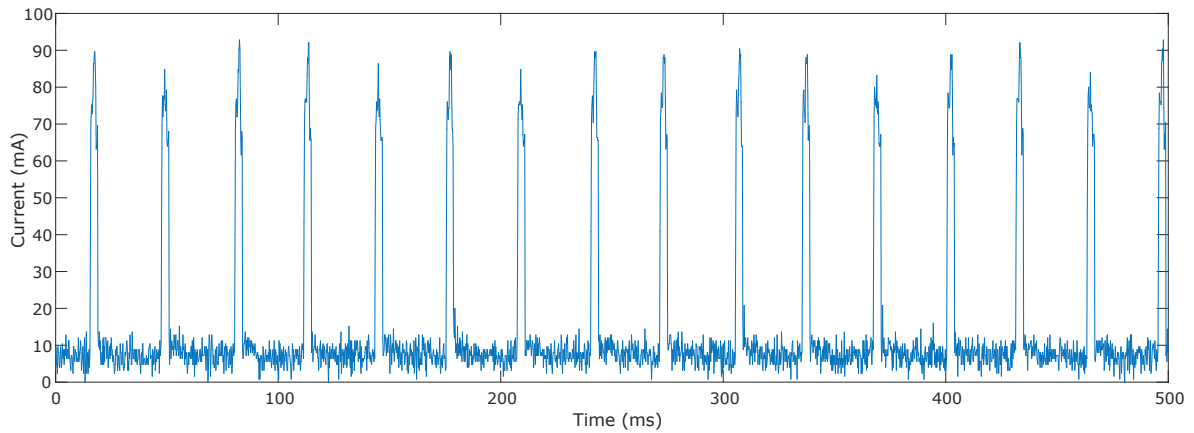


Figure 4.7: NB-IoT RCC connected current-consumption profile at 3.4V

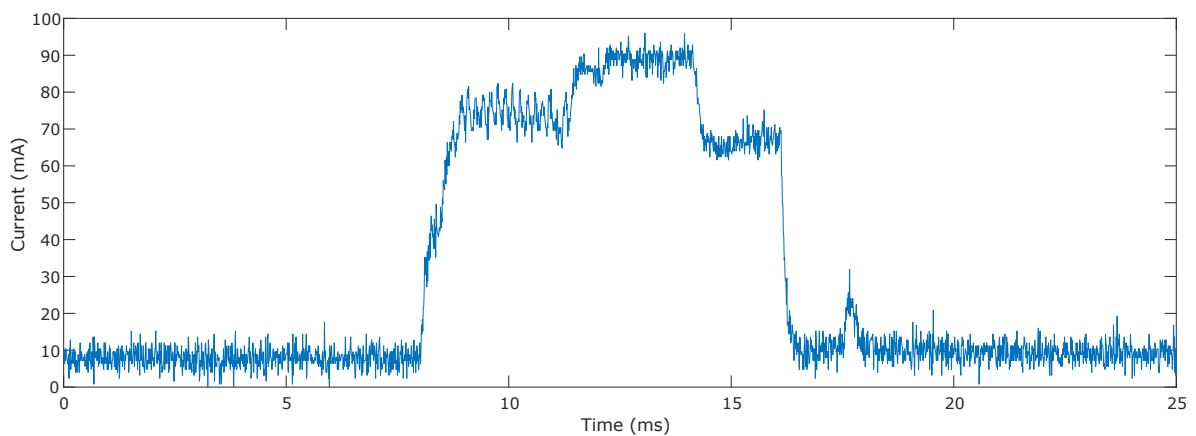


Figure 4.8: NB-IoT RCC window close-up current-consumption profile at 3.4V

Due to the excessively long RRC-idle state currently required by the MTN-network, no decisive conclusion can be made regarding the power-consumption of NB-IoT. Further cooperation between the network operator is needed to minimize the RRC-idle state to optimize the network for battery-driven applications.

If the packet transmission time in seconds is denoted by  $T_a$  and the transmissions per hour is known as  $d$ , the device remains in sleep mode ( $T_s$ ) for  $T_s = (3600 - T_a * d)$ . Thus, the current consumption of the modems and MCU in idle and sleep mode is crucial as it will contribute to a large part of the overall power-consumption. The same testing current logging device described in Section 3.7 is used to measure sleep and idle mode power consumption. The results of the modems sleep and idle tests can be seen in Table 4.2.

Using the information in Figures 4.2 to 4.8 and Table 4.2, a predictive analysis of the expected battery-life of the devices based on measured results can be made. To estimate the battery life it is assumed an ideal 9.25 Wh, 3.3 V (Sigfox and LoRaWAN) or 3.4 V (NB-IoT) battery is used. The ideal battery has no self-discharge rate, stays constant at 3.3 V/3.4 V and no voltage regulator is used. Table 4.3 highlights the current power differences between the varying technologies. In Table 4.3, it is assumed that each device transmits a single 12-byte message per hour and spend the remainder of the time in sleep mode. The current consumption and timing information is based on the measured values,



Table 4.2: Measured Sigfox, LoRaWAN, NB-IoT modem and MCU sleep and idle currents

Modem state	Operating Voltage (V)	Current
LoRa RN2483 idle	3.3	3.0 mA
LoRa RN2483 sleep	3.3	993 nA
Sigfox SFM10R1 idle	3.3	526 uA
Sigfox SFM10R1 sleep	3.3	1.04 uA
Sigfox SFM10R1 deep sleep	3.3	150 nA
NB-IoT Sara-N200 idle	3.4	7 mA
NB-IoT Sara-N200 sleep	3.4	3.7 uA
ATMega328P idle	3.4	4 mA
ATMega328P sleep	3.4	8 uA

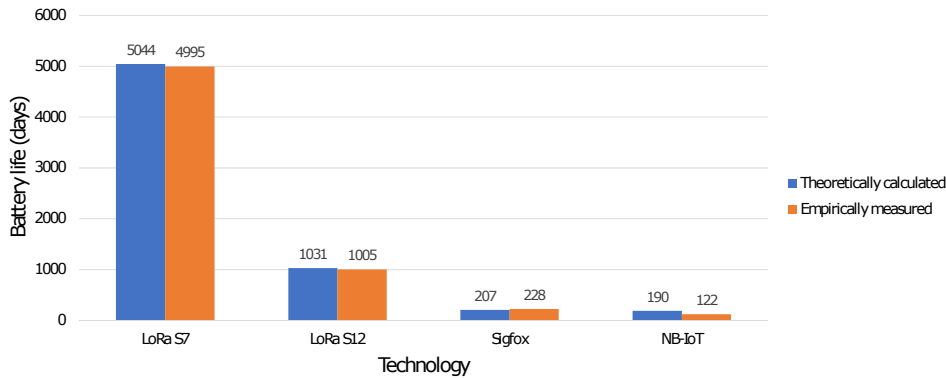


Figure 4.9: Theoretically calculated vs. empirically measured battery life expectation of the different communication technologies transmitting 6, 12-byte messages per hour, no MCU included

with no MCU power-consumption included. Using total average uW power-usage over an hour of each technology, shown in Table 4.3, a comparison can be drawn on the power consumption of each technology. It is clear that LoRaWAN SF7 is the most power-efficient, due to the short transmission burst. NB-IoT displays the worst power-consumption, due to the extended RRC-idle state.

To validate the measured power consumption of the different technologies, the measured transmission, receive and idle times and currents of the different modems are compared in Figure 4.9, with no MCU power consumption included using the ideal 9.25Wh battery. In the case of LoRaWAN and Sigfox, the expected empirically measured battery-life can be compared to theoretical data sheet current consumption values. The theoretical transmission time for Sigfox is based on the theoretical 100bps transmission speed. The theoretical transmission time for LoRaWAN SF7 and SF12 is based on the theoretical transmission speed calculated using Equation 2.2. In the case of NB-IoT, the practical measured transmission times are used in the theoretical data sheet calculations. Only the transmission time (through the use of the "AT+NEUSTATS" command), RRC-idle state and deep-sleep current of the NB-IoT modem is considered. For all NB-IoT measurements, it is assumed that the device will only stay in RRC-idle state for 20s as per data sheet opposed to the measured 250s.

From Figure 4.9 the low power consumption, due to the short transmission bursts, of LoRaWAN SF7 is evident. LoRaWAN SF12 and Sigfox has similar transmission times,

Table 4.3: Power consumption calculations for the different technologies transmitting a single 12-byte message once per hour

LoRaWAN SF7	Voltage (V)	Current (mA)	Power (mW)	Duty cycle (s/h)	Average power (uW)
LoRa Tx	3.3	38.7	127.71	0.0616	2.18526
LoRa Rx 1	3.3	13.8	45.54	0.0906	1.14609
LoRa Rx 2	3.3	13.8	45.54	0.26	3.289
LoRa Idle	3.3	3	9.9	1.88	5.17
LoRa Sleep	3.3	0.000993	0.003277	3597.708	3.274814
<b>Total:</b>					<b>15.06516</b>

LoRaWAN SF12	Voltage (V)	Current (mA)	Power (mW)	Duty cycle (s/h)	Average power (uW)
LoRa Tx	3.3	37.8	124.74	1.48	51.282
LoRa Rx 1	3.3	13.8	45.54	0.28	3.542
LoRa Rx 2	3.3	13.8	45.54	0.28	3.542
LoRa Idle	3.3	3	9.9	1.68	4.62
LoRa Sleep	3.3	0.000993	0.003277	3596.28	3.273514
<b>Total:</b>					<b>66.25951</b>

Sigfox	Voltage (V)	Current (mA)	Power (mW)	Duty cycle (s/h)	Average power (uW)
Sigfox Idle	3.3	2.8	9.24	6.48	16.632
Sigfox Trans	3.3	56.7	187.11	2.4	124.74
Sigfox Sleep	3.3	0.00104	0.003432	3591.12	3.423534
<b>Total:</b>					<b>144.7955</b>

NB-IoT	Voltage (V)	Current (mA)	Power (mW)	Duty cycle (s/h)	Average power (uW)
NB-Transmit	3.4	300	1020	0.0621	17.595
NB-RRC cycle 1	3.4	70	238	3.75	247.9167
NB-RRC cycle 2	3.4	85	289	1.875	150.5208
NB-IoT idle	3.4	8	27.2	14.125	106.7222
NB sleep	3.4	0.006	0.0204	3580.188	20.28773
<b>Total:</b>					<b>543.0425</b>

however the three duplicate transmissions of Sigfox significantly decrease battery life expectancy. NB-IoT's battery life is the worst, due to the 20s RRC-idle state following a transmission. NB-IoT also has a large discrepancy between the theoretically calculated battery life and empirically measured values, as the datasheet for the NB-IoT modem only provided averaged power consumption data.

Since the battery life of LoRaWAN and Sigfox can be modelled accurately, real world device use cases are investigated. NB-IoT is excluded from this comparison, since the measured power consumption values are significantly higher than the theoretical values due to the longer RRC-idle phase. The following battery life prediction aims to compare 1) packet-size and 2) transmission rate. For this experiment, the same ideal 9.25 Wh battery is assumed, with the power consumption of the ATmega328P included. It is assumed that the MCU and modem only wakes to transmit and then returns to sleep mode. The measured power-consumption values are used in a model, which considers the MCU idle and sleep power-consumption and time, as well as modem transmit, receive, idle and sleep power-consumption and time. The results can be seen in Figure 4.10 and Figure 4.11

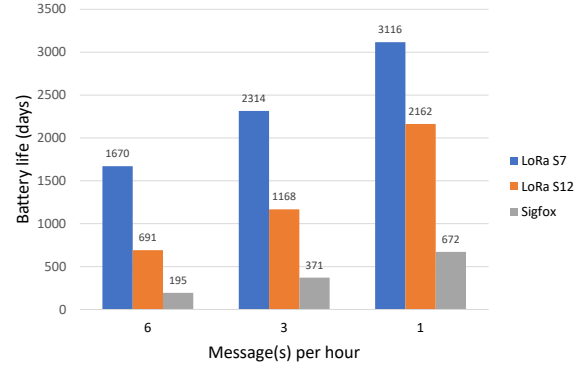
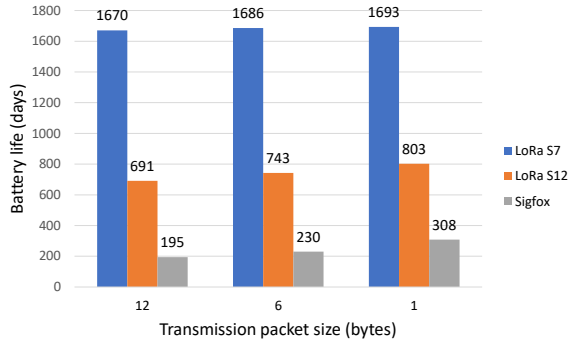


Figure 4.10: LPWAN battery life vs transmission packet size @ 6 messages per hour

Figure 4.11: LPWAN battery life vs transmission rate @ 12 byte messages

Figure 4.10 indicates that an increase in message size only drastically affects technologies with slow data-rates (Sigfox and LoRaWAN SF12). Although LoRaWAN SF7, will also experience decreased power-consumption by decreasing the transmission duration, the power-consumption savings is overshadowed by the sleep currents of the MCU and modem.

Changing the transmission rate from 3 packet per hour to 1 packet, as seen in Figure 4.11, it is expected to increase battery lifetime by nearly three times. However, changing the update rate only provides a limited increase in battery life, due to the relatively high sleep-currents of the MCU and modems.

As LPWAN devices are typically battery powered, investigating the power consumption of the different transmission power settings is of interest to device manufacturers. Table 4.4 indicates the measured current consumption of LoRaWAN SF7, LoRaWAN SF12 and Sigfox, as these are the only LPWAN technologies with user defined transmission power.

Table 4.4: LoRaWAN and Sigfox transmission current draw at different transmission powers

Technology	Transmission power (dBm)	Average transmission current @ 3.3V (mA)
Sigfox	0	25.6
	5	31.2
	10	36.1
	15	56.7
LoraWAN SF7	2	25
	8	33.1
	14	38.7
LoraWAN SF12	2	25.1
	8	33.3
	14	37.8

The trade off, by decreasing the transmitted power can be seen in the reduced received power as indicated in Figures 4.12 to 4.14. By decreasing the transmitted power, the link budget error margin is decreased. Therefore packet may fall below the base station receiver sensitivity, as can be seen by the missing packets in Figures 4.13.

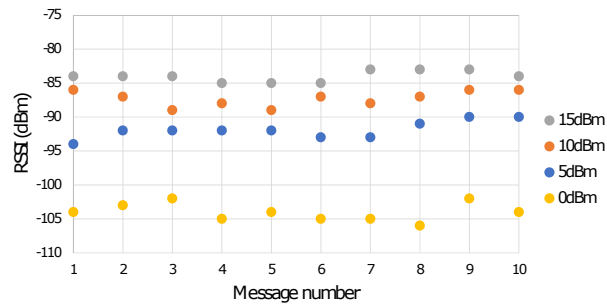


Figure 4.12: Sigfox transmitted power vs received power for 10 tests

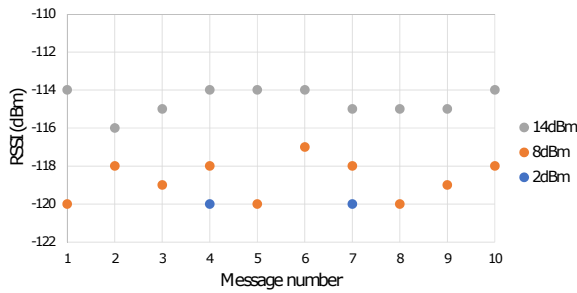


Figure 4.13: LoRaWAN SF7 transmitted power vs received power for 10 tests

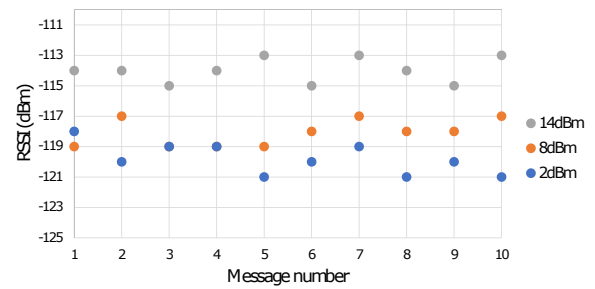


Figure 4.14: LoRaWAN SF12 transmitted power vs received power for 10 tests

#### 4.1.2.2 GSM

GSM current consumption is more sophisticated than the simplified LPWAN technologies, Sigfox and LoRaWAN. Due to the complex GSM standard, the device needs to communicate constantly with mobile network (paging) to be attached to the network. Upon start-up the device pages (transmission followed by reception frame) the network constantly, as can be seen in Figure 4.15. This constant connection between the device and the network bases station is used to register the SIM and IMEI to the mobile network.

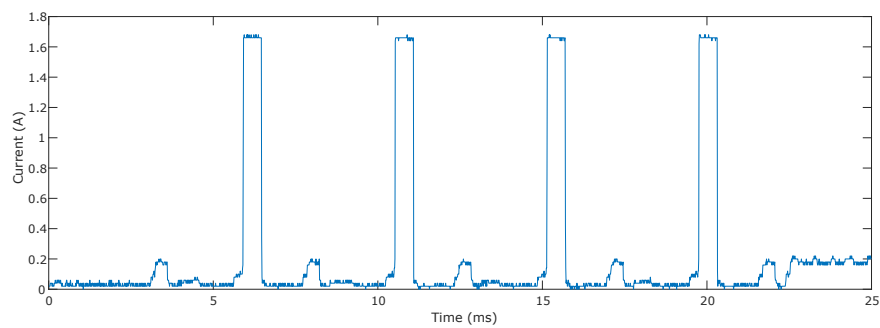


Figure 4.15: GPRS current consumption profile during network connection at 3.4 V

Once the device is connected to the GSM network, the current consumption is reduced to a idle state followed by reception windows, as can be seen in Figure 4.16.

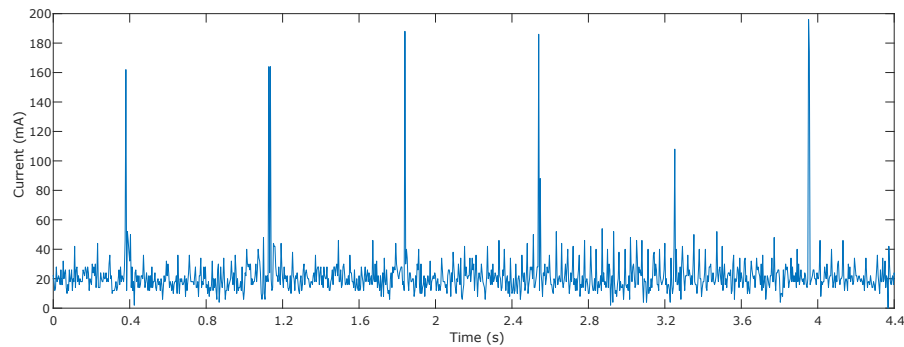


Figure 4.16: GPRS current consumption profile during network idle at 3.4 V

In order to measure the complete current consumption of a GPRS device, the current consumption profile needs to be logged from deep-sleep until transmission. However, the connecting to the GPRS network is dependent on network conditions. The time it requires a device to register ("`+COPS=0,0,\"MTN-SA\"`"), varies drastically, depending on the network conditions. Two connection attempt, depicted in the vast amounts of transmission frames transmitted by the device, is shown in Figure 4.17.

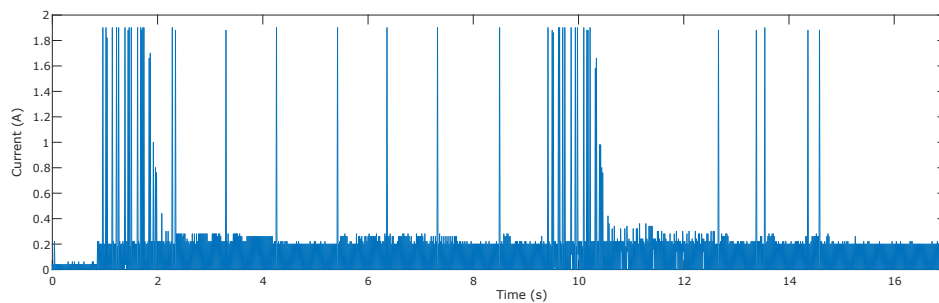


Figure 4.17: GPRS current consumption profile connecting to network from sleep at 3.4 V

Figures 4.16 to 4.17, identifies the major problems with GSM current consumption measurement. The measurement limitation is the short transmission/reception frames. The transmission/reception frames are typically 576.88 microseconds, therefore the extremely high sampling rate as defined in Section 3.7. Further, as the connection time to a GPRS network is dependent on network conditions connections can take be in the order of 50 seconds. This long duration and high amounts of sampled points creates a vast amount of sampled data, which is beyond the 2500 samples of a normal oscilloscope. Further, there are numerous other factors which influences the power-consumption of GPRS. The transmission power is dependent on the received signal quality and is adapted by the mobile-network. Populated mobile-networks can reduce the throughput of a device, therefore increasing the power consumption. Mismatched antennas can cause the transmission current to peak at 2.5 A at 3.4V.

Due to these various variables and measuring limitations, the power-consumption of GPRS could not be accurately modeled. However, from the data gathered, it is clear that GPRS is not optimized for battery-driven applications requiring years of operation. A simple example of the high-current draw of GPRS can be seen in the standby-time of early pre smart-phone GPRS cellphones.

### 4.1.3 Throughput

LoRaWAN supports data rates from 0.3 to 38.4kbps depending on the SF, however as a frame consists of the actual data and a 13 byte preamble (LoRaWAN protocol) the practical measured time on air varies drastically. The tested transmission times for different data packet sizes (excluding preamble) can be seen in Figure 4.18. In order to ensure packet delivery, TTN proposed a solution that defines a fair access/use policy that limits the Time on Air of each end device to a maximum of 30 seconds per day. This is based on 86400 seconds in a day, 8 frequencies on which data can be received, a 5% receive duty cycle on the gateway (minimalist stance of gateway reception time) and ensuring that 1000 nodes is supported per gateway. TTN also limits the amount of down link message to 10 12-byte messages per 24h, as base station is not able to receive transmissions from devices while it is transmitting.

$$(8 \text{ frequencies} \times 86,400 \text{ sec} \times 0.05 \text{ duty-cycle}) / 1,000 \text{ nodes} = 30 \text{ seconds per device}$$

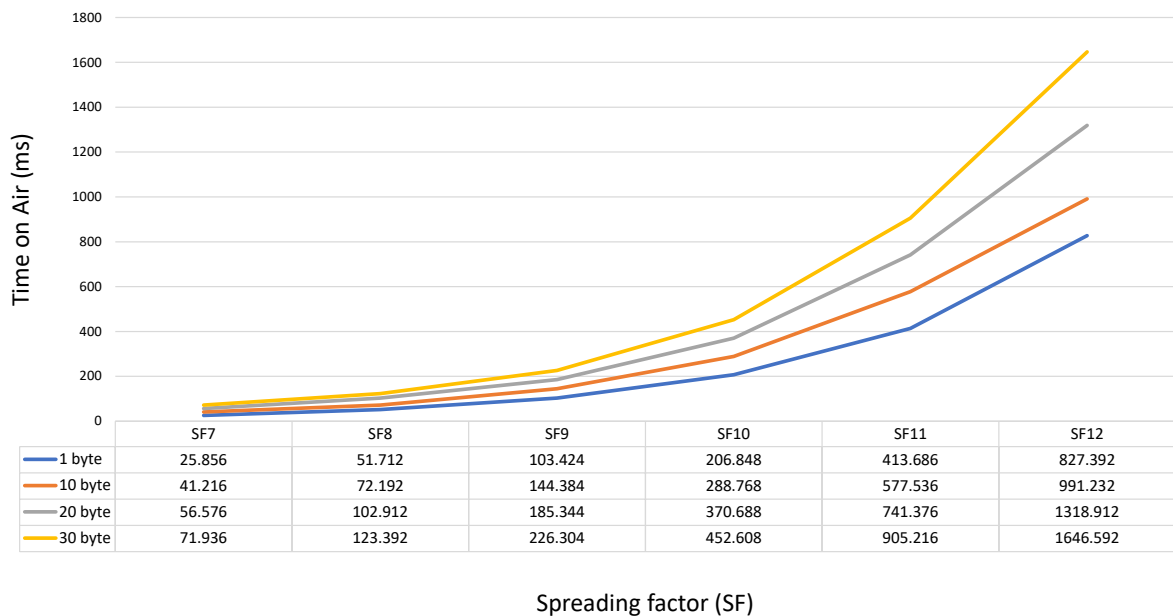


Figure 4.18: LoRa time on air vs spreading factor with CR 4/5 and 125 kHz bandwidth

Considering Figure 4.18, the 1% ISM band duty-cycle limitations and TTN's 30 s time-on air limitation the maximum data throughput per 24h can be determined as seen in Table 4.5. Although Table 4.5 list the maximum data throughput per 24h, it is also important to adhere to the per sub-band duty-cycle limitation. The time-off a specific sub-band required can be calculated using Equation 4.1, where  $T_{offsub}$  is the require time of a sub band,  $ToA$  is the time on air and  $D_{sub}$  is the duty cycle of the sub band. The time-off sub-band limitation will not limit the throughput per 24 hours, however it will limit the rate at which messages can be sent simultaneously.

$$T_{offsub} = (ToA/D_{sub}) - ToA \quad (4.1)$$

Table 4.5: LoRaWAN max messages per 24h vs spreading factor at CR=4/5 and BW=125 kHz

	Message size (bytes)				
	1	6	12	20	30
LoRaWAN SF 7	18646	16791	14004	12010	9897
LoRaWAN SF 12	748	655	582	477	404
LoRaWAN (TTN) SF 7	647	583	486	417	343
LoRaWAN (TTN) SF 12	25	22	20	16	14

Table 4.6: LoRaWAN measured transmission speed vs spreading factor at CR=4/5 and BW=125 kHz

Packet transmitted	Total frame size (bytes)	Time measured (ms)	Data rate (bps)
1 byte SF 7	14	46.4	2410
6 bytes SF 7	19	51.2	2970
12 bytes SF 7	25	61.6	3246
216 bytes SF 7	229	343.3	5336
1 byte SF 12	14	1160	96.55
6 bytes SF 12	19	1320	115.2
12 bytes SF 12	25	1480	135.1
48 bytes SF 12	25	2302	212

Unlike LoRaWAN, Sigfox is not only limited by duty-cycle and data rate, but additionally by business model. There is no sub-band duty-cycle limitation, thus all of the 140 12 byte messages can be transmitted sequentially with no time off sub-band required. To determine the data rate, the transmission time for different frames (data + protocol overhead) is measured, and the results are shown below in Table 4.7

Table 4.7: Sigfox measured transmission speed

Bytes transmitted (bytes)	Total frame size (bytes)	Time measured (s)	Data rate (bps)
1	15	1.32	90.91
6	20	1.84	86.96
12	26	2.2	94.55

As NB-IoT operates in the licenced spectrum there is no throughput restrictions, other than the data-rate restriction. Table 4.8 shows the measured uplink and downlink data rates in different signal quality environments (distances from gateway). Measurements were recorded using the "AT+NUESTATS="THP"" command to receive throughput information from the device. There is no clear correlation between the downlink data rate and the signal quality environment. Typically, the throughput of a NB-IoT network is network condition dependent, therefore results may vary. The results vary drastically from the theoretical physical layer data rate in Table 2.5, indicating that the NB-IoT network is still under development. Based on Table 4.8, 4.5 and 2.2, an overview of the number of 12-byte messages per 24h can be concluded in Table 4.9. The throughput values for NB-IoT and GPRS were theoretically calculated, using the maximum theoretical data rate of the two technologies. This was done to highlight the vast difference between the amount of data that can be transmitted via licensed and unlicensed band. NB-IoT and GPRS's

Table 4.8: NB-IoT measured up link and down link rate

RSSI (dBm)	TX pwr (dBm)	SNR (dB)	Physical UL rate (bps)	Physical DL rate (bps)
-76.2	1	124	2750	14193
-73.3	0	112	2750	14193
-67.2	14	83	2750	2250
-66.2	-4	10	2933	14193
-61.1	-10	167	2357	6939
-60.6	-11	138	2933	14193
-60.6	-11	139	2933	14193
-60.1	-11	155	2933	14193
-59.8	-11	140	2933	14193
-59.5	-7	76	2933	8461
-57.8	-25	139	2933	7096
-55	-18	129	2933	14193
-52.6	-16	151	2933	13750
-50.1	-19	156	2933	9736
-46.8	-22	225	2933	8921
-45	-23	93	2750	14193
-45.2	-23	91	2750	14193
-100.3	23	34	15625	11200
-100.1	23	39	15625	11200
-99.5	23	38	15625	11200

Table 4.9: Throughput comparison of the different technologies

Technology	Throughput (12-byte packets/24h)
Sigfox	140
LoRaWAN SF7	486
LoRaWAN SF12	20
NB-IoT	14 062 500
GPRS	19 260 000

throughput is highly dependent on the network conditions and operator configuration and is therefore beyond the scope of the project.

#### 4.1.4 Scalability

The simulation designed in Section 3.1.4 is adapted to model a typical LoRaWAN LPWAN star network. Two situations are considered, one where devices transmit a single 12-byte message every 1000s to a single base station, and another where each device transmits a single 12-byte message sequentially to utilise the full 1% duty cycle. No down link message or message acknowledgements are sent by the base station and it is assumed that the base station is only able to demodulate the packet with the higher RSSI level. Figures 4.19 to 4.22 demonstrate the packet delivery ratio for a varying amount of device at two different transmission rates.

Figures 4.19 and 4.20 illustrates that although LoRaWAN SF7 only operates on 3 channels, compared to the 8 available channels for LoRaWAN SF12, the scalability of LoRaWAN SF7 is drastically higher due to the short transmission bursts. Figures 4.21 and 4.22 highlights the reduced scalability, when operated at the maximum duty cycle, of LoRaWAN SF7 compared to LoRaWAN SF12, due to the reduced number of channels. The results indicates the low scalability of LoRaWAN per base station compared to NB-



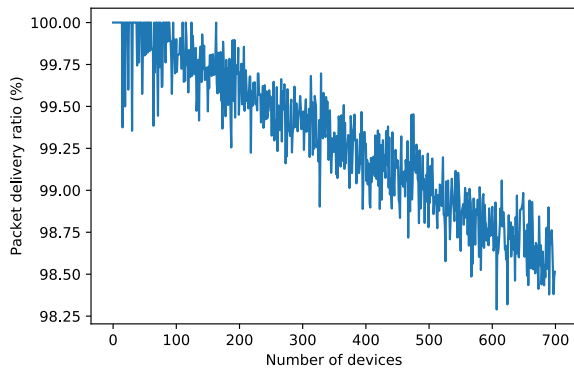


Figure 4.19: LoRaWAN SF7 packet delivery ratio vs. number of devices @ a single 12-byte message every 1000 s

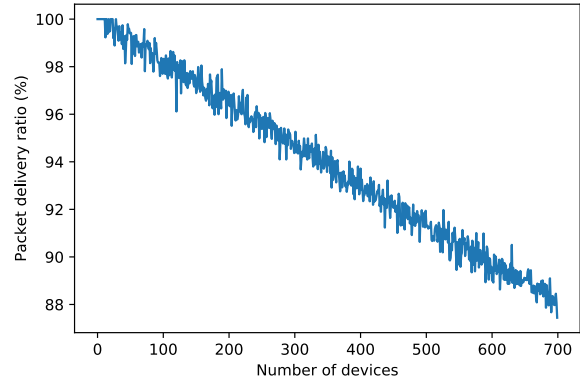


Figure 4.20: LoRaWAN SF12 packet delivery ratio vs. number of devices @ a single 12-byte message every 1000 s

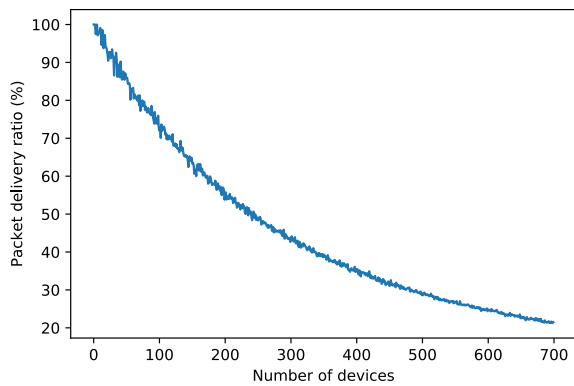


Figure 4.21: LoRaWAN SF7 packet delivery ratio vs. number of devices @ a single 12-byte message every 6.16 s (1% duty cycle)

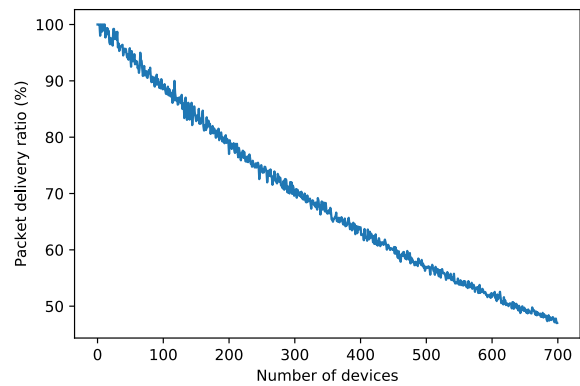


Figure 4.22: LoRaWAN SF12 packet delivery ratio vs. number of devices @ a single 12-byte message every 148 s (1% duty cycle)

IoT and GSM, which is due to the limited amount of channels and lack of any scheduling between devices. To compensate for the low scalability, an increase in spatially diverse base stations will allow packet to be received by multiple base stations at varying received power level.

To determine the scalability of Sigfox, two simulations is established. The first simulation, shown in Figure 4.23, determines the maximum amount of Sigfox devices transmitting a 12 byte message every 1000s to a single base station. The simulation deducted that 55000 devices transmitting the base station will reach the 270 simultaneously transmitting devices which ensures a 99.9% PDR. The second simulation demonstrates a varying amount of devices transmitting a 12 byte message every 1000s to a single base station. The simulation analyses any collision in time and frequency domain for each message, and determines if at least one of the three frames are correctly received. The simulation, shown in Figure 4.24, indicates the extremely high scalability of a single Sigfox base station. The computational requirements to calculate more than 8000 devices increases drastically, therefore, this simulation only aims to support the first Sigfox scalability simulation.

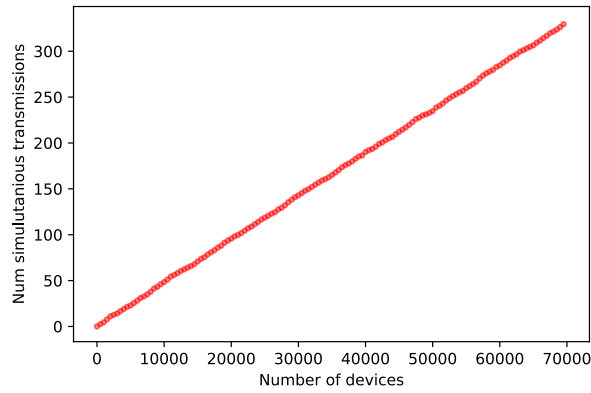


Figure 4.23: Sigfox number of simultaneous transmissions vs. number of devices transmitting

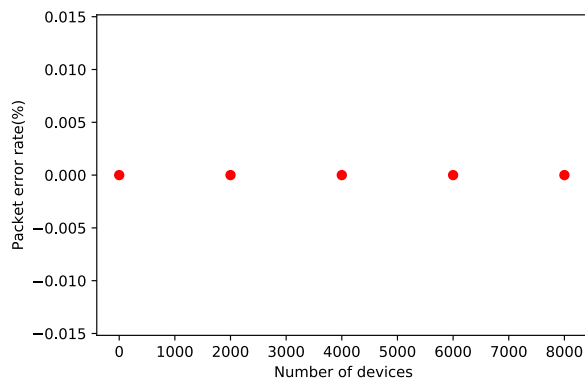


Figure 4.24: Sigfox packet error rate vs. number of devices transmitting

## 4.2 Application results analysis

This section investigates the extent to which different application metrics affects performance of the different communication technologies.

### 4.2.1 Antenna

As all of the mk III boards were designed with a SMA connector, antennas were simply exchanged as all of the modems a required  $50\Omega$  impedance antenna.

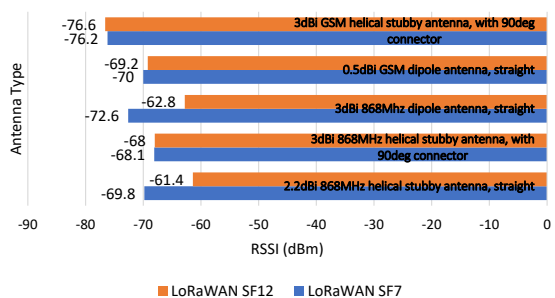


Figure 4.25: Comparison of different antennas in terms of signal strength (LoRaWAN)

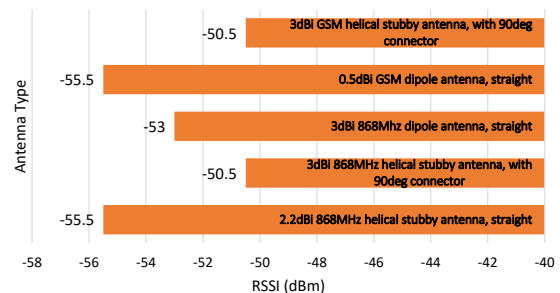


Figure 4.26: Comparison of different antennas in terms of signal strength (GSM)

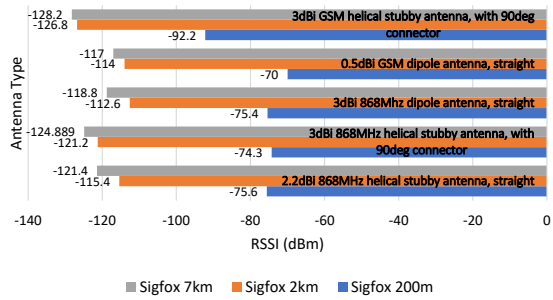


Figure 4.27: Comparison of different antennas in terms of signal strength (Sigfox)

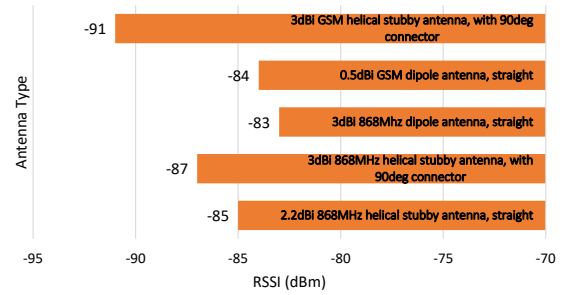


Figure 4.28: Comparison of different antennas in terms of signal strength (NB-IoT)

The results, seen in Figures 4.25 to 4.28, indicate that the 3dBi 868MHz dipole antenna delivered consistently good performance. This is substantiated by the anechoic chamber tests, seen in Appendix A, which verifies the low VSWR and good omni-directional radiation pattern of the 3dBi 868MHz dipole antenna. The 3dBi GSM helical antenna with 90 degree connector performed the worst in the tests, except for the GSM test. This degraded performance is due to the irregular radiation pattern of the antenna indicated by the Anechoic chamber tests. The antenna test attests to the importance of choosing a high quality antenna with a verifiable radiation pattern, as this will significantly improve the link budget of the communication system. Moreover, it is important to utilize an antenna designed for the application's specific frequency.

## 4.2.2 Polarization

Polarisation tests results, using a vertically polarized 3 dBi dipole 868 MHz omni-directional antenna, can be seen in Figure 4.29. As the LoRaWAN gateway was designed in Section 3.8.3, the receiving antenna model is chosen as vertically polarized, similar to the antenna used by the Sigfox base station receiver antenna. The polarization mismatch verifies the drastic reduction in received power. The polarization mismatch RSSI reduction measured is not nearly as drastic as the theoretical 100% reduction calculated by Equation 2.5. This is due to the effects of multiple paths from transmitter to receiver introducing reflections. Minimal, negligible RSSI reduction is experienced by NB-IoT as mobile network operators utilizes a dual polarization base station antenna design [89].

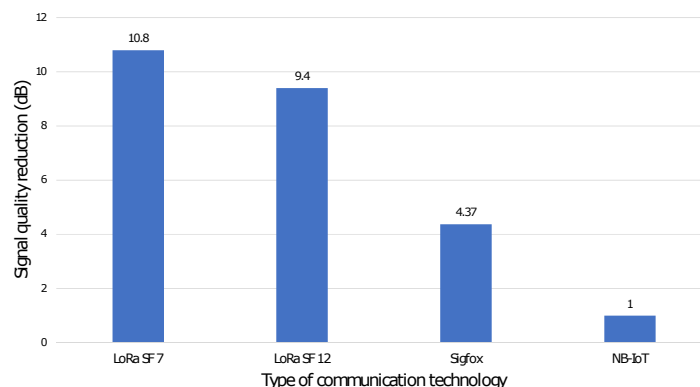


Figure 4.29: % RSSI reduction due to 90° angle polarization shift

### 4.2.3 Near-field interference

To ensure accuracy, five 12-byte messages are sent by the LoRaWAN and Sigfox device, the RSSI values retrieved from the corresponding back-ends, and the average calculated. The GSM measurements were done through adapting the firmware to check the signal quality from the device ("AT+CSQ") and transmitting the returned RSSI value to MQTT broker. The NB-IoT measurements were directly tested through a USB-UART connection utilizing the "AT+UESTATS" command, as no CoAP integration has been implemented. In the case of NB-IoT and GSM, the transmission power is measured constantly to ensure that it is kept consistent throughout the tests. The transmission environment is kept constant for all devices through all of the tests. A baseline signal quality test is done, and with the different near field interference objects introduced and measured. The results can be seen in Figure 4.30, with the near field interference reduction displayed as a percentage of the baseline signal quality, as this provides a better comparative overview.

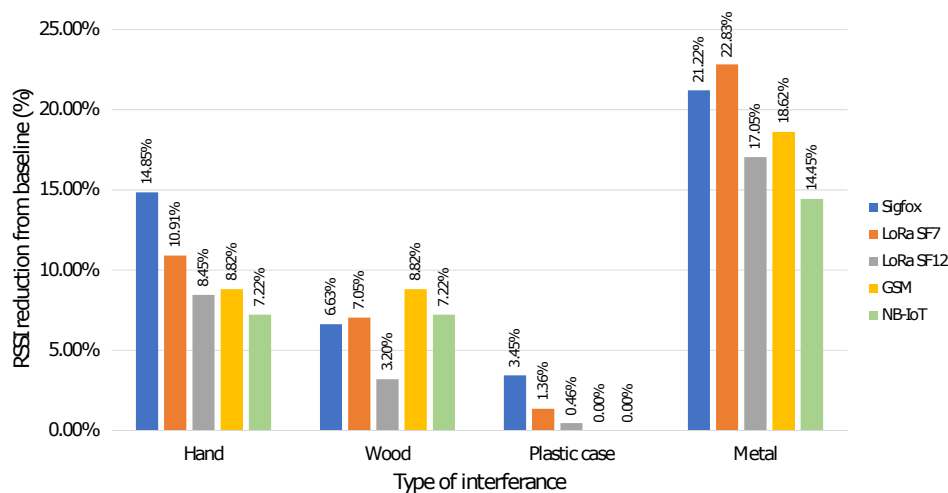


Figure 4.30: Average % RSSI drop from baseline caused by near-field interference

From the results of the different tests, seen in Figure 4.30, it is clear that the type of material causing the near-field interference is the most important factor to consider. Near-field interference caused by metal-produced the largest antenna-detuning, and therefore resulted in the largest reduction in RSSI, while the PVC enclosure produces minimal negligible interference. The human body consists mostly of salt water, which is a lossy dielectric which absorb RF energy and attenuate electric fields, therefore leading to the illustrated high performance loss. As the location of the GSM base station is unknown, no clear conclusion could be drawn from a comparison of the resilience to near-field interference between the different technologies. The tested values indicate that the important factor to consider, will be the effect of near-field interference will be on the VSWR of the antennas.

## 4.2.4 Path Loss

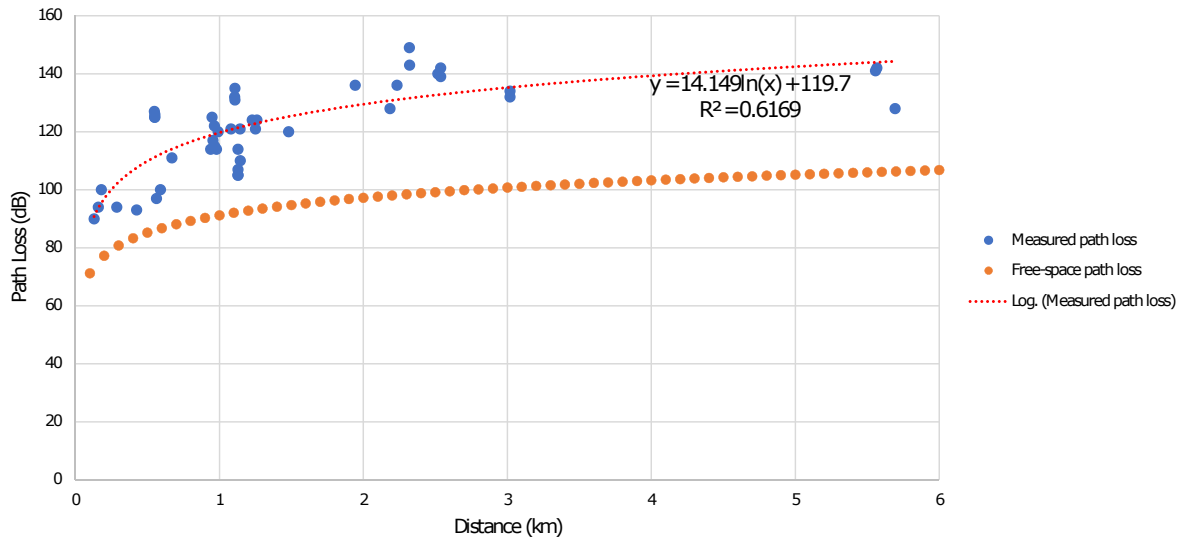


Figure 4.31: Sigfox theoretical free-space path-loss vs measured path-loss

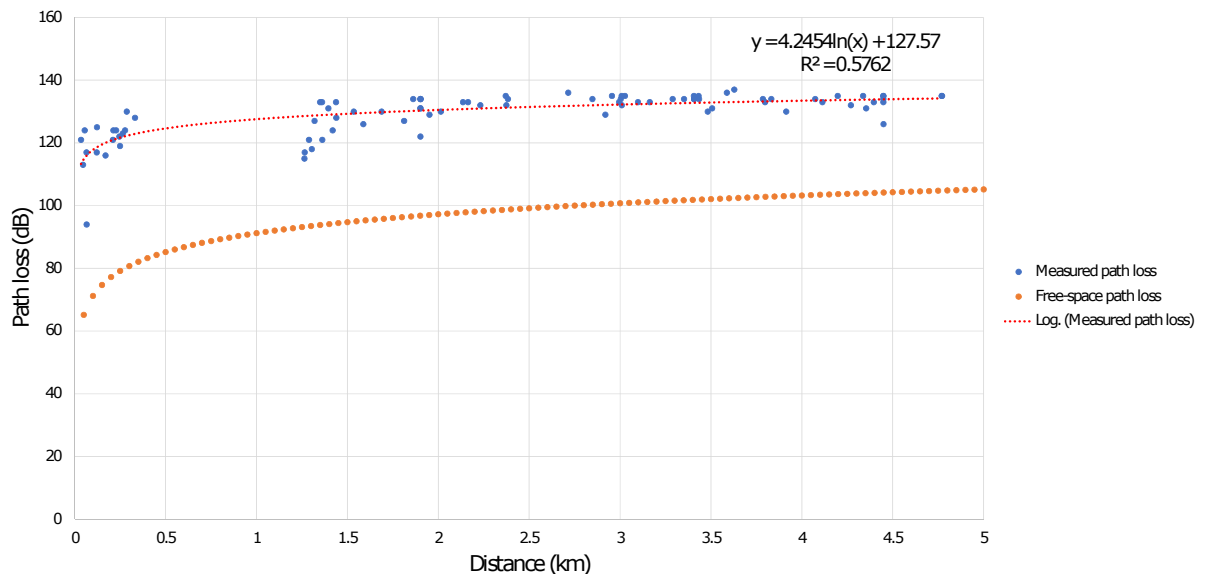


Figure 4.32: LoRaWAN theoretical SF7 free-space path-loss vs measured path-loss

The practical measurements for Sigfox and LoRaWAN produced a trend line data correlation  $R^2$  value of 0.6169 and 0.5762 respectively, correlated to a logarithmic regression line shown in the Figures 4.31 and 4.32. The values are lower than expected, due to extreme variance in the semi-urban environment conditions in Stellenbosch, with wide-open areas followed by extremely densely populated areas. Although the  $R^2$  values are not accurate enough to draw concrete conclusions, as regression line systematically over and under-predicts the data at different points along the curve, the data can be used as a proof of concept test. The GPS path-loss modelling technique can be used by network operators who aim to place new base stations at sites.

## 4.2.5 Coverage



Figure 4.33: Measured RSSI (dB) network coverage of the different networks in the testing area

The coverage map provided in Figure 4.33 shows the excellent coverage provided by the legacy GPRS network (MTN). Moreover, it highlights the current lack of multiple LoRaWAN base stations covering the testing area, as no coverage was detected at one testing location. Sigfox coverage is consistent, as there are multiple base stations covering the testing area. NB-IoT's coverage is relatively good considering that only a single base station is covering the entire testing area. This is due to the high unobstructed base station location and the increased transmission power of NB-IoT.

## 4.3 Practical results analysis

In order to validate the certain aspects of the performance results obtained in Section 4.1, data is collected from a Sigfox and LoRaWAN application, shown in the following sections.

### 4.3.1 Sigfox results

Data is collected from 20 Sigfox water-meters installed in random locations across the Western-Cape. The water meters utilizes the same ATmega328P MCU, 3.3V linear regulator and WsSfm10r1 Sigfox modem and are programmed to report a 6-byte water meter reading every 10 minutes. These water-meters typically reside in manholes, thus signal quality is degraded through the lack of line of sight as well as the the far field interference caused by the manhole cover. The data collected from the Sigfox water meters

can be seen in Table 4.10. In Table 4.10, the T#msg is the number of packets received by the Sigfox network in total for the complete duration of the measured period, A#msg is the calculated number of messages that was transmitted by the device, based on the preprogrammed transmission frequency of the device's firmware, %PDR is the Packet delivery ratio calculated based on the previous two values, RSSI(dBm) and SNR(dB) are averaged values across the whole testing period.

Table 4.10: Sigfox water meters signal quality analysis

Dev ID	Start Date	T #msg	A #msg	%PDR	RSSI (dBm)	SNR (dB)
397AD1	3/16/2018 9:06	7437	11149	66.71%	-136.43	14.68141
397BC6	3/14/2018 12:43	9855	11568	85.19%	-137.952	13.04
2E61C5	5/14/2018 10:54	2194	2568	85.44%	-129.8	15.27
3C6E91	5/18/2018 9:30	1597	1731	92.26%	-121.083	23.23
3979E9	5/2/2018 8:46	3933	4129	95.25%	-140.589	9.961526
3D596F	5/18/2018 11:18	1673	1723	97.10%	-107.916	22.42971
373706	4/24/2018 14:30	5085	5212	97.56%	-131.99	18.98
397A89	4/10/2018 8:31	7477	7566	98.82%	-123.27	27.65
397D18	3/13/2018 7:44	11759	11889	98.91%	-126.584	24.32
397B08	3/26/2018 10:21	9536	9576	99.58%	-124.19	26.1556
397B04	3/29/2018 10:27	9281	9281	100.00%	-134.74	15.8991
397B10	3/13/2018 14:05	11727	11727	100.00%	-130.204	20.985
397BA3	4/11/2018 9:42	7337	7337	100.00%	-126.72	24.54
3979DD	3/29/2018 10:51	9596	9596	100.00%	-128.783	21.589
3979EE	4/11/2018 13:53	7150	7150	100.00%	-131.1	19.8
37371C	3/15/2018 17:21	9513	9513	100.00%	-121.69	27.85
39432C	3/29/2018 9:59	8778	8778	100.00%	-123.65	26.35
39433A	3/12/2018 9:32	11927	11927	100.00%	-107.62	41.47
39796A	3/26/2018 10:25	9340	9340	100.00%	-138.03	12.532
391636	3/13/2018 15:58	11950	11950	100.00%	-113.68	35.76

The RSSI and SNR remained consistent for most devices, except Dev ID: 2E61C5, where signal quality drastically improved at 5/21/2018 11:51:21 AM, from 67.44%PDR to 96.67%PDR, -138.06 dB to -126.21 dB RSSI and 11.4951 dB to 16.9148 dB SNR. Dev ID: 3C6E91 saw a drastic signal quality increase between 5/21/2018 11:53:01 AM and 5/24/2018 8:23:54 PM, from 90.82%PDR to 97%PDR, -128.51 dB to -97.98 dB RSSI, 22.44 dB to 25.70 dB SNR and Dev ID: 3D596F saw drastic fluctuations in RSSI. These fluctuations can be attributed to the variation in the Sqwidnet network being changed, with new base stations added and base stations being offline. The PDR achieved by the water meters at different RSSI levels validates the Sigfox results in Figure 4.1. The total RSSI distribution of the packets received can be seen in Figure 4.34, while the total SNR distribution of the packets received can be seen in Figure 4.35. These figures illustrate the advantage of the larger link budget of LPWAN technologies when used in extended coverage situation such as in manholes or indoors.

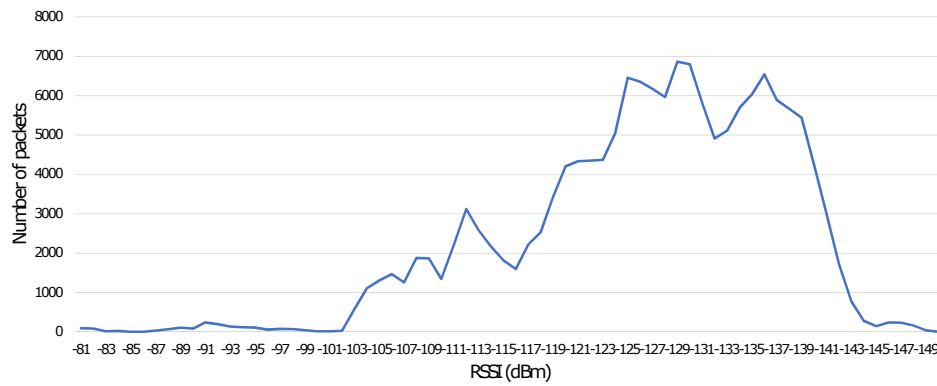


Figure 4.34: Sigfox field-test RSSI

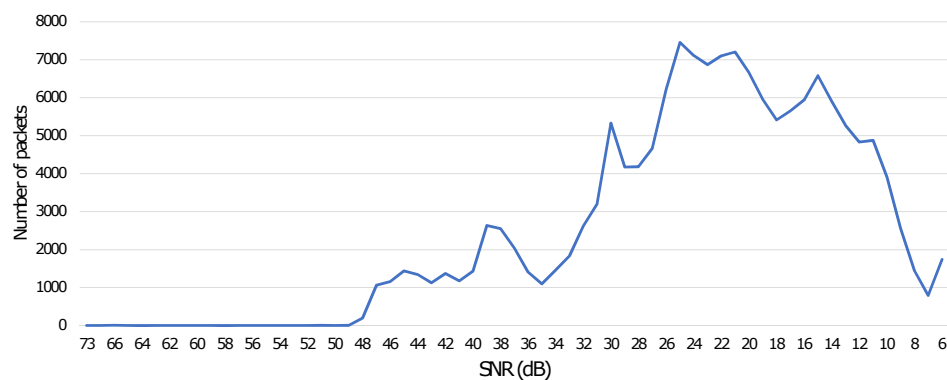


Figure 4.35: Sigfox field-test SNR

The average RSSI value for packets for which all three of the transmitted frames were received was  $-124.175$  dB, which accounted for 76.24% of the total packet, for two frames the average RSSI value was  $-133.03$  dB (16.19% of total packets) and for only a single frame, the RSSI average was  $-137.95$  dB accounting for 7.57% of the total packets.

### 4.3.2 LoRaWAN results

LoRaWAN results were obtained through the crowd sourcing application, TTN Mapper. This is an open source TTN coverage mapping application. The data is either gathered through a combination of a TTN LoRaWAN device transmitting a message and a smart phone application which is within proximity of the device logging the GPS and RSSI values, or through a GPS equipped TTN LoRaWAN device transmitting the coordinates. These measurements therefore are all devices which tend to be mobile. The dataset used in this test is messages sent to the DIY gateway built in Section 3.8.3 on a random day. Figures 4.36 and 4.37 highlights the choice of device makers to use LoRaWAN SF7, as it allows a higher throughput in a 24h cycle. The results further indicate that devices tend to be used in various deep coverage locations, specifically environments where signal quality is sub-optimal. Figure 4.38 verifies the assumption in the LoRaWAN scalability simulations that devices using LoRaWAN SF7 only operates on 3 channels, compared to the 8 available channels for LoRaWAN SF12.



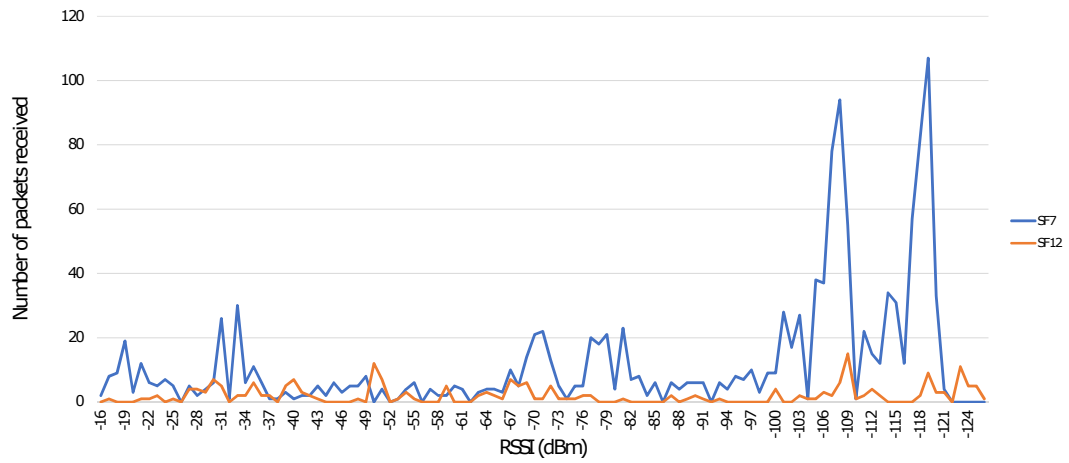


Figure 4.36: TTN LoRaWAN packets RSSI distribution at CR=4/5, BW=125

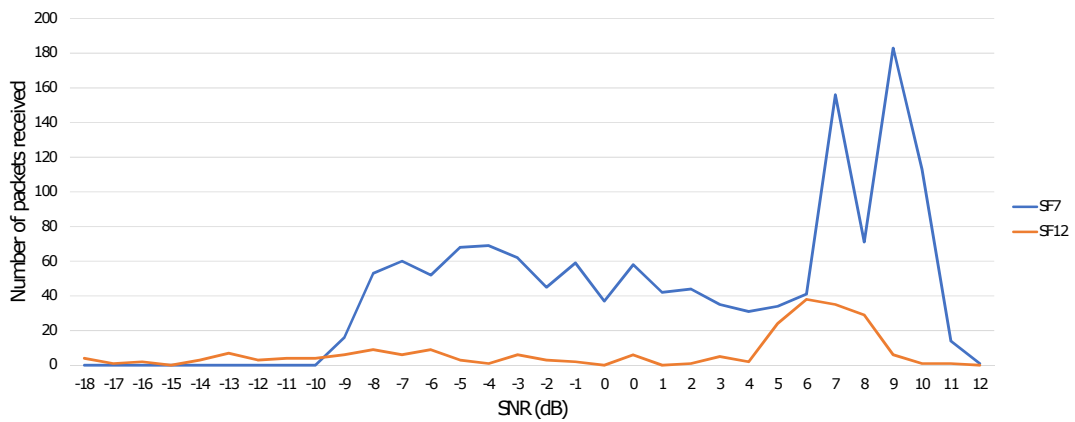


Figure 4.37: TTN LoRaWAN packets SNR distribution at CR=4/5, BW=125

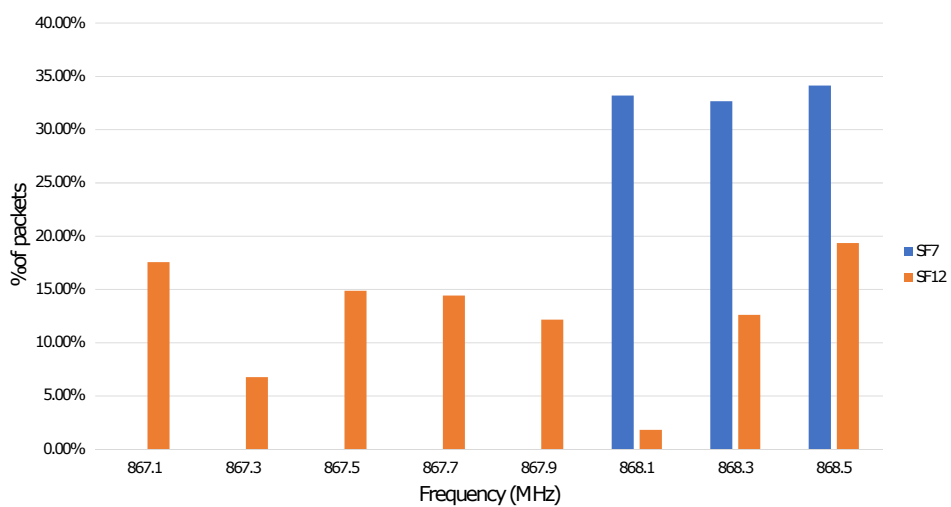


Figure 4.38: TTN LoRaWAN packet frequency distribution at CR=4/5, BW=125

### 4.3.3 Summary

The performance comparison, based on the literature review, experimental testing and simulation of the different communication technologies can be summarized in Figures 4.39 to 4.42. This summary only aims to provide a visualised qualitative overview of the different technologies, however it highlights the vast performance differences of the networks.

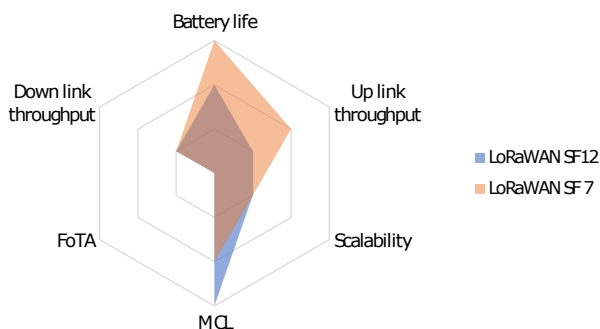


Figure 4.39: LoRaWAN performance summary

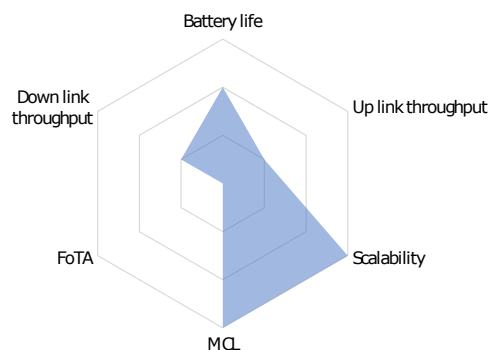


Figure 4.40: Sigfox performance summary

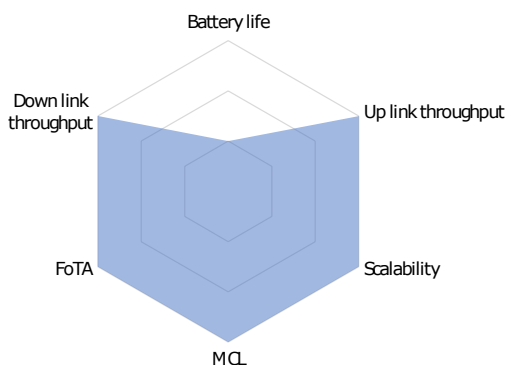


Figure 4.41: NB-IoT performance summary

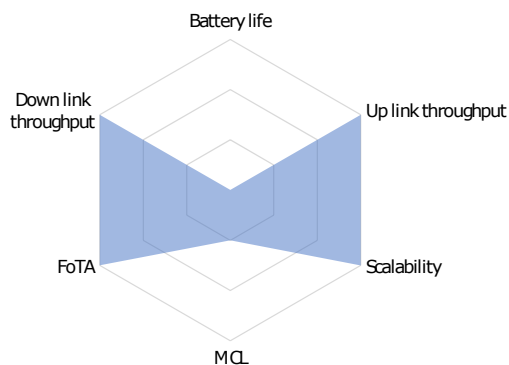


Figure 4.42: GPRS performance summary

# Chapter 5

## Conclusion and recommendations

### 5.1 Comparative conclusion

Based on the performance analysis of the different communication technologies it is clear that there is no single solution to all IoT applications. However, certain technologies fair better in IoT applications with varying throughput, scalability, coverage and power-consumption requirements.

**Battery life:** In applications where device battery life is a crucial factor, either LoRaWAN or Sigfox is recommended, due to the completely asynchronous nature of these technologies. Practically measured values indicated a battery life advantage of LoRaWAN SF 7 of five times greater than LoRaWAN SF 12 and nearly 25 times that of Sigfox. This is mainly due to the extremely long time-on-air of LoRaWAN SF 12 and Sigfox. Through continuous development with the mobile network operators to reduce the RRC-idle phase of NB-IoT, NB-IoT could potentially also feature minimal power consumption comparable with the likes of LoRaWAN and Sigfox.

**Throughput:** Throughput between the different technologies is vastly different, and should rather be compared in either the licensed spectrum category (NB-IoT and GPRS) or the unlicensed spectrum (Sigfox and LoRaWAN). Applications that require vast amounts of data to be transmitted, such as real time vehicle fleet monitoring, GPRS and NB-IoT is recommended as they are not duty-cycle limited. The decision between GPRS and NB-IoT will be based on the battery life requirements of the IoT device, with NB-IoT having the advantage. In the case of extremely low-throughput applications, such as water-meters, power meters and weather stations, Sigfox is recommended, as it offers a scalable solution with no base station costs involved. Although it limits the 12-byte throughput per 24h to 140 messages, it is more than the 20 messages offered by LoRaWAN SF12.

**Scalability:** In deployments where vast amounts of devices needs to be connected, such as in smart-cities, either Sigfox, NB-IoT or GPRS is recommended, as they offer more than 50 000 devices being supported by a single base station. However, through increasing the amount of spatially diverse base stations, LoRaWAN will also work in a scalable deployment.

**Down-link latency:** In applications where down-link latency is a critical component, only GPRS will suffice, as it is the only technology that requires constant paging between the base station and the end device.

**Down-link throughput:** Any applications requiring bi-directional communication, more than 120 bytes per 24h, should use NB-IoT or GPRS, as Sigfox and LoRaWAN is limited by the duty-cycle limitations of the base station.

**Coverage:** For, IoT devices used in extended coverage situations, such as deep-indoor devices or remote locations, either Sigfox or NB-IoT is recommended, as these technologies offer a maximum MCL of higher than 158 dB. IoT devices used in general use case, would benefit from the large scale deployment of the GPRS network, which provides excellent coverage due to the legacy infrastructure.

**FoTa:** Only GPRS and NB-IoT are able to offer firmware over the air upgrades to IoT devices, as LoRaWAN and Sigfox are limited in band-width.

## 5.2 Use cases

To conclude the different metrics, a typical array of IoT-applications are identified and explored, with the suitable IoT-network identified in each case. To expand these IoT-applications, a brief summary of the requirements of various other IoT-applications is provided in Table 5.1, with the usability of each technology in evaluated in Table 5.2.

### 5.2.1 Smart farming

IoT application in smart-farming, such as soil-sensors, temperature sensors, animal tracking ect. allows monitoring and controlling certain factors to allow optimum conditions for plants and animals to maximize the harvest capacity and animal health. Typically, these applications are geographically distributed in locations that has no main-power available, require low-throughput (typically 10 bytes/h) and a long life-cycle (5 years+). Implementing either a Sigfox or LoRaWAN solution is ideal, as they feature low power consumption and long range.

### 5.2.2 Smart cities

Smart cities IoT applications typically consists of utility measurements and metering and smart parking. These applications require high scalability, low throughput (typically 10 bytes/ 10 minutes) and long-battery life (5 years+). Sigfox offers an ideal solution, due to its high scalability, good urban coverage and low power consumption.

### 5.2.3 Vehicle tracking

Vehicle tracking requires a network that offers excellent coverage in both urban and rural areas. Low-throughput is generally required (single coordinate/ 10 minutes), however in the case of theft higher throughput rates are required to enable accurate tracking. Currently GPRS is the only technology that offers country-wide coverage, and therefore the best solution. NB-IoT could offer a more battery efficient solution, however coverage needs to be improved. Due to Sigfox and LoRaWAN's limited throughput these IoT-networks would not suffice in vehicle tracking applications. Hybrid Sigfox or LoRaWAN and GPRS solutions is ideal, as it could offer long battery life along with selectable accurate tracking.

### 5.2.4 Smart homes

Smart homes utilize IoT connected devices to enable remote monitoring of appliances and systems, such as lighting and security systems. These devices and systems typically

Table 5.1: IoT use case requirements

IoT-application	Up link throughput	Down link throughput	Battery life duration	Scalability
Smart bicycle	M	L	H	L
Smart parking	H	L	H	H
Smart garbage bins	L	L	H	L
Pet tracking	M	L	M	L
Point of sale terminals	H	H	L	M
Healthcare	H	H	M	H
Smart agriculture	L	L	H	L
Intelligent buildings	M	M	H	H
Asset tracking	H	L	H	M
Utility metering	H	L	H	M

Table 5.2: IoT use case applicability

IoT-application	LoRaWAN SF7	LoRaWAN SF12	Sigfox	NB-IoT	GPRS
Smart bicycle	Excellent	Excellent	Excellent	Average	Poor
Smart parking	Excellent	Average	Excellent	Average	Poor
Smart garbage bins	Excellent	Excellent	Excellent	Average	Poor
Pet tracking	Excellent	Excellent	Excellent	Excellent	Poor
Point of sale terminals	Poor	Poor	Poor	Excellent	Excellent
Healthcare	Poor	Poor	Poor	Excellent	Average
Smart agriculture	Excellent	Excellent	Excellent	Average	Poor
Intelligent buildings	Average	Poor	Poor	Average	Poor
Asset tracking	Excellent	Excellent	Excellent	Poor	Poor
Utility metering	Excellent	Excellent	Excellent	Poor	Poor

require high up link and down link throughput communication with low latency. Sigfox, NB-IoT and LoRaWAN would not suffice due to the high down link latency. GPRS is ideal as it supports the throughput and latency requirements, and main power supplies are typically available in household environments.

### 5.2.5 Predictive maintenance

IoT devices are used to observe devices and systems in industrial applications to monitor wear and usage. These devices are required to be active for years (10 years+), reporting small usage data packets (typically 10 bytes/day) irregularly. Sigfox and LoRaWAN offers the ideal solution, as devices can offer multiple year battery life.

## 5.3 Conclusion

The work in this thesis covered the following aspects successfully as outlined in the objectives in Section 1.2.

Four communication technology testing devices were developed to compare the different communication standards performances successfully. The developed testing devices resemble testing devices used in the industry and can, with minimal firmware or hardware changes, be used in a variety of real world applications.

To support performance testing, an additional LoRaWAN gateway and a current measurement device was successfully built, tested and implemented.

A complete back-end system was developed to store data transmitted by devices. Through

the addition of a front-end website, the complete system can be used in industry application.

Performance testing metrics were successfully identified, motivated, investigated, tested and results compared in this work. The metrics allowed the different standards to be compared successfully, which allowed recommendations to be made based on the use case of each technology. Different non-performance metric which affect the performance in real world deployment were successfully identified, motivated, investigated, tested and results compared. This allowed recommendations to be made regarding the deployment of the different technologies.

Through competition in the LPWAN space, the different technologies will continue to develop and improve to support more features and expand the coverage network. This was clearly evident, as at the start of the research, there was no coverage for NB-IoT, and LoRaWAN and Sigfox coverage was extremely limited. Currently, the complete testing area is covered, as can be seen in the coverage tests. Due to the performance of each technology, with its own advantages and disadvantages, it is difficult to imagine that one solution will force all other competing technologies out of the market.

## 5.4 Open research challenges

As the market for LPWAN technology is ever growing, the following recommendation can be for future research challenges:

**Software defined radios (SDR):** An future research challenge, could be to design and code a SDR base station that is capable of receiving both LoRaWAN and Sigfox messages. Sigfox offers a SDR device to emulate a sigfox network [90], and there are open source SDR LoRaWAN solutions available as well [91].

**6LoWPAN:** This protocol enables sending data as IPv6 packets and using LoRaWAN, which allows wireless internet connectivity at low data rates and with a low duty cycle.

**IoT Blockchain:** The IoT networks tested in this work, either rely on a network operator or a private individual to construct a network base station to provide coverage. Crowd sourcing this infrastructure instead, could result in greater coverage. Implementing a block chain architecture, as shown in [92], would allow users to receive crypto currency in exchange for building a decentralized IoT network.

## 5.5 Recommendations

Based on the results and conclusions, the following recommendations for future improvements can be made regarding the testing devices and testing system.

### 5.5.1 Test devices

**Improve battery and regulator:** Although the focus of this work is not to develop ultra-low power consumption IoT devices, the current testing devices identified the possibility of multiple years of battery life. Through implementing an ultra efficient voltage regulator, reducing the operating voltage or designing a battery solution that does not require a voltage regulator, the current testing device architecture could be used in real world multiple year IoT device applications.

**MCU choice:** Practically developing the LPWAN firmware indicated the reduction in

firmware complexity compared to GPRS. Progressing to an MCU with reduced complexity, such as a ATtiny from Atmel could potentially reduce device cost and improve power consumption.

**CoAp integration:** Implementing the CoAp protocol in the NB-IoT firmware would allow the devices to be practically implemented in real world IoT use cases.

### 5.5.2 Test system

**Front-end web development:** Implementing a front-end website to access and visualize the data gatered by the IoT devices would vastly increase the usability of the complete system. This would allow the testing system to be used by IoT device developers a full-stack web solution for all the various IoT communication standards.

**CoAp integration:** The back-end system lacks the support of receiving CoAp packet. Implementing this section, along with the suggested CoAp firmware integration would allow the system to fully support the NB-IoT standard.

**LoRaWAN gateway:** Currently, the LoRaWAN base station utilizes Resin.io to manage the TTN packet forwarding application. The issue is the overhead regarding the data usage of Resin.io. Either replacing the LTE back haul network with an ADSL solution or changing the management software could solve this issue.

**Scalability analysis:** The scalability analysis for LoRaWAN and Sigfox can be improved to reduce the amount of assumptions made and include a multi gateway scalability analysis. Moreover, more LoRaWAN SF7 tests need to be conducted to measure the common distribution of packets on the 8 available channels.

# List of References

- [1] Sigfox. Sigfox technical overview. [Online]. <https://www.disk91.com/wp-content/uploads/2017/05/4967675830228422064.pdf>, 05 2017. [Accessed: 08- September- 2018].
- [2] Ericsson. Mobility report, Massive IoT coverage in the city. [Online]. <https://www.ericsson.com/en/mobility-report/massive-iot-coverage-in-the-city/>. [Accessed: 11- September- 2018].
- [3] GPRS architecture: Interfaces and protocols. Technical report, Nokia, 2004.
- [4] Technical Marketing Workgroup 1.0. LoRaWAN What is it? A technical overview of LoRa and LoRaWAN. Technical report, LoRa Alliance, November 2015.
- [5] Sakshama Ghosly. All about LoRa and LoRaWAN : Symbol generation. [Online]. Available: <http://www.sghosly.com/p/lora-is-chirp-spread-spectrum.html>. [Accessed: 10- Oct- 2017].
- [6] Aloys Augustin, Jiazi Yi, Thomas Clausen, and William Mark Townsley. A study of LoRa: Long Range and Low Power Networks for the Internet of Things. *Sensors*, 16(9), 2016.
- [7] Link Labs. LTE eDRX and PSM explained for LTE-M1. [Online]. <https://www.link-labs.com/blog/lte-e-drx-psm-explained-for-lte-m1>. [Accessed: 12- June- 2018].
- [8] Indoor path loss. Technical Report XST-AN005a-Indoor, DIGI, June 2012. Application Note.
- [9] D. Girbau, J. Lorenzo, A. Lazaro, and R. Villarino. Effects of antenna detuning and gain penalty on the read range of UHF RFID. In *European Workshop on Smart Objects: Systems, Technologies and Applications*, pages 1–7, June 2010.
- [10] Appendix C: Microstrip Transmission Line Design and Discontinuities | Engineering360. [Online]. <http://www.globalspec.com/reference/70606/203279/appendix-c-microstrip-transmission-line-design-and-discontinuities>. [Accessed: 19- October- 2017].
- [11] MultiMedia LLC. TTN Mapper. [Online]. "<http://ttnmapper.org/gateways/packets.php?gwaddr=B827EBFFFE5FA31F>", 2018. [Accessed: 03- Augusts- 2018].
- [12] Yi-Bing Lin, Herman C.-H. Rao, and Imrich Chlamtac. General packet radio service (gprs): architecture, interfaces, and deployment. *Wireless Communications and Mobile Computing*, 1(1):77–92.
- [13] Internet of things forecast - ericsson. [Online]. <https://www.ericsson.com/en/mobility-report/internet-of-things-forecast>, May 2018. [Accessed: 12- June- 2018].
- [14] Rebeca Kates. What you need to know about the 2G network shutdown, Apr 2017.



- [15] Youngsun K Namhoon K. Terminating 2g service in korea: Policy issues and suggestions. *International Telecommunications Policy Review*, 21, 2014.
- [16] Dominic Adriaanse. Deal with Chinese telecoms giant to drive Stellies innovation | Cape Times, Aug 2017.
- [17] JP Meijers. The Things Network in and around Cape Town. [Online]. <https://www.thethingsnetwork.org/community/western-cape/post/the-things-network-in-and-around-cape-town>, Dec 2017. [Accessed: 18- September- 2017].
- [18] Sandra Mulder. News - smart water meter helps schools to save water...| Stellenbosch University News, Aug 2017.
- [19] U. Raza, P. Kulkarni, and M. Sooriyabandara. Low power wide area networks: An overview. *IEEE Communications Surveys Tutorials*, 19(2):855–873, Secondquarter 2017.
- [20] Kais Mekki, Eddy Bajic, Frederic Chaxel, and Fernand Meyer. A comparative study of lpwan technologies for large-scale iot deployment. *ICT Express*, 2018.
- [21] Rashmi Sharan Sinha, Yiqiao Wei, and Seung-Hoon Hwang. A survey on LPWA technology: LoRa and NB-IoT. *ICT Express*, 3(1):14 – 21, 2017.
- [22] M. Lauridsen, I. Z. Kovacs, P. Mogensen, M. Sorensen, and S. Holst. Coverage and capacity analysis of LTE-M and NB-IoT in a rural area. In *2016 IEEE 84th Vehicular Technology Conference (VTC-Fall)*, pages 1–5, Sept 2016.
- [23] Norbert Blenn and Fernando A. Kuipers. Lorawan in the wild: Measurements The Things Network. *CoRR*, abs/1706.03086, 2017.
- [24] F. Adelantado, X. Vilajosana, P. Tuset-Peiro, B. Martinez, J. Melia-Segui, and T. Watteyne. Understanding the limits of LoRaWAN. *IEEE Communications Magazine*, 55(9):34–40, 2017.
- [25] Joseph Finnegan and Stephen Brown. A comparative survey of LPWA networking. *CoRR*, abs/1802.04222, 2018.
- [26] M. Lauridsen, H. Nguyen, B. Vejlggaard, I. Z. Kovacs, P. Mogensen, and M. Sorensen. Coverage comparison of gprs, nb-iot, lora, and sigfox in a 7800 km<sup>2</sup> area. In *2017 IEEE 85th Vehicular Technology Conference (VTC Spring)*, pages 1–5, June 2017.
- [27] Mahmoud Elkhodr, Seyed A. Shahrestani, and Hon Cheung. Emerging wireless technologies in the Internet of Things: a comparative study. *CoRR*, abs/1611.00861, 2016.
- [28] Hans-Jörg Vögel Christian Bettstetter and Jörg Eberspächer. Gsm phase 2+ general packet radio service GPRS: Architecture, protocols, and air interface.
- [29] Xiaoyan Fang and D. Ghosal. Performance modeling and qos evaluation of mac/rlc layer in gsm/gprs networks. In *IEEE International Conference on Communications, 2003. ICC '03.*, volume 1, pages 271–275 vol.1, May 2003.
- [30] Tutorialspoint. GPRS - quality of service. [Online].<https://www.tutorialspoint.com/gprs>. [Accessed: 05- September- 2018].
- [31] O2. Gprs: How it works. [Online]. <http://www.o2.co.uk/assets2/PRODIImages/PDF/GPRS-howitworksMar07.pdf>. [Accessed: 05- September- 2018].

- [32] Sigfox - The Global Communications Service Provider for the Internet of Things (IoT). [Online]. <https://www.sigfox.com/en>. [Accessed: 05- September- 2018].
- [33] SqwidNET. Sqwidnet - the fastest growing iot network in south africa. [Online]. <https://www.squidnet.com/squidnet-the-fastest-growing-iot-network-in-south-africa/>. [Accessed: 05- September- 2018].
- [34] Sigfox expanding its Global IoT network into South Africa in partnership with DFA. [Online]. <https://www.sigfox.com/en/news/sigfox-expanding-its-global-iot-network-south-africa-partnership-dfa>. [Accessed: 08- September- 2018].
- [35] SIGFOX - Signal Identification Wiki. [Online]. <https://www.sigidwiki.com/wiki/SIGFOX>. [Accessed: 12- May- 2018].
- [36] Make things come alive in a secure way. Technical report, Sigfox, February 2017.
- [37] LoRa Alliance. Coverage & Operator Map. [Online]. <https://loro-alliance.org/>. [Accessed: 18- September- 2017].
- [38] P. S. Cheong, J. Bergs, C. Hawinkel, and J. Famaey. Comparison of LoRaWAN classes and their power consumption. In *2017 IEEE Symposium on Communications and Vehicular Technology (SCVT)*, pages 1–6, Nov 2017.
- [39] Juha Petajarvi, Konstantin Mikhaylov, Marko Pettissalo, Janne Janhunen, and Jari Iinatti. Performance of a low-power wide-area network based on LoRa technology: Doppler robustness, scalability, and coverage. *International Journal of Distributed Sensor Networks*, 13(3):1550147717699412, 2017.
- [40] AN1200.22. LoRa modulation basics. Technical report, Semtech, May 2015.
- [41] U. Noreen, A. Bounceur, and L. Clavier. A study of LoRa low power and wide area network technology. In *2017 International Conference on Advanced Technologies for Signal and Image Processing (ATSIP)*, pages 1–6, May 2017.
- [42] The Things Network. LoRaWAN Adaptive Data Rate. [Online]. <https://www.thethingsnetwork.org/docs/lorawan/adr.html>. [Accessed: 13- November- 2018].
- [43] The Things Network. Network architecture. [Online]. <https://www.thethingsnetwork.org/docs/network/architecture.html>. [Accessed: 08- September- 2018].
- [44] Ublox. Iot and the four reasons why licensed spectrum technologies have been worth the wait. [Online]. <https://www.u-blox.com/en/iot-and-four-reasons-why-licensed-spectrum-technologies-have-been-worth-wait>. [Accessed: 17- August- 2018].
- [45] Vodacom and Vodafone. White paper: Narrowband-iot: pushing the boundaries of iot systems. Technical report, Vodacom, Sptember 2017.
- [46] S. Grant and L. Purnell. Nb-iot deployment guide to basic feature set requirements. Technical report, GSMA, April 2018.
- [47] Weightless. Weightless - Setting the standard for IoT. [Online]. <http://www.weightless.org/>. [Accessed: 05- September- 2018].
- [48] Link Labs. A comprehensive look at low power, wide area networks. for 'Internet of Things' Engineers and Decision makers. Technical report. [Accessed: 05- September- 2018].

- [49] WavIOT. WAVIOT NB-FI LPWAN technology products and tech description. Technical report.
- [50] WavIOT. Low-power long-range (lpwan) solutions for iot and m2m. [Online]. <https://waviot.com/>. [Accessed: 05- September- 2018].
- [51] INGENU. An educational guide a white paper by INGENU how RPMA works. Technical report. [Accessed: 05- September- 2018].
- [52] G. Ergeerts, M. Nikodem, D. Subotic, T. Surmacz, B. Wojciechowski, P. D. Meulenaere, and M. Weyn. Dash7 alliance protocol in monitoring applications. In *2015 10th International Conference on P2P, Parallel, Grid, Cloud and Internet Computing (3PGCIC)*, pages 623–628, Nov 2015.
- [53] M. Weyn, G. Ergeerts, R. Berkvens, B. Wojciechowski, and Y. Tabakov. Dash7 alliance protocol 1.0: Low-power, mid-range sensor and actuator communication. In *2015 IEEE Conference on Standards for Communications and Networking (CSCN)*, pages 54–59, Oct 2015.
- [54] Tellit. *LE51-868s RF module user guide*, 1 edition, 4 2014. Datasheet.
- [55] Microchip. *RN2483 Low-Power Long Range LoRa Technology Transceiver Module*, 2017. Datasheet.
- [56] U-Blox. *LEON-G1 series quad-band GSM GPRS data & voice modules*, 3 edition, 1 2018. Datasheet.
- [57] Juha Petäjäjärvi, Konstantin Mikhaylov, Antti Roivainen, Tuomo Hänninen, and Marko Pettissalo. On the coverage of LPWANs: Range evaluation and channel attenuation model for LoRa technology. *2015 14th International Conference on ITS Telecommunications (ITST)*, pages 55–59, 2015.
- [58] Otto Wireless Solutions. By-868-01 2db stubby antenna. Technical report, 58 Wakis Avenue, Randburg, South-Africa. Datasheet.
- [59] Otto Wireless Solutions. Lte-yd-11 lte/3g/4g/gsm yagi ottenna 11db with bracket and 10 meter cable. Technical report, 58 Wakis Avenue, Randburg, South-Africa. Datasheet.
- [60] Otto Wireless Solutions. Dbds-800/900-11-120 11db high gain 360 outdoor sector antenna. Technical report, 58 Wakis Avenue, Randburg, South-Africa. Datasheet.
- [61] Otto Wireless Solutions. Aird530lw 30db rocket dish antenna. Technical report, 58 Wakis Avenue, Randburg, South-Africa. Datasheet.
- [62] P.J. Bevelacqua. Polarization - EM Waves and Antennas. [Online]. [www.antenna-theory.com/basics/polarization.php](http://www.antenna-theory.com/basics/polarization.php). [Accessed: 14- July- 2018].
- [63] Hendrik Linka, Michael Rademacher, Karl Jonas, and Osianah Glenn Aliu. Path Loss Models for Low-Power Wide-Area Networks: Experimental Results using LoRa. *VDE ITG-Fachbericht Mobilkommunikation*, 2018.
- [64] Dr R. Wolhuter. Communication Fundamentals Applications to Smart Grid Technology. Department of Electrical and Electronic Engineering, Faculty of Engineering, University of Stellenbosch, 2018.
- [65] RichardWallace. Achieving optimum radio range. Technical Report SWRA479A, Texas Instruments, September 2017.

- [66] M. Loy and I. Sylla. Ism-band and short range device antennas. Technical Report SWRA046A, Texas Instruments, August 2005.
- [67] Martin C. Bor, Utz Roedig, Thiemo Voigt, and Juan M. Alonso. Do LoRa Low-Power Wide-Area Networks Scale? In *Proceedings of the 19th ACM International Conference on Modeling, Analysis and Simulation of Wireless and Mobile Systems, MSWiM '16*, pages 59–67, New York, NY, USA, 2016. ACM.
- [68] H. D. Pham, M. Drieberg, and C. C. Nguyen. Development of vehicle tracking system using GPS and GSM modem. In *2013 IEEE Conference on Open Systems (ICOS)*, pages 89–94, Dec 2013.
- [69] M. I. Hoque, A. A. Amin, M. J. Rahaman, and M. Hossam-E-Haider. Designing and performance evaluation of GSM/GPS based helicopter tracking device. In *2017 IEEE International Conference on Telecommunications and Photonics (ICTP)*, pages 77–81, Dec 2017.
- [70] SIMCom. *GSM/GPRS Module SIM800C*. Datasheet.
- [71] WISOL. *WISOL / WSSFM10R1AT*, 14 edition. Datasheet.
- [72] HopeRF. *RFM95/96/97/98(W) - Low Power Long Range Transceiver Module*, 1 edition. Datasheet.
- [73] Ublox. *SARA-N2 Power-optimized NB-IoT (LTE Cat NB1) modules*, 14 edition, 06 2018. Datasheet.
- [74] Atmel. *ATmega128A4U / ATmega64A4U / ATmega32A4U / ATmega16A4U*, 09 2014. Datasheet.
- [75] Atmel. *ATmega328/P Datasheet*, 11 2016. Datasheet.
- [76] Nicolaas Hendrik Naude. Firmware and functional test platform developed for a smart controller. Master's thesis, Faculty of Engineering, Stellenbosch University, 12 2017.
- [77] ST electronics. *LEON-G100/G200 quad-band GSM/GPRS Data and Voice Modules System Integration Manual*, 05 2012. Datasheet.
- [78] UBLOX. *L5987 3 A step-down switching regulator*, 2014. Datasheet.
- [79] Microwaves 101. Coplanar Waveguide Calculator. [Online]. <https://www.microwaves101.com/calculators/864-coplanar-waveguide-calculator>. [Accessed: 18- September- 2017].
- [80] Rainee N Simons. *Coplanar Waveguide Circuits, Components, and Systems*. Wiley, 2004.
- [81] Electronic Design. What's the difference between high-side and low-side current sensing? [Online]. <http://www.electronicdesign.com/power/what-s-difference-between-high-side-and-low-side-current-sensing>. [Accessed: 07- July- 2018].
- [82] D.L. Jones. uCurrent GOLD. [Online]. [www.eevblog.com/projects/ucurrent/](http://www.eevblog.com/projects/ucurrent/). [Accessed: 10- August- 2018].
- [83] The Things network. The Things Gateway. [Online]. Available: [www.thethingsnetwork.org/docs/gateways/gateway/](http://www.thethingsnetwork.org/docs/gateways/gateway/). [Accessed: 10- Sept- 2018].

- [84] Lorrier. Carrier grade LPWAN. [Online]. Available: <https://lorrier.com/introducing-lr2>. [Accessed: 10- August- 2018].
- [85] The Things network J. Kersing. Build your own RAK831 based gateway. [Online]. Available: [www.thethingsnetwork.org/docs/gateways/rak831/](http://www.thethingsnetwork.org/docs/gateways/rak831/). [Accessed: 10- August- 2018].
- [86] R. Kaiser. From zero to LoRaWAN in a weekend. [Online]. [github.com/ttn-zh/ic880a-gateway/wiki](https://github.com/ttn-zh/ic880a-gateway/wiki). [Accessed: 10- August- 2018].
- [87] IMST GmbH. *WiMOD iC880A*, 03 2015. Datasheet.
- [88] Andrew Hector Cloete. A domestic electric water heater application for smart grid. Master's thesis, Faculty of Engineering, Stellenbosch University, 12 2017.
- [89] T. Isenlik, M.M. Bilgic, K. Yegin, and M. Ciydem. Gsm/umts dual polarization base station antenna design. In *2011 XXXth URSI General Assembly and Scientific Symposium*, pages 1–4, Aug 2011.
- [90] Sigfox. Sigfox SDR Dongle. [Online]. <https://build.sigfox.com/sdr-dongle>. [Accessed: 10- August- 2018].
- [91] RTL-SDR.COM. Decoding the LoRa IoT protocol with an RTL-SDR. [Online]. <https://www.rtl-sdr.com/decoding-the-iot-lora-protocol-with-an-rtl-sdr>. [Accessed: 10- August- 2018].
- [92] A. Thompson M. Nijdam R. Garg A. Haleem, A. Allen. Helium a Decentralized Machine Network. 2018.

# Appendix A

## Antenna Tests

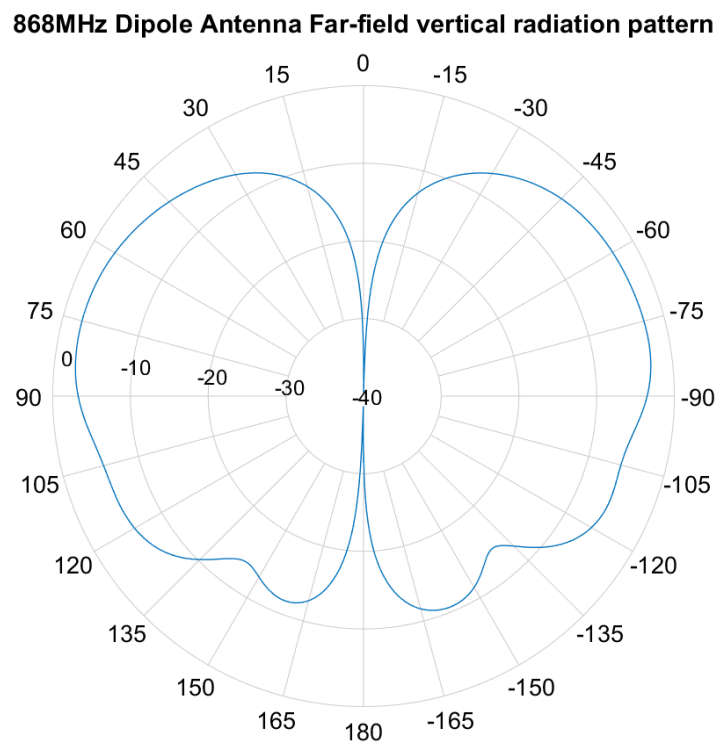


Figure A.1: 868MHz Dipole Antenna Far-Field vertical radiation pattern tested at 868MHz

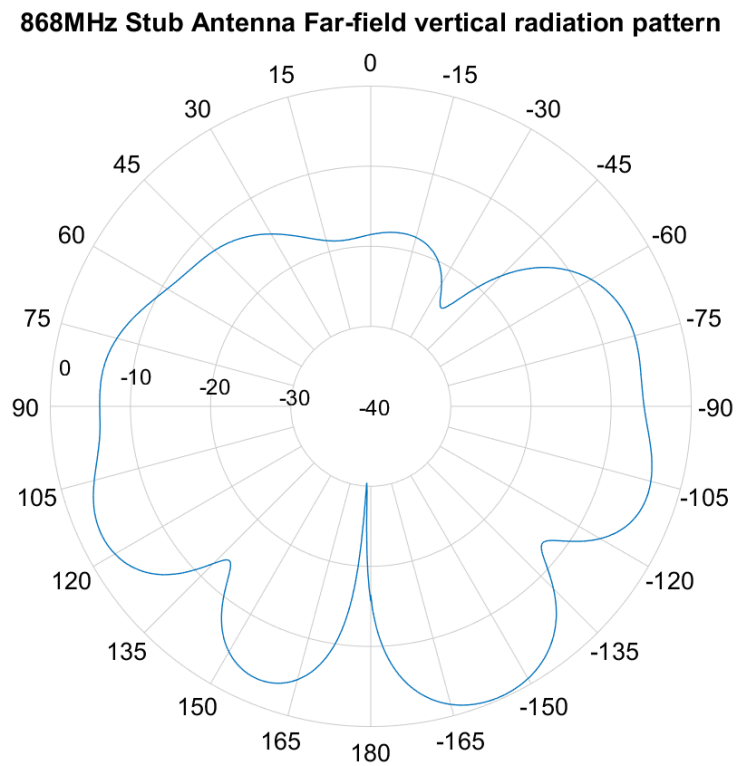


Figure A.2: 868MHz Stub Antenna Far-Field vertical radiation pattern tested at 868MHz

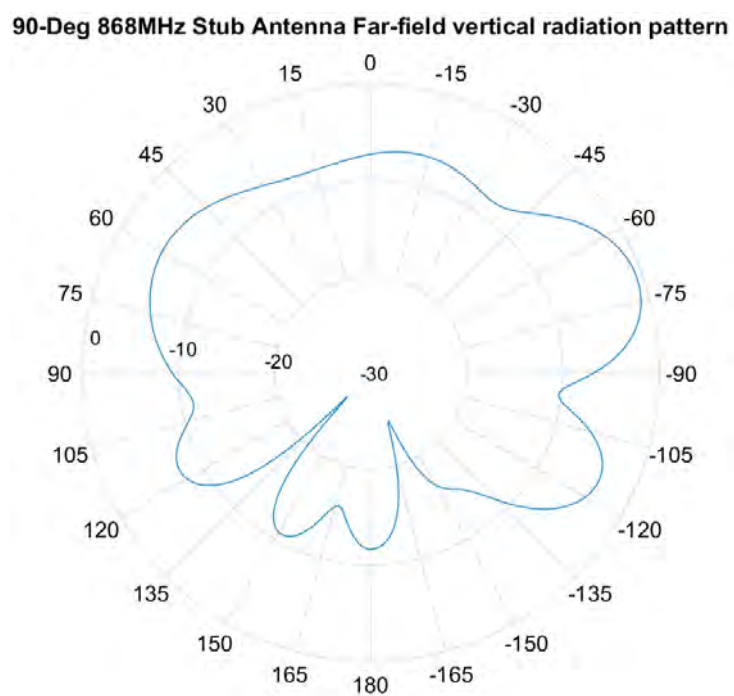


Figure A.3: 90 Deg 868MHz Stub Antenna Far-Field vertical radiation pattern tested at 868MHz

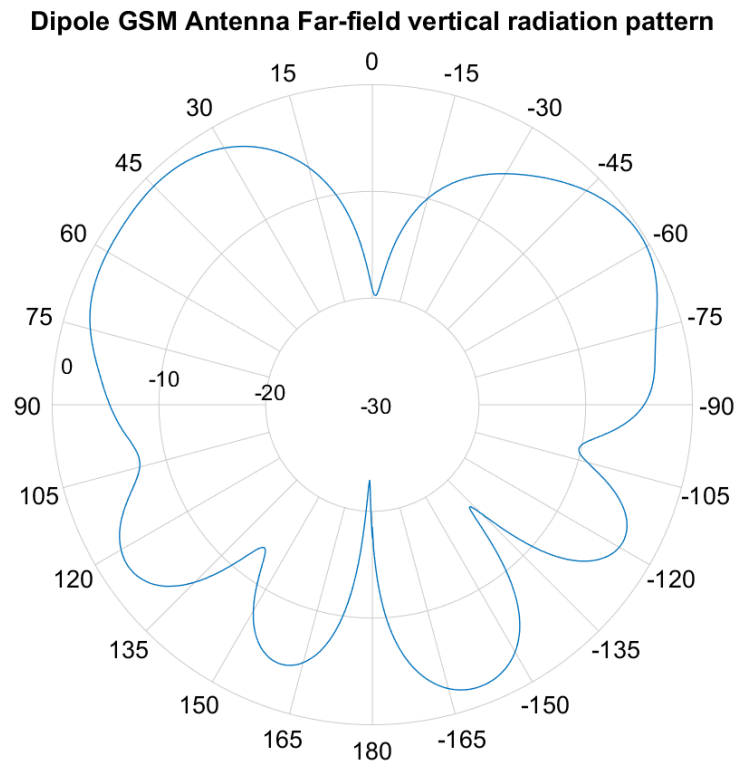


Figure A.4: GSM Dipole Antenna Far-Field vertical radiation pattern tested at 868MHz

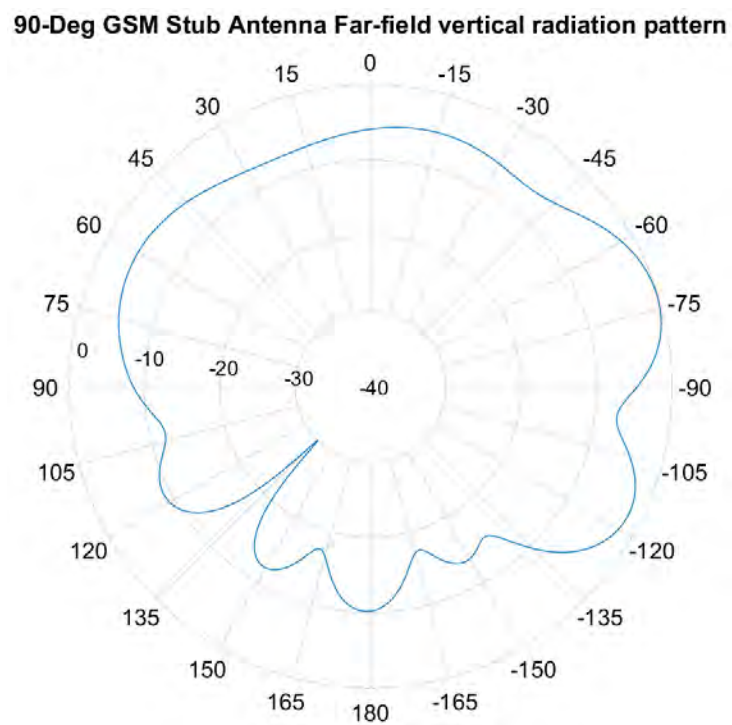


Figure A.5: 90 Deg GSM Stub Antenna Far-Field vertical radiation pattern tested at 868MHz



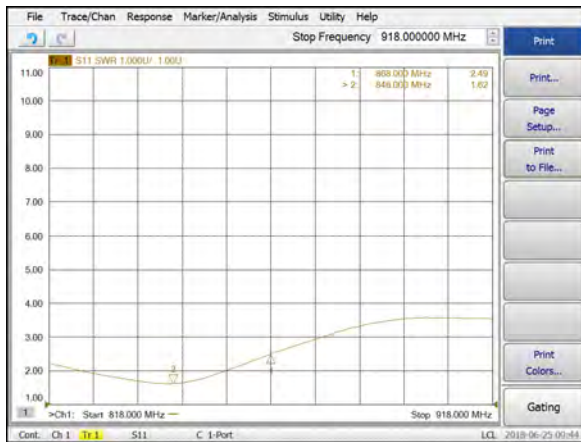


Figure A.6: 3dBi GSM helical stubby antenna, with 90deg connector VSWR

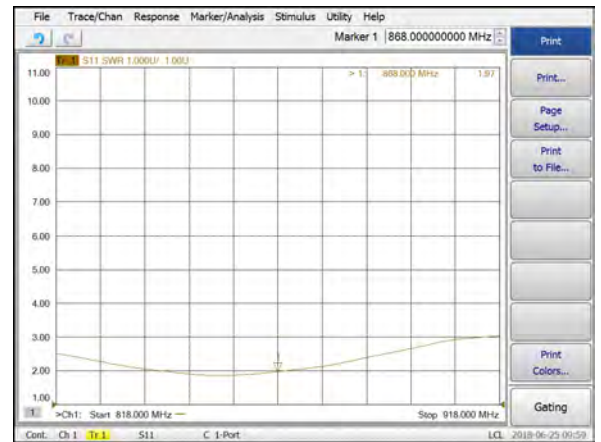


Figure A.7: 3dBi 868MHz helical stubby antenna, with 90deg connector VSWR

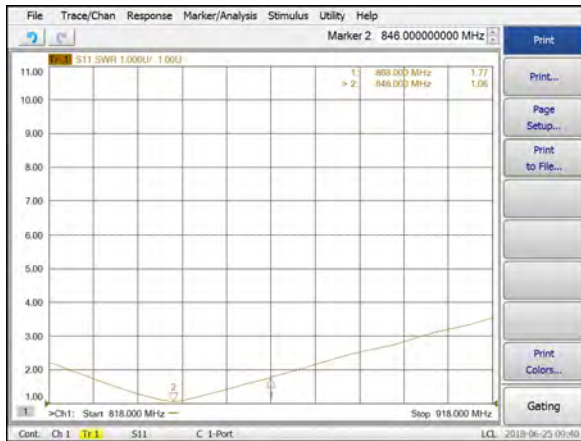


Figure A.8: 3dBi 868Mhz dipole antenna, straight VSWR

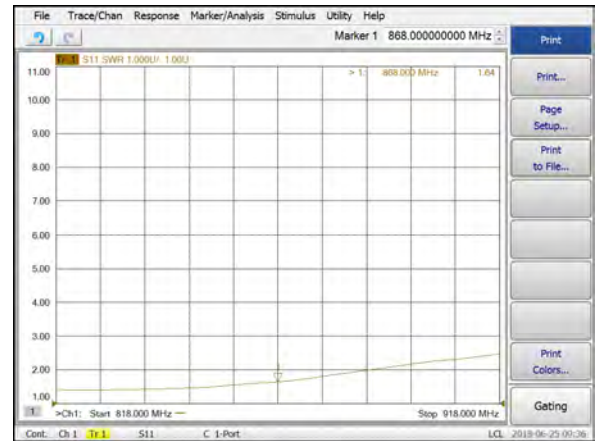


Figure A.9: 0.5dBi GSM dipole antenna, straight VSWR

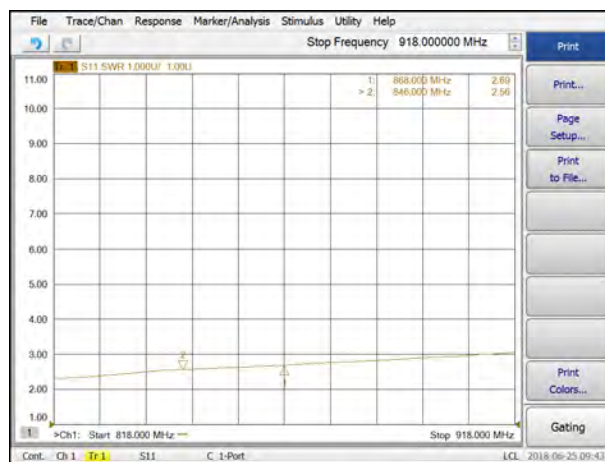


Figure A.10: 2.2dBi 868MHz helical stubby antenna, straight VSWR

# Appendix B

## Hardware Development



(a) NB-IoT base station



(b) Sigfox base station



(c) LoRaWAN gateway

Figure B.1: Different base stations deployed

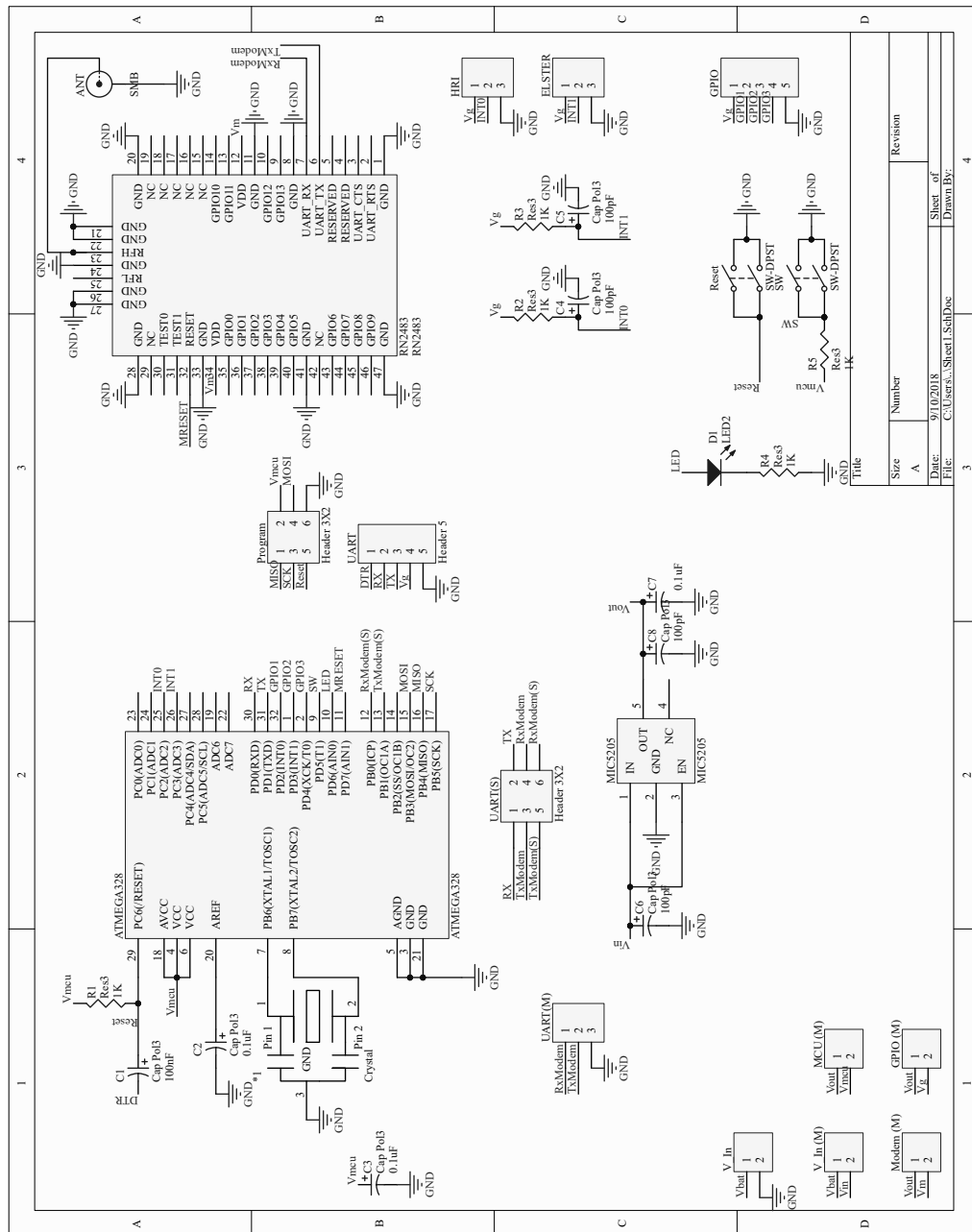


Figure B.2: LoRaWAN device PCB design

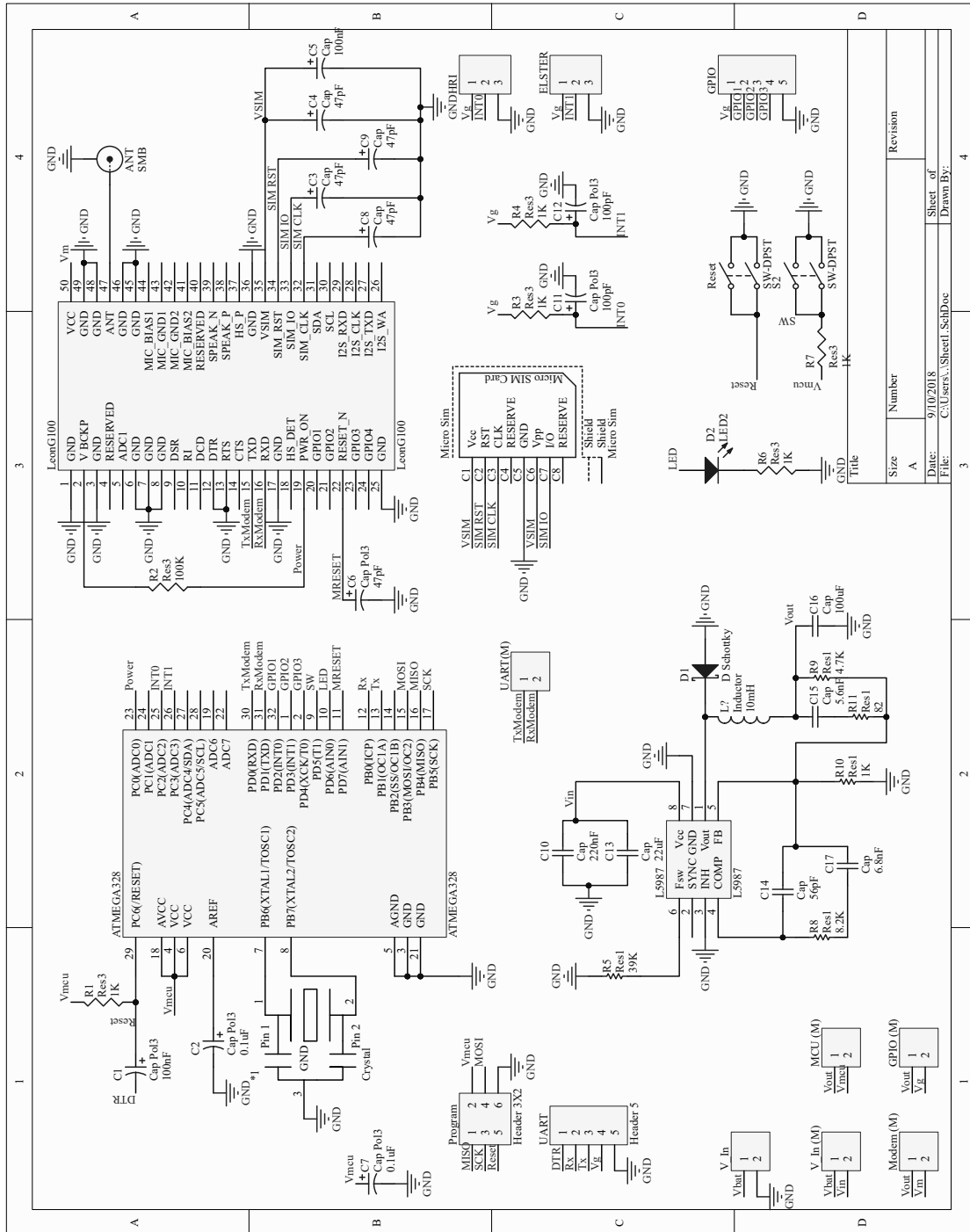


Figure B.3: GPRS device PCB design

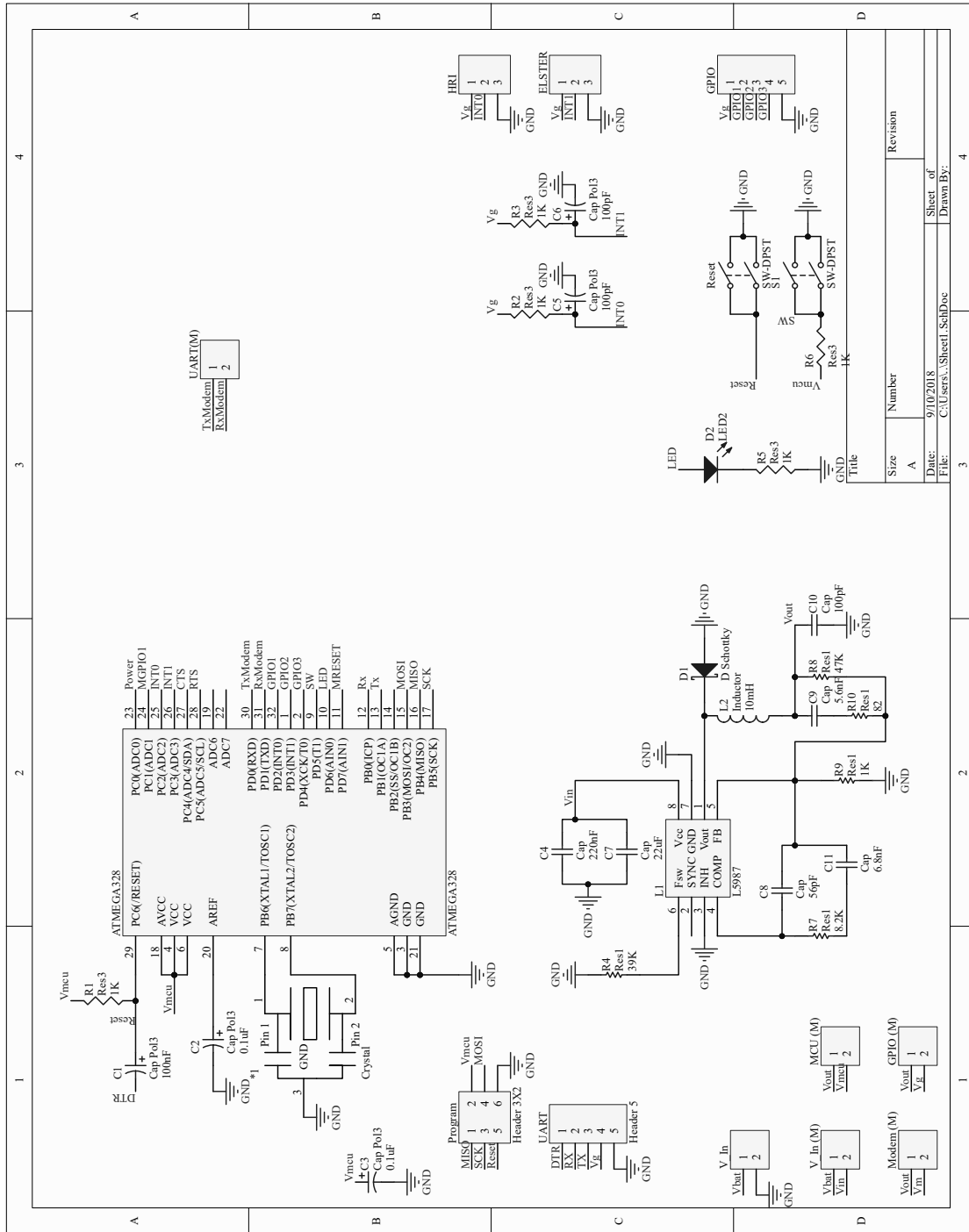


Figure B.4: NB-IoT device PCB design Part I

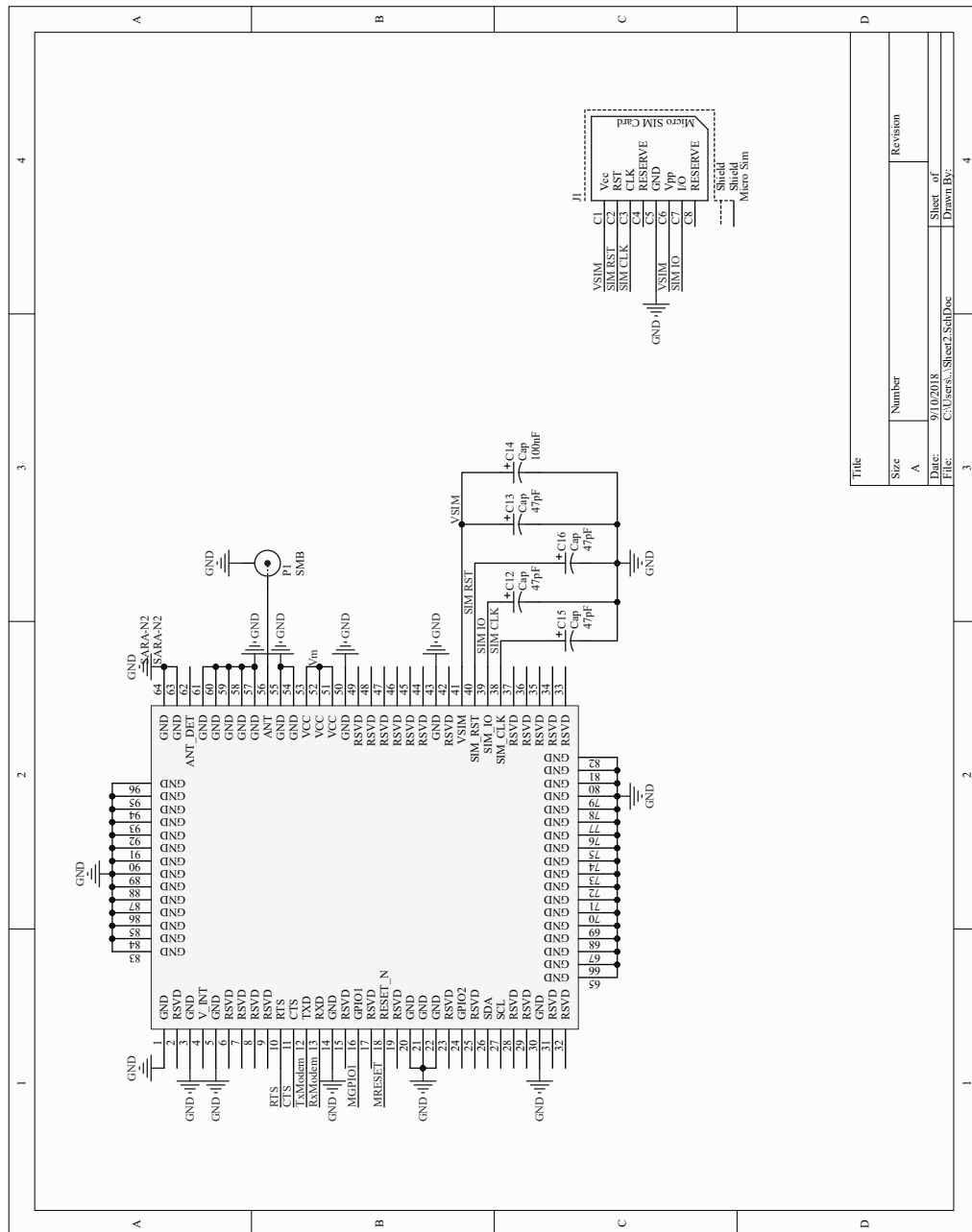


Figure B.5: NB-IoT device PCB design Part II

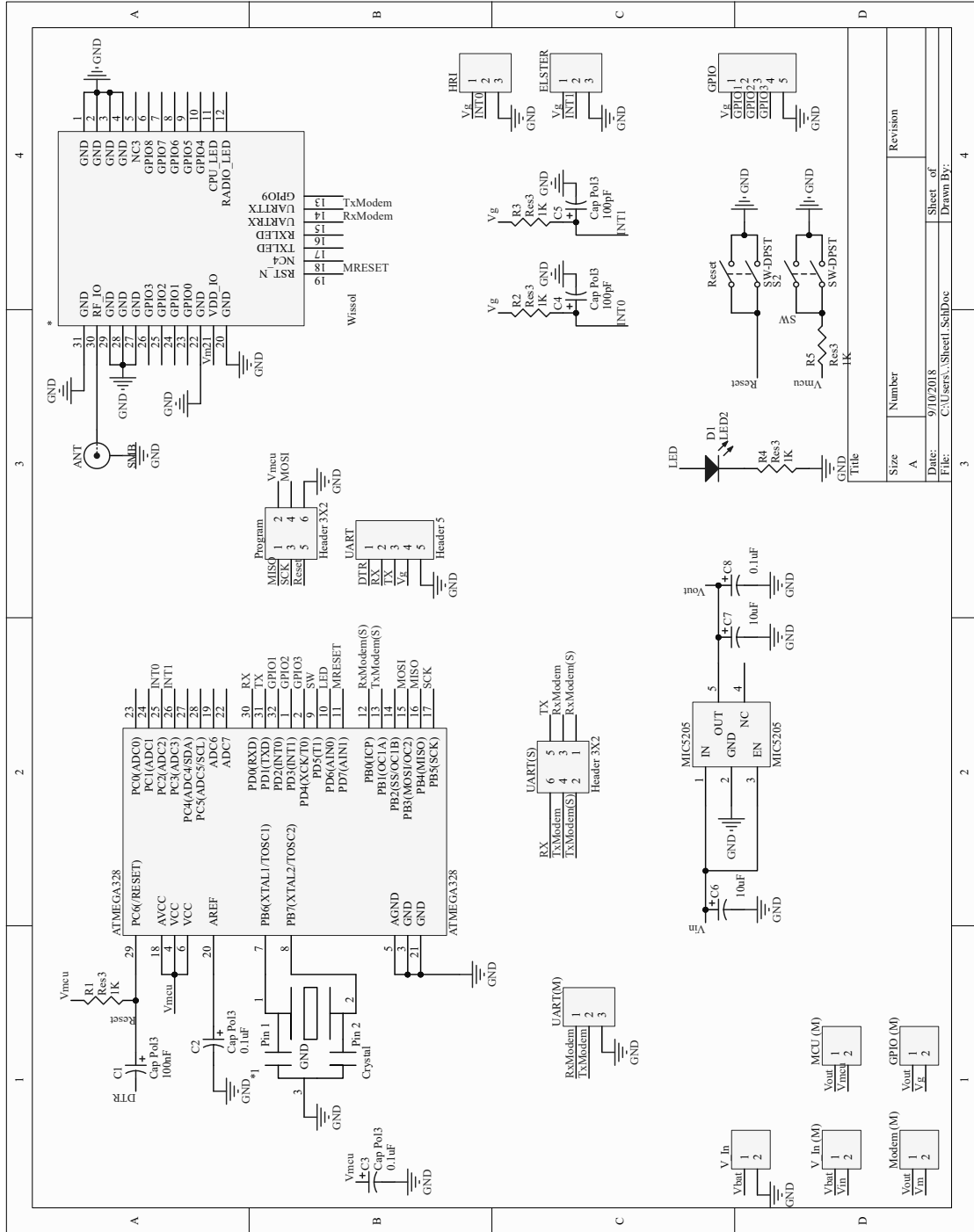


Figure B.6: Sigfox device PCB design

$$Z_o = \frac{60 \times \pi}{\sqrt{\epsilon_{eff}}} \times \frac{1.0}{\frac{K(k)}{K(k')} + \frac{K(kl)}{K(kl')}} \quad (\text{B.1})$$

$$k' = \sqrt{1.0 - k^2} \quad (\text{B.2})$$

$$kl' = \sqrt{1.0 - kl^2} \quad (\text{B.3})$$



$$kl = \frac{\tanh\left(\frac{\pi \times a}{4.0 \times h}\right)}{\tanh\left(\frac{\pi \times b}{4.0 \times h}\right)} \quad (\text{B.4})$$

$$\epsilon_{eff} = \frac{1.0 + \epsilon_r \times \frac{K(k')}{K(k)} \times \frac{K(kl)}{K(kl')}}{1.0 + \frac{K(k')}{K(k)} \times \frac{K(kl)}{K(kl')}} \quad (\text{B.5})$$

# Appendix C

## Backend systems

The screenshot displays the 'loraserver' application overview in the The Things Network Console. The interface includes a navigation bar with 'Applications', 'Gateways', and 'Support', and a user profile for 'ThomasDurand'. The main content area is divided into three sections: 'APPLICATION OVERVIEW', 'APPLICATION EUIs', and 'DEVICES'. The 'APPLICATION OVERVIEW' section shows the Application ID as 'loraserver', Description as 'Lora Server', Created as 'last year', and Handler as 'ttn-handler-eu (current handler)'. The 'APPLICATION EUIs' section shows a single EUI: '70 B3 D5 7E F0 00 4D A4'. The 'DEVICES' section shows '4 registered devices'.

**THE THINGS NETWORK CONSOLE** COMMUNITY EDITION

Applications Gateways Support **ThomasDurand** ▾

Applications > loraserver

Overview Devices Payload Formats Integrations Data Settings

### APPLICATION OVERVIEW

[documentation](#)

**Application ID** loraserver

**Description** Lora Server

**Created** last year

**Handler** ttn-handler-eu (current handler)

### APPLICATION EUIs

[manage euis](#)

<> 70 B3 D5 7E F0 00 4D A4

### DEVICES

[register device](#) [manage devices](#)

4 registered devices

Figure C.1: The Things network LoRaWAN device back-end

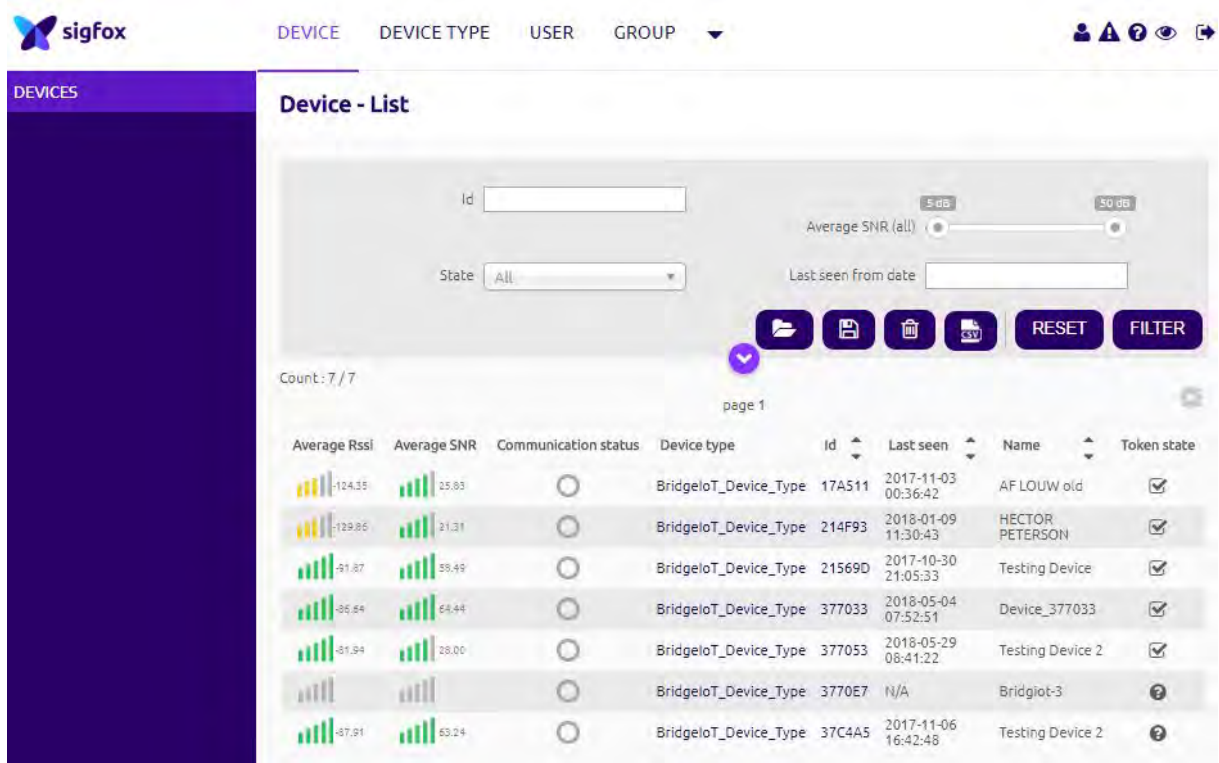


Figure C.2: Sigfox device back-end

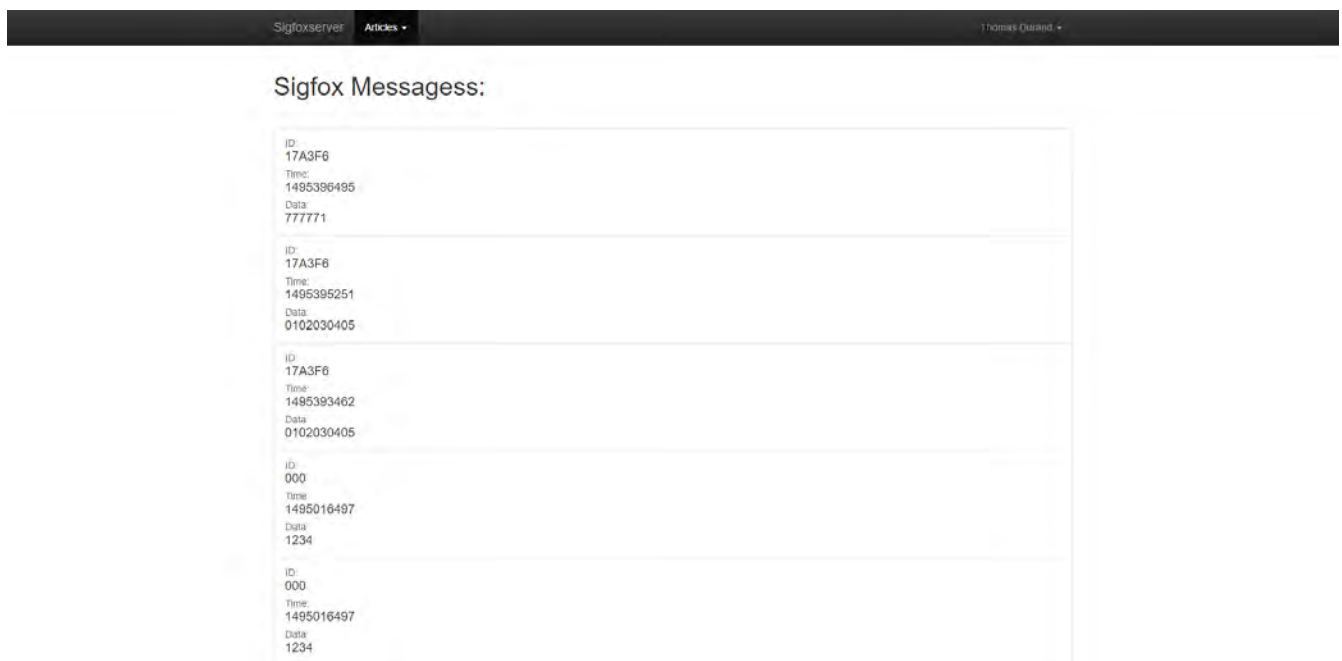


Figure C.3: MEAN-stack front-end web development

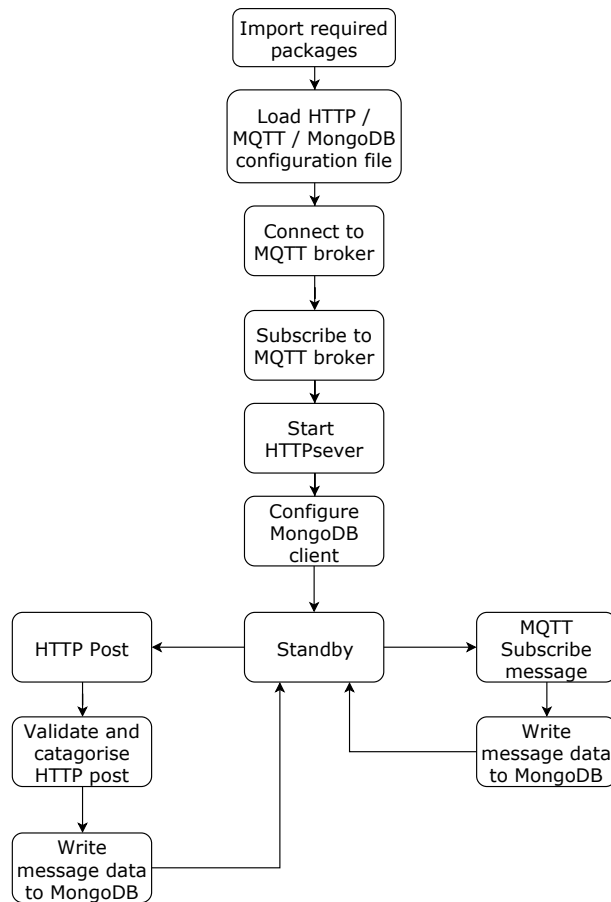


Figure C.4: Data translation layer overview

# Appendix D

## Power consumption calculations

To calculate the expected battery life of an ideal device which only consists of a modem, powered by an ideal 9250mWh battery (as described in Section 4.1.2.1), Tables D.2 to D.5 is measured. These table consider all phases of the modems transmitting a 12 byte message every 10 minutes. The expected battery life of the technologies can be seen in Table D.1.

<b>Technology</b>	<b>Total power consumption (mWh)</b>	<b>Battery life (days)</b>
LoRaWAN SF7	0.077421	4978
LoRaWAN SF12	0.364862	1056
Sigfox	2.062497	187
NB-IoT	3.156255	122

Table D.1: Battery life estimation of each type of technology

<b>LoRaWAN SF7</b>	<b>V</b>	<b>mA</b>	<b>mW</b>	<b>s/h</b>	<b>mWh</b>
LoRa Tx	3.3	38.7	127.71	0.3696	0.01311156
LoRa Rx 1	3.3	13.8	45.54	0.54	0.006831
LoRa Rx 2	3.3	13.8	45.54	1.56	0.019734
LoRa Idle	3.3	3	9.9	12.5304	0.0344586
LoRa Sleep	3.3	0.001	0.0033	3585	0.00328625

Table D.2: LoRaWAN SF7 power consumption calculations

<b>LoRaWAN S12</b>	<b>V</b>	<b>mA</b>	<b>mW</b>	<b>s/h</b>	<b>mWh</b>
LoRa Tx	3.3	37.8	124.74	8.88	0.307692
LoRa Rx 1	3.3	13.8	45.54	0.6	0.00759
LoRa Rx 2	3.3	13.8	45.54	1.56	0.019734
LoRa Idle	3.3	3	9.9	9.66	0.026565
LoRa Sleep	3.3	0.001	0.0033	3579.3	0.003281025

Table D.3: LoRaWAN SF12 power consumption calculations

<b>Sigfox</b>	<b>V</b>	<b>mA</b>	<b>mW</b>	<b>s/h</b>	<b>mWh</b>
Sigfox Sleep	3.3	0.0005	0.00165	3593.141	0.0.0016468
Sigfox Idle	3.3	0.6	1.98	4.8	0.00264
Sigfox Trans	3.3	56.7	187.11	39.6	2.05821

Table D.4: Sigfox power consumption calculations

<b>NB-IoT</b>	<b>V</b>	<b>mA</b>	<b>mW</b>	<b>s/h</b>	<b>mWh</b>
NB-Transmit	3.4	300	1020	0.3726	0.10557
NB-RRC cycle 1	3.4	70	238	22.5	1.4875
NB-RRC cycle 2	3.4	85	289	11.25	0.903125
NB-RRC cycle 3	3.4	8	27.2	84.75	0.640333333
NB sleep	3.4	0.006	0.0204	3481.13	0.019726403

Table D.5: NB-IoT power consumption calculations

# Appendix E

## Scalability simulations

```

num_dev = 700 #Number of devices to simulate
N = 10 #Number of simulations
ToA = 1.48 #Time on air per device
dev = np.zeros((num_dev, 3)) #Devices simulation matrix
devs = np.zeros((num_dev, 1)) #Per num of devices simulation matrix
coll = 0 #total number of collisions

for r in range(num_dev): #Devices
    for h in range(N): #Simulations
        list = set() #Message collision unique set
        for i in range(r):
            #Populate each device transmission at a random time
            dev[i][0] = random.uniform(0, (1000-ToA))
            #Populate each device transmission at a random frequency
            dev[i][1] = random.randint(1, 8)
            #Populate each device transmission at a RSSI
            dev[i][2] = random.uniform(-60, -140)
        for i in range(0,r,1):
            #Check all possible packet collisions with each other
            for j in range(0,r,1):
                #Calculate the end time of dev (j) transmission
                end = dev[j][0]+ToA;
                #Check if collision occurred
                if(dev[i][0]>dev[j][0] and dev[i][0]<end and dev[i][1]==dev[j][1]):
                    #List.add(i);
                    #List.add(j);
                    if(dev[i][2]>dev[j][2]):
                        list.add(j);
                    else:
                        list.add(i);
                coll = coll + len(list) #add the amount of collisions
            devs[r][0] = 100 - coll/N/(r+1)*100
            coll = 0
plt.xlabel('Number of devices')
plt.ylabel('Packet delivery ratio (%)')
plt.plot(devs);
plt.show();

```

Figure E.1: LoRaWAN SF12 Scalability simulation, for device transmitting a single packet in 1000s intervals

```

num_dev = 700 #Number of devices to simulate
N = 10 #Number of simulations
ToA = 0.0616 #Time on air per device
dev = np.zeros((num_dev, 3)) #Devices simulation matrix
devs = np.zeros((num_dev, 1)) #Per num of devices simulation matrix
coll = 0 #total number of collisions

for r in range(num_dev): #Devices
    for h in range(N): #Simulations
        list = set() #Message collision unique set
        for i in range(r):
            #Populate each device transmission at a random time
            dev[i][0] = random.uniform(0, (1000-ToA))
            #Populate each device transmission at a random frequency
            dev[i][1] = random.randint(1, 3)
            #Populate each device transmission at a RSSI
            dev[i][2] = random.uniform(-60, -120)
        for i in range(0,r,1):
            #Check all possible packet collisions with each other
            for j in range(0,r,1):
                #Calculate the end time of dev (j) transmission
                end = dev[j][0]+ToA;
                #Check if collision occurred
                if(dev[i][0]>dev[j][0] and dev[i][0]<end and dev[i][1]==dev[j][1]):
                    #list.add(i);
                    #list.add(j);
                    if(dev[i][2]>dev[j][2]):
                        list.add(j);
                    else:
                        list.add(i);
                coll = coll + len(list) #add the amount of collisions
            devs[r][0] = 100 - coll/N/(r+1)*100
            coll = 0
plt.xlabel('Number of devices')
plt.ylabel('Packet delivery ratio (%)')
plt.plot(devs);
plt.show();

```

Figure E.2: LoRaWAN SF7 Scalability simulation, for device transmitting a single packet in 1000s intervals

```

num_dev = 70001
N = 1
ToA = 1.84 #Time on air per device
dev = np.zeros((num_dev, 3)) #Devices simulation matrix
devs = np.zeros((num_dev, 1)) #Per num of devices simulation matrix
coll = 0 #total number of collisions

for i in range(num_dev):
    #Populate each device transmission at a random time
    dev[i][0] = random.uniform(0, (991))
    #Populate each device transmission at a random time
    dev[i][1] = dev[i][0]+2.3
    #Populate each device transmission at a random time
    dev[i][2] = dev[i][0]+4.6
for y in range(1, num_dev, 500):
    list = set()
    for x in range(100, 800, 100):
        for h in range(y): #Simulations
            end1 = dev[h][0]+ToA;
            end2 = dev[h][1]+ToA;
            end3 = dev[h][2]+ToA;
            if(dev[h][0]<x and x<end1 or dev[h][1]<x and x<end2 or dev[h][2]<x and x<end3):
                list.add(h);
        devs[y][0] = len(list)/8
    plt.scatter(y,devs[y][0],alpha = 0.5, c='r', s=10);
plt.xlabel('Number of devices')
plt.ylabel('Num simulutanous transmissions')
plt.show()

```

Figure E.3: Sigfox Scalability simulation, for device transmitting a single packet in 1000s intervals